Ollscoil na Gaillimhe
University of Galway

Provided by the author(s) and University of Galway in accordance with publisher policies. Please cite the published version when available.

Title	Centrosome cohesion: functions of C-NAP1
Author(s)	Flanagan, Anne-Marie
Publication Date	2016-01-07
Item record	http://hdl.handle.net/10379/5458

Downloaded 2024-05-09T00:23:08Z

Some rights reserved. For more information, please see the item record link above.

Centrosome Cohesion: Functions of C-NAP1

Anne-Marie Flanagan
Centre for Chromosome Biology,
School of Natural Sciences,
National University of Ireland, Galway

A thesis submitted to the National University of Ireland, Galway
for the degree of Doctor of Philosophy

September 2015

Supervisor: Prof. Ciaran Morrison

Table of Contents

List of figures

List of tables

Abreviations

53BP1	p53 binding protein 1
9-1-1	Rad9-Rad1-Hus1
AID	auxin-inducible degron
Aki1	Akt kinase-interacting protein 1
ALMS1	Alström syndrome 1
APC/C	anaphase promoting complex/cyclosome
APS	ammonium persulphate
Arl13B	ADP-ribosylation factor-like 13B
ATM	ataxia telangiectasia, mutated
ATP	adenosine-5‟-triphosphate
ATR	ATM-Rad3 related
ATRIP	ATR-interacting protein
BBS	Bardet-Biedl syndrome
BLAST	basic local alignment search tool
Bld10	Basal body 10
BLM	bloom syndrome protein
Bp	base pair(s)
BRCA1	breast cancer associated gene1
BRCA2	breast cancer associated gene 2
BSA	bovine serum albumin
BUB	budding uninhibited by benzimidazole
CDC	cell division cycle
CDK	cyclin-dependent kinase
cDNA	complementary DNA
Cas9	CRISPR associated protein 9
CEP	Centrosomal protein
Chk	checkpoint kinase
C-NAP1	centrosomal NEK2-associated protein 1
CPAP	Centrosomal P4.1-associated Protein
CRISPR	clustered regularly interspaced short palindromic repeat
C-terminus	carboxy terminus
DAPI	4‟, 6-diamidino-2-phenylindole
DDR	DNA damage response
DEPC	Diethylpyrocarbonate
DMSO	dimethylsulfoxide
DNA-PK	DNA-dependent protein kinase
dNTP	deoxyribonucleotide-5‟-triphosphate
DSB	double-strand break
dsDNA	double-stranded DNA
E2F	adenovirus E2 promoter binding factor
ECL	enhanced chemiluminesence
EDTA	ethylenediaminetetraacetic acid
EGTA	ethylene glycol tetraacetic acid
EM	electron microscopy
Exo1	Exonuclease 1
FACS	fluorescence-activated cell sorting
FANCD2	Fanconi anaemia, complementation group D2
FBS	foetal bovine serum
FITC	fluorescein isothiocyanate
G	gravity
γ-TURC	γ-tubulin ring complex
γ-TUSC	γ-tubulin small complex
GCP	γ-tubulin complex protein
Gen1	Gen homologue, endonuclease 1
GFP	green fluorescent protein
Hh	Hedgehog
HR	homologous recombination
hTERT-RPE1	human telomerase reverse transcriptase- retinal pigment epithelial

HU	hydroxyurea
IF	immunofluorescence microscopy
IFT	intraflagellar transport
IR	ionizing radiation
kb	kilobase pair(s)
kDa	kilodaltons
Kiz	kizuna
LB	luria-Bertani medium
MAD	mitotic arrest deficient
MAP	microtubule associated protein
MCC	mitotic checkpoint complex
MCPH	Microcephalin
MDC1	mediator of DNA damage checkpoint protein 1
MDM2	mouse double minute 2
MRE11	meiotic recombination 11
MRN	MRE11-RAD50-NBS1 complex
Mst2	Mammalian Sterile 20-like kinase 2
MTOC	microtubule-organising centre
NBS1	Nijmegen breakage syndrome 1
NCBI	National Center for Biotechnology Information
NCS	newborn calf serum
NEDD1	Neural precursor cell expressed, developmentally down-regulated 1
NEK	NIMA-related kinase
NHEJ	non-homologous end joining
NIMA	Never-in-mitosis A
ODF2	Outer dense fiber protein 2
OFD1	Oral-facial-digital syndrome 1
PBS	phosphate buffered saline
PCM	pericentriolar material
PCR	polymerase chain reaction
PDGF	platelet-derived growth factor
Pen/Strep	penicillin/streptomycin
PIKK	phosphoinositide 3-kinase related protein kinase
Plk	polo-like kinase
PNK	polynucleotide kinase
POC	Protein of Centriole
PP1	Protein phosphatase 1
Rad	radiation sensitive
RCC1	Regulator of Chromosome Condensation 1
Rb	Retinoblastoma
RFC	Replication factor C
RNA	ribonucleic acid
RNAi	RNA interference
RNase	ribonuclease
RPA	replication protein A
SAC	spindle assembly checkpoint
SAP	shrimp alkaline phosphatese
SAS	Spindle assembly abnormal protein
Sav	scaffold protein Salvador
SCC	Sister Chromatid Cohesion protein
SCF	Skp, Cullin, F-box containing complex
SDS	sodium dodecyl sulphate
SDS-PAGE	SDS polyacrylamide gel electrophoresis
SEM	standard error of the mean
Ser/Thr	serine/threonine
Sgo1	Shugosin 1
Shh	Sonic hedgehog
siRNA	short interfering RNA
SPB	spindle pole body
ss	serum starved

ssDNA	single-stranded DNA
STIL	SCL/TAL1 interrupting locus
TAE	tris acetate EDTA
TEM	transmission electron microscopy
TEMED	N,N,N‘,N‘‘-tetramethylethylenediamine
TIR1	Transport inhibitor response 1
TG	tris-glycine
TopBP1	Topoisomerase II DNA binding protein 1
Tris	tris(hydroxymethyl)aminomethane
UV	ultraviolet
Wnt	wingless-type MMTV integration site family
WT	Wild-type
XLF	XRCC4-like factor

Acknowledgements

Firstly, I would like to thank my supervisor Professor Ciaran Morrison for giving me the opportunity to do a PhD in his lab. I am very grateful for all the support and guidance you provided over the last four years. It was a pleasure to work with you.

To the lab members that have been there from day one, Owen and Lisa, thank you for making me work hard, we've been there through all the highs and lows of lab life and I want to say thank you for helping me through the difficult and frustrating times in particular. To my current lab members, Shiva, Yetunde and Ebtissal; thanks for all the chats and distractions. I needed the breaks even though I was reluctant to take them at times.

To previous lab members including Anna, Loretta, Chiara, Alicja, Tiago, Sandra and David, I am hugely appreciative of all the assistance and advice you have given over the past four years even though some of you have been many miles away. I also want to thank the other members of the CCB for creating such a friendly and helpful working environment, in particular Emma, Meller Anna, Karen, Mike and all the admin staff. I especially want to thank Janna and Nikolay for their unending friendship and encouragement. You carried me when I could barely stand and I honestly don't know where I'd be without you both.

Thank you to the people that make up my sporting life, players and coaches. I am grateful for all the opportunities you have given me to play sport, whether it was soccer, Gaelic football or tag rugby, my sanity was saved because of these activities.

Finally, I want to thank my family. My parents didn't know what I was doing so much but as long as I was happy they were happy too. Thank you for putting yourselves out so many times just to accommodate my life. Thanks to Deirdre for being a good housemate, it was always good to see ya after a long day in the lab.

Abstract

Double stranded DNA encodes the genetic material of the cell. Replication and segregation cycles are regulated in order to maintain the integrity of the DNA sequence from one cell cycle to the next. Detection of lesions in the genetic material directs specific signalling and repair pathways to conserve the DNA sequence at the site of damage. The DNA damage response can arrest the cell cycle. Functions of other organelles, such as the centrosome, can proceed during this time, although their activities can become desynchronized from the cell cycle.

The main microtubule organising centre in animal cells is the centrosome. The centrosome is composed of two barrels of microtubule triplets connected by a fibrous intercentriolar linker held in a lattice of proteins called the pericentriolar material and surrounded by a clustering of centriolar satellite complexes. C-NAP1 anchors the linker to the centrioles and is removed following centrosome duplication to facilitate the centrosome-mediated organisation of the bipolar spindle in mitosis.

C-NAP1 depletion causes premature loss of centrosome cohesion and centrosome splitting. To address the impact of DNA damage on split centrosomes, we investigated *C-NAP1* in chicken and human systems. We observed that chicken C-NAP1 localises to the centrosome, between the centrioles. Conditional depletion of chicken C-NAP1 using an auxin-inducible degron did not affect centrosome cohesion or centrosomal responses to DNA damage.

We generated stable human cell lines with a disrupted *C-NAP1* coding region and noticed a significant increase in split centrosomes. We also discovered a disorganised localisation pattern of centriolar satellite complexes in cells lacking C-NAP1, where the key satellite components PCM1 and OFD1 showed decreased clustering at the centrosome although their total expression remained unchanged. The ability to generate primary cilia was not affected by C-NAP1 loss, although we observed the formation of aberrant rootletin structures in the cytosol of ciliated cells. We exposed *C-NAP1*-disrupted cells to ionising radiation to induce a DNA damage response and found the level of centriole amplification was decreased when compared to wildtype cells. We propose that the decrease in the local concentration of centriolar satellite components at the centrosome hinders the DNA damage-induced amplification of centrioles.

1. Introduction

1.1 Cell cycle overview

The eukaryotic cell cycle is an ordered series of events that involve DNA replication and equal division of chromosomes into two daughter cells. This highly controlled process is characterised by the replication of the genomic DNA in synthesis phase (S phase) and the segregation of the replicated chromosomes in mitosis (M phase). Between cyclic S and M phases, there are G1 and G2 gap phases in which the cell prepares for the coming S or M phase. There also exists a G0 cell state where the cell reversibly exits from cycling to a quiescent state. DNA replication and segregation defects are associated with tumorigenesis, therefore intrinsic cell cycle checkpoints play an important role in maintaining genome stability (Molinari 2000).

The cell cycle is carefully controlled through a series of cyclin-dependent kinases (Cdks) in association with their regulatory cyclin binding partners. Cyclins are synthesised and degraded in a cyclic manner during the cell cycle (Fig. 1.1). Cyclins bind their Cdk partners, which act as the catalytic subunits to mediate cell cycle progression. Cdk activity facilitates the transition from one cell cycle stage to the next via phosphorylation of target proteins on serine and threonine residues (Satyanarayana and Kaldis 2009).

In G1, the cell prepares machinery to duplicate the cell contents before entry into S phase. There is also the possibility to exit the cell cycle for an indefinite length of time in response to external stimuli. Cell cycle re-entry is triggered upon mitogenic stimulation and cyclin D bound to Cdk4 or Cdk6 initiates the transcription of E2F-regulated cyclin A and cyclin E in addition to other cell cycle progression proteins. Cyclin E in cooperation with Cdk2 induces further transcription of E2F, thus transitioning to S phase. Cdk2, in conjunction with cyclin A, phosphorylates proteins required for DNA replication in S phase, allowing the duplication of the genetic material of the cell (Malumbres and Barbacid 2005).

Cyclin A/Cdk2 activity remains high for the duration of S phase and for most of G2 before decreasing as the cell transitions from the prophase to prometaphase stages of mitosis (M phase). Chromosome condensation occurs in prophase and the centrosomes begin to migrate to opposite poles of the cell. Nuclear envelope breakdown (NEBD) and centrosome-chromatin attachments begin to form via microtubule attachment to kinetochores in prometaphase. The chromosomes then

align between the centrosomes and form the metaphase plate, followed by anaphase where the chromatids separate and are pulled towards the centrosomes. The nuclear envelope is re-established and chromosomes start to decondense in telophase before cytokinesis separates the two new daughter cells (Hunt and Kirschner 1993).

Cdk1 activation via cyclin A is required for initiation of prophase and later cyclin B-dependent activation of Cdk1 is induced by Cdc25 phosphatase to promote chromosome condensation, NEBD and spindle assembly in prometaphase. The anaphase promoting complex/cyclosome (APC/C) rapidly degrades cyclin B after all kinetochores have attached to the bipolar spindle at the metaphase-to-anaphase transition resulting in a sharp decrease in Cdk1 activity. Cyclin-mediated activation of Cdk proteins regulates cell cycle progression. Cells can control the rate of cell cycle progression to deal with stress or DNA damage through degradation and inhibition of cyclins (Hochegger *et al.* 2008).

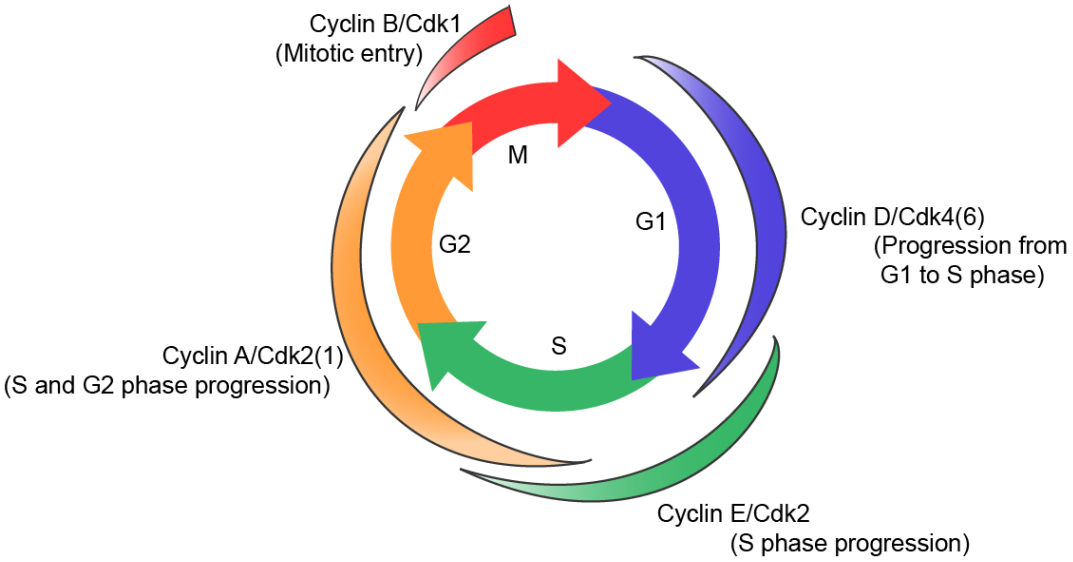

Figure 1.1: The cell cycle and cyclin/Cdk activity. G1 exit is facilitated by a decrease in cyclin D/Cdk4 activity, with cyclin E/Cdk2 taking over to promote S phase initiation. Cyclin A/Cdk2(1) drives S and G2 phase followed by cyclin B/Cdk1-mediated control of mitosis. Curved segments indicate the increases and decreases in cyclin/Cdk activation state.

1.2 DNA damage

Cells are exposed to agents that attack the structure and integrity of their DNA at such a rate that 10^4 DNA lesions are encountered in a cell per day (Martin *et al.* 1985, Lieber and Karanjawala 2004). The most potent threats to DNA stability are UV (ultraviolet) light, ionising radiation (IR), oxidative stress and genotoxic substances. DNA lesions resulting from distortions to individual bases in the DNA sequence are generally repaired quite efficiently and accurately by base excision repair (BER) and nucleotide excision repair (NER) pathways (Lieber 2010, Kamileri *et al.* 2012, Wallace *et al.* 2012). The DNA replication process can also incorporate errors into the genome that require repair by direct excision during replication or by mismatch repair after the strands are released by the polymerase (Martin *et al.* 2010). IR is one of the strongest methods of introducing DNA damage and can trigger the entire cellular complement of cell cycle checkpoints to repair single and double stand breaks by DNA repair pathways (Nakajima *et al.* 2015).

1.2.1 Single strand breaks

Single strand breaks (SSBs) are detected by members of the phosphatidylinositol 3-kinase like protein kinase (PIKK) family which include ATM (ataxia telangiectasia, mutated), ATR (ataxia telangiectasia and Rad3 related) and DNA-PK (DNA dependent protein kinase) protein kinases (Liu *et al.* 2006). Although ATM and DNA-PK can localise to SSBs after they have been converted to double strand breaks, it is mainly ATR which is responsible for eliciting the damage response from SSBs by activating Chk1 (checkpoint kinase 1) through which the signal is transduced to effector proteins, including Cdc25 (Fig. 1.2) (Shiloh 2003, Zou and Elledge 2003). ATR is recruited to single strands of DNA that are coated in RPA (replication protein A) via the ATR-interacting protein, ATRIP, although ATM and the MRN (MRE11-RAD50-NBS1) complex can initially detect the DNA break and (Brown and Baltimore 2000, Lee and Paull 2005). ATR and ATRIP, together with the Rad17-RFC (replication factor C) complex, recruit Rad9-Rad1-Hus1 (9-1-1) complexes to the DNA break resulting in the activation of Chk1 (Bermudez *et al.* 2003, Niida and Nakanishi 2006). Topoisomerase II DNA binding protein 1 (TOPBP1) is recruited by the 9-1-1 complex and is necessary for complete ATR activation (Ueda *et al.* 2012). Claspin also localises to the SSB site via Rad17, further contributing to the activation of ATR, which phosphorylates Chk1 to induce

checkpoint activation (Chini and Chen 2003).

1.2.2 Double strand breaks

ATM kinase localises to the site of double strand breaks (DSBs). Present in the cell as an inactive homodimer, ATM autophosphorylation on serine 1981 in the presence of DNA damage releases active monomers which phosphorylate target proteins (Bakkenist and Kastan 2003). The recruitment of ATM to DSBs is mediated by the MRN (Mre11-Rad50-Nbs1) complex which acts as a sensor to detect DNA damage and localises to sites of double strand breaks, where it dictates the recruitment of factors necessary for DNA repair (Lee and Paull 2005). The phosphorylation of γH2AX on serine 139 by ATM marks the DNA as a docking site for other DNA damage response (DDR) mediator proteins, such as MDC1 (Mediator of DNA Damage Checkpoint protein 1), resulting in the amplification of the damage signal (Burma *et al.* 2001, Lou *et al.* 2003). MDC1 acts as a scaffold protein stabilised at the DSB by NBS1 and γH2AX which interacts with Rad51 to mediate checkpoint control during homologous recombinational DNA repair (Lou *et al.* 2003). DNA damage mediator proteins 53BP1 (p53 binding protein) and BRCA1 are activated by ATM in response to DSBs. 53BP1 further activates ATM and induces G2/M checkpoint activation to mediate homologous repair of DNA (Liu *et al.* 2006). BRCA1 also activates the G2/M checkpoint and is required by ATM to carry out ATM-specific phosphorylation of p53 in the G1 DNA damage checkpoint (Fabbro *et al.* 2004).

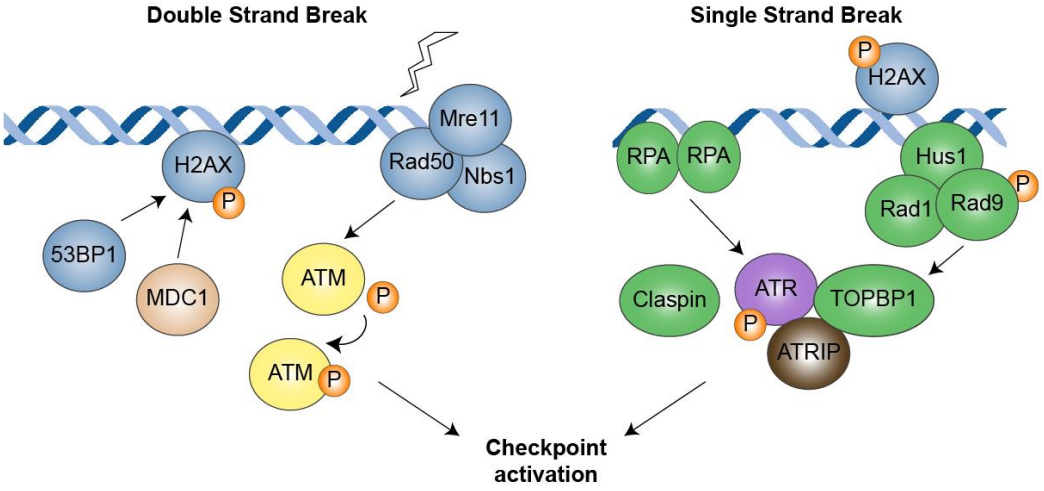

Figure 1.2: Detection of double and single stranded DNA damage. Double strand breaks are detected by the MRN (Mre11-Rad50-Nbs1) complex which recruits and phosphorylates ATM. The presence of γH2AX amplifies the damage signal and allows the recruitment of 53BP1 and MDC1. RPA coated single strand breaks activate ATR via ATRIP and the recruitment of γH2AX and the 9-1-1 (Rad9-Rad1-Hus1) complex. TOPBP1 and Claspin contribute to further ATR activation.

1.3 DNA break repair

Part of the function of DNA damage signalling pathways outlined above is to recruit repair factors to restore the damaged DNA. The repair method employed by the cell depends on the type of DNA lesion and the stage of the cell cycle in which the damage is detected (Bernstein and Rothstein 2009). The two main pathways for dealing with SSBs and DSBs are homologous recombination (HR) and non-homologous end joining (NHEJ) (Fig. 1.5).

1.3.1 Homologous recombination

HR-mediated DNA repair utilises the sequence of the sister chromatid in most cases in order to restore the DNA to its original state. This conservative method of DNA repair is only available when the DNA structure is unwound in S phase before cell division and can be accessed by the factors necessary for repair (Moynahan and Jasin 2010). In general, HR is regulated by Chk1 which has been activated by ATR and, to a lesser extent, ATM (Morrison *et al.* 2000, Wang *et al.* 2004). The recruitment of the MRN complex in cooperation with the Cdk phosphorylation target, the endonuclease CtIP, controls exodeoxyribonuclease 1 (Exo1) 5' to 3' resection of the DNA strands at DS sites (Zhu *et al.* 2008, Huertas and Jackson 2009).

The exposed DNA is then coated in RPA, with RAD51 playing a role in preventing

the formation of DNA secondary structures (Chen *et al.* 2008). RAD51 also facilitates the cross-over of DNA strands to provide a template DNA sequence for repair (Fig. 1.5) (Baumann *et al.* 1996). The interaction between RAD51 and the DNA is assisted by XRCC2, XRCC3, RAD52 and BRCA2, where BRCA2 is involved in transporting RAD51 to the DNA and maintaining the protein in its active form (Sonoda *et al.* 2001, H. Yang *et al.* 2002, Carreira *et al.* 2009, Somyajit *et al.* 2013). The ssDNA binds to the opposite continuous strand in a RAD51-dependent manner and forms a displacement loop (D loop) in a process called strand exchange (Sung and Robberson 1995). After DNA polymerases fill in the gap caused by the break, the resulting Holliday junction is cleaved and resolved by the topoisomerase TOPOIII or BLM (Bloom syndrome protein) or by the endonuclease action of proteins such as GEN1 (Gen homologue, endonuclease 1) (Wu and Hickson 2003, Rass *et al.* 2010). HR prevents the loss of genetic information but at the expense of heterozygosity.

1.3.2 Non-homologous end joining

NHEJ is an error-prone repair mechanism of DNA break repair as there is no DNA template used (Lieber 2010). NHEJ is employed by the cell to repair DNA damage encountered in interphase, when the DNA is in a closed, repressed state, but is also important for V(D)J recombination in immune cells (Takata *et al.* 1998, Gellert 2002). DSB repair can be carried out by HR or NHEJ with the recruitment of the Ku70/Ku80 ring complex by the MRN complex directing the repair towards the NHEJ pathway (Walker *et al.* 2001). Ku70/Ku80 interacts with and activates DNA-dependent protein kinase (DNA-PK), which inhibit DNA resection and promote repair by phosphorylating DNA repair proteins (Gottlieb and Jackson 1993, West *et al.* 1998, Meek *et al.* 2004, Goodarzi *et al.* 2006). XRCC4 bound to DNA ligase IV mediates repair by ligating the broken DNA ends after terminal deoxynucleotidyl transferase (TdT) and resolvase activity extend the DNA (Gu *et al.* 2007, Lieber 2010, Rass *et al.* 2010). The presence of XLF (XRCC-like factor) is thought to aid the ligation of incompatible DNA ends in an attempt to retain all the nucleotides in the sequence (Ahnesorg *et al.* 2006). Artemis interacts with DNA-PKcs to trim the DNA and modify damaged nucleotides (Ma *et al.* 2002). The repair is complete but is generally accompanied by addition or deletion of a small number of bases.

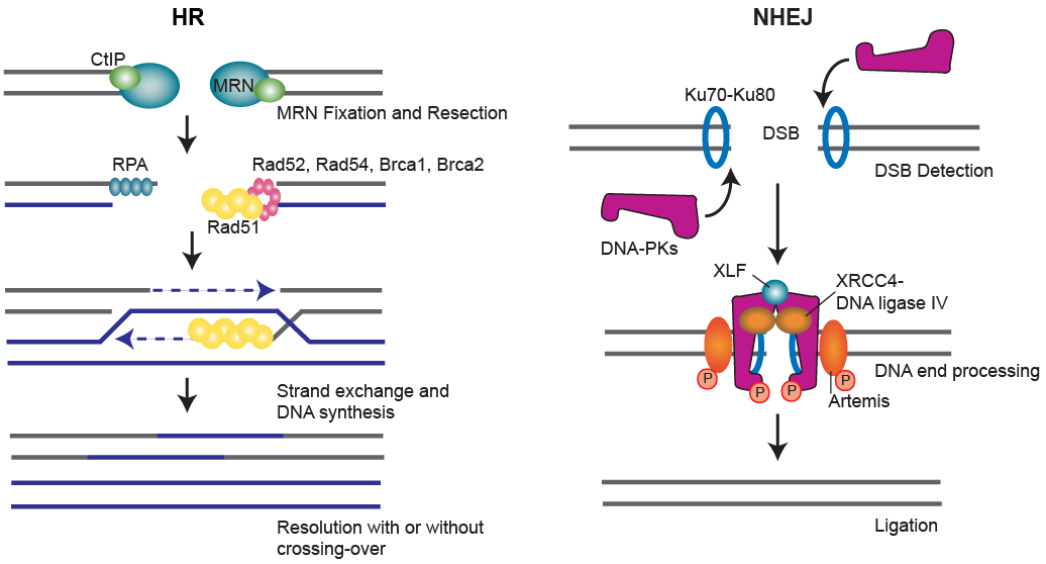

Figure 1.3: Homologous recombination (HR) and non-homologous end joining (NHEJ) DNA repair pathways. DNA repair via HR is detected and resected by the MRN complex and CtIP. Rad proteins mediate the DNA-DNA interaction between the strands before resolution by TOPOIII, BLM and GEN1. Ku protein complex binding at DSBs initiates NHEJ. DNA-PKs facilitate the recruitment of DNA end-processing and ligation factors Artemis, XLF and XRCC4-DNA Ligase IV to repair the DNA. Adapted from (Saito *et al.* 2013).

1.4 DNA damage checkpoints

Maintenance of DNA integrity is regulated at four points in the cell cycle which are coordinated with the stages of the cell cycle. These checkpoints are implemented in response to Chk1 and Chk2 (Checkpoint kinases 1 and 2) activation to ensure the cell cycle is slowed down or halted in order to deal with DNA damage (Abraham 2001). Cell cycle arrest plays an important role in preventing the replication and transmission of damaged DNA into the next cell cycle (Ishikawa *et al.* 2006).

1.4.1 G1 checkpoint

DNA damage occurring in G1 phase of the cell cycle uses the ATM (ataxia telangiectasia, mutated) and ATR (ATM-Rad3 related) pathways to detect DNA breaks and activate Chk1 and Chk2 kinases (Fig. 1.3). ATM/ATR induce the G1 checkpoint through the stabilisation and activation of p53 through phosphorylation on the serine-15, threonine-18 and serine-20 residues of the p53 protein (Chehab *et al.* 1999, Shieh *et al.* 2000, Takai *et al.* 2002, Bartek and Lukas 2003). Chk1 and Chk2 phosphorylate the p53 regulatory protein Mdm2, leading to its inactivation, thus preventing p53 ubiquitination and degradation (Schon *et al.* 2002). Active p53

then induces the transcription of p21, which inhibits cyclin E and Cdk2 to prevent entry into S phase (Harper *et al.* 1995). Chk1-mediated phosphorylation of the cyclin E/Cdk2 activator, Cdc25, also acts to halt the cell cycle in G1 by promoting Cdc25 degradation. The 14-3-3 protein complex recognises the phosphorylation sequence of Cdc25 and binds to the protein, sequestering it in the cytoplasm until the Cdc25 is degraded (Chen *et al.* 2003, Cann and Hicks 2007). Although Chk1 is the main Cdc25 inhibitor, Chk2 also plays a role to enhance Cdc25 degradation enhancing Chk1 activity (Madlener *et al.* 2009). By preventing Cyclin E/Cdk2 activation, the Rb retinoblastoma protein cannot be phosphorylated. The release of E2F transcription factors, which are dependent on Rb phosphorylation, control the transcription of the cyclin A and E genes necessary for S phase initiation. This ultimately results in cell cycle delay by preventing entry into S phase in the presence of DNA damage (Wu *et al.* 1996, Satyanarayana and Kaldis 2009).

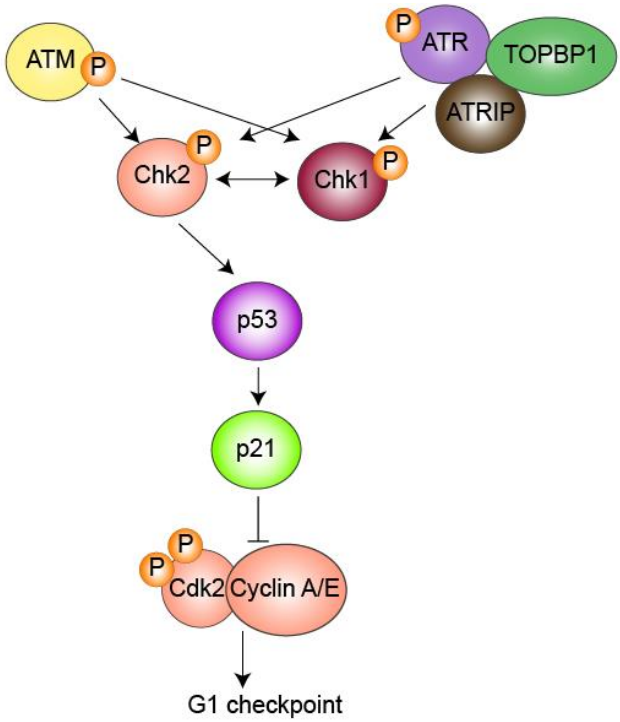

Figure 1.4: The G1 checkpoint activation pathway. ATM and ATR phosphorylate and activate Chk1 and Chk2. Stabilisation of p53 by Chk2 phosphorylation allows transcription of p21 which inhibits cyclin A/E/Cdk2 activation, arresting the cell cycle in G1.

1.4.2 Intra S checkpoint

DNA damage that occurs in S phase or which has slipped through the G1 checkpoint results in damage signalling and repair pathway activation via the damage response

kinases ATM and ATR (Falck *et al.* 2001). DNA lesions and blocked replication forks trigger the intra-S-phase checkpoint, which can slow or halt the rate of DNA synthesis depending on the level of damaged DNA in the cell. The large amount of single stranded DNA (ssDNA) present in S phase determines a preferentially ATR-mediated repair pathway, although ATM can also drive the DDR signal should the single stranded DNA lesions persist and create DSBs (Fig. 1.4) (Zou and Elledge 2003). The intra S checkpoint targets Cdk2 to prevent cell cycle progression via phosphorylation and degradation of Cdc25 (Sorensen *et al.* 2003). Cdk2 is required for replication complex assembly, particularly Cdc45 and DNA polymerase α and therefore can prevent replication from origins of replication that has not already been initiated (Takisawa *et al.* 2000). Inhibition of DNA replication is also prevented in association with the SMC (structural maintenance of chromosomes) complex. ATM and ATR can phosphorylate the SMC1 and SMC3 subunits of cohesin to initiate DNA repair, while ATM phosphorylation of BRCA1 (breast cancer 1), Nbs1 (Nijmegen breakage syndrome 1) and FANCD2 (Fanconi anaemia, complementation group D2) in S phase mediates cell cycle arrest in order to process and repair damaged DNA (Yazdi *et al.* 2002, Sancar *et al.* 2004, Bunting *et al.* 2010, Lossaint *et al.* 2013).

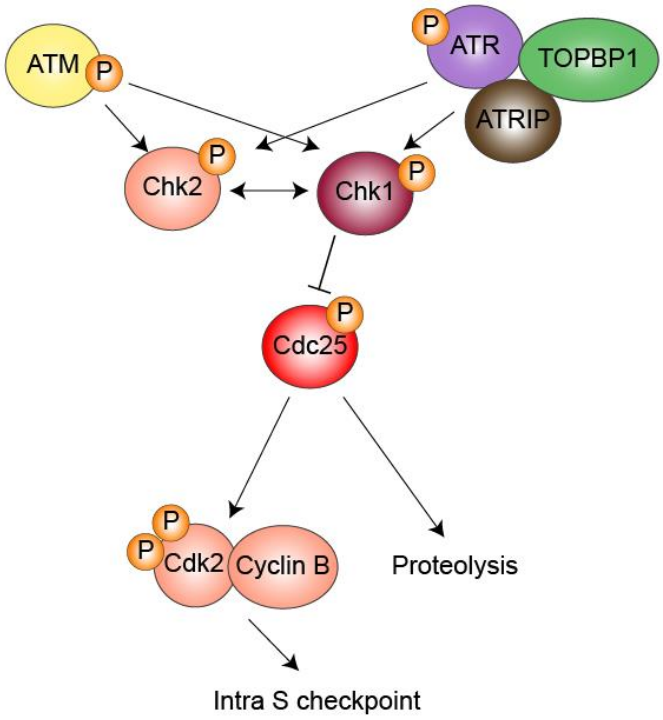

Figure 1.5: Schematic of intra S checkpoint activation pathway. Activation of ATM and ATR regulate Cdc25 phosphorylation via Chk1 and Chk2, leading to degradation of Cdc25 and inhibition of cell cycle progression due to the presence of inactive cyclin B/Cdk2.

1.4.3 G2/M checkpoint

Cdk2/cyclin B is critical for cell cycle progression into mitosis and therefore is the main target for inactivation following DNA damage in G2 (Satyanarayana and Kaldis 2009). DNA lesions that are detected at the end of G2 phase bring about the G2/M checkpoint. Activated Chk1, Chk2 and p53 resulting from ATM and ATR phosphorylation, induce p21 and 14-3-3 complex activity (Shaltiel *et al.* 2015). p21 inhibits cyclin A/Cdk2 and cyclin D/Cdk4(6) complexes that in turn inhibit E2F which results in the down regulation of the Cdk1, cyclin A, cyclin B1 and cyclin B2 genes (Harper *et al.* 1993, Harper *et al.* 1995). Transcription of the 14-3-3 complex, in combination with p21, inhibits and sequesters the Cdk2/cyclin B1 complex in the cytoplasm (Taylor and Stark 2001). Cdk2/cyclin B1 is also inhibited through Cdc25 activation by Chk1 and Chk2 (Sorensen *et al.* 2003). Wee1 and Myt1 are important for the regulation of Cdk proteins and Chk1 is responsible for stabilising Wee1 in order to phosphorylate and inhibit Cdk1 activity in G2 (Ayeni and Campbell 2014).

1.4.4 Spindle assembly checkpoint

The spindle assembly checkpoint regulates the metaphase-to-anaphase transition by blocking the progression of mitosis until all kinetochores have formed correct microtubule attachments. It is important that the cell avoids the unequal division of chromosomes due to the resulting aneuploidy and genetic disorders from missing/extra chromosomes in daughter cells (Kops *et al.* 2005). The APC/C complex is responsible for the separation of chromosomes at anaphase by mediating the degradation of separase-bound securin and cyclin B/Cdk1 inactivation (King *et al.* 1995, Ciosk *et al.* 1998, Nasmyth 2001). Active separase cleaves the cohesin ring complex and allows the separation of the chromosomes (Ciosk *et al.* 1998, Peters 2006). Removal of cyclin B and subsequent Cdk1 inactivation facilitates the progression of the cell cycle, permitting the transition from metaphase to anaphase.

Misaligned kinetochore attachments attract proteins that comprise the mitotic checkpoint complex (MCC); MAD2, BUBR1, Cdc20 and BUB3 (Skoufias *et al.* 2001, Sudakin *et al.* 2001, Johnson *et al.* 2004). The recruitment of the MCC complex at sites of unattached kinetochores activates its MAD2 subunit via a

conformational change induced upon MAD1 binding (Luo *et al.* 2002). MAD2 then associates with Cdc20, and also promotes BUBR1-BUB3-Cdc20 complex formation, to inhibit the activation of the APC/C by mediating Cdc20 ubiquitination and degradation (Fang *et al.* 1998, Sironi *et al.* 2001). The BUBR1-BUB3-Cdc20 complex mediates Cdc20 removal in addition to occupying the APC/C substrate binding site (Herzog *et al.* 2009, Chao *et al.* 2012). APC/C regulation of the SAC, to ensure the bi-orientation and attachment of chromosomes before anaphase, prevents aberrant chromosome segregation (Kops *et al.* 2005).

1.5 The centrosome

Described by Theodor Boveri at the turn of the 19th century, the centrosome is now known to be the main microtubule organising centre (MTOC) in animal somatic cells. The centrosome was originally identified in sections of early sea urchin and *Ascaris* embryos stained with iron haematoxylin as a dense concentration of molecules that appeared darker than the surrounding matrix. Boveri documented a specific localisation pattern of the mass during cell division which intrigued his curiosity. He was interested in the possible function of these accumulations and created detailed sketches of sea urchin cells in various mitotic stages of the cell cycle (Boveri 1887). Although investigations lay dormant for many years in the century that followed, his early research initiated the snowball effect of interest and dedication in studying the roles of the centrosome in the cell. Today, we count over 6000 papers in this field (source: PubMed).

In the 1960s and 70s, the invention of electron microscopy facilitated the detailed resolution of centrosome structure. The work of Sergei Sorokin laid the foundation of investigations into the arrangement of centrosome proteins, based on his initial sketches depicting the nine-fold radial symmetry of the centriole barrels and the pathways for the formation of primary cilium (Sorokin 1968a, Sorokin 1968b). We now know that the centrosome is composed of two centrioles, each one comprised of nine sets of microtubule triplets arranged in a barrel shape, surrounded by a set of large coil-coiled proteins collectively named the pericentriolar material (PCM, Fig. 1.6). The microtubules confer a polarity on the centrioles. The stabilised minus ends of the α- and β-tubulin polymers are referred to as the proximal end of the barrel,

while the microtubule plus ends are termed centriole distal ends, where the microtubule triplets taper to doublets (Luders and Stearns 2007).

The two centrioles are maintained in close proximity to one another via an intercentriolar linker (Fig. 1.6). The linker connects the proximal ends of the centrioles through a combination of fibrous proteins anchored at the centriole by a small number of scaffold proteins such as C-NAP1 (centrosomal Nek2-associated protein 1) (Mardin and Schiebel 2012). The structure of the surrounding PCM remained unclear for many years. Only recently, it was revealed to be a highly organised cylindrical arrangement of Cep 120, Cep192, Cep152, Cdk5Rap2, NEDD1 (neural precursor cell expressed, developmentally down-regulated 1) and TUBG1 (γtubulin). These proteins form a layered effect by encircling the centriole, with PCNT (pericentrin) threading the layers from the centriole wall through to the intracellular space (Dictenberg *et al.* 1998, Fu and Glover 2012, Lawo *et al.* 2012, Mennella *et al.* 2012, Sonnen *et al.* 2012). The PCM is an important site of γTuRC (γ-tubulin ring complex) anchoring. γTuRCs are the structures responsible for nucleating microtubules (Bettencourt-Dias and Glover 2007). The two centrioles that make up a single centrosome differ in their protein composition. The mature centriole, also called the mother centriole, is distinguished by its distal and subdistal appendages whereas the less mature "daughter" centriole lacks these extra proteins. The appendage proteins are crucial for cilium anchoring and assembly, which occur during withdrawal from the cell cycle in G0 (Jana *et al.* 2014). In addition to the PCM, the centrosome is surrounded by centriolar satellites that have the large PCM1 protein at their core. Centriolar satellites, however, are not as tightly associated around the centrosome as the PCM, but are critical during the formation of primary cilia (Dammermann and Merdes 2002).

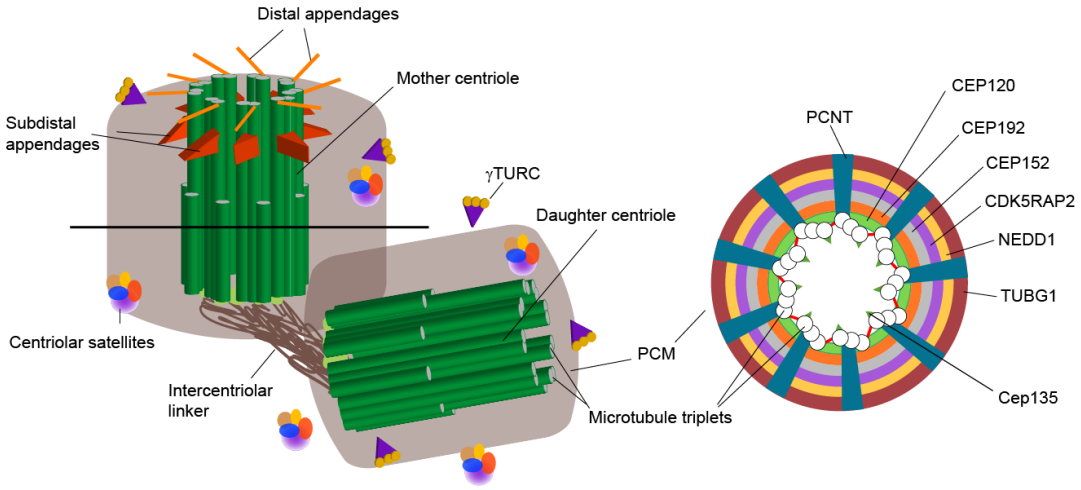

Figure 1.6: Centrosome, centriole and PCM structure. Schematic view of the centrosome shows the two centrioles in close proximity tethered via an intercentriolar linker. The mother is distinguished by the presence of distal and subdistal appendages. The pericentriolar material (PCM) surrounds the microtubule barrels with embedded γTURC complexes and centriolar satellites. A detailed through section of the PCM indicated by the black line (left) can be seen on the right. Adapted from (Bettencourt-Dias and Glover 2007, Kitagawa *et al.* 2011, Lawo *et al.* 2012).

1.6 Functions of the centrosome

1.6.1 Microtubule nucleation

Centrosomes are present in most higher eukaryote species, where they function in organising microtubules during cell division. Lower eukaryotes and plants lack centrosomes, although this does not confer any apparent disadvantage at the cellular level. In yeast, the role of the centrosome is completed by a functionally equivalent spindle pole body (SPB) apparatus (Luders and Stearns 2007). The centrosome is responsible for the nucleation of most cellular microtubules by initiating *de novo* microtubule formation. Microtubule nucleation is the initiation event in which α- and β-tubulin dimers interact to form microtubule polymers. The γTuRC complexes embedded in the PCM nucleate polymerisation of α and β tubulin heterodimers into microtubules. In lower organisms, γTuSC (γ-tubulin small complex) assemblies composed of two γ-tubulin subunits, GCP2 and GCP3 (γ-tubulin complex proteins 2 and 3) are sufficient to nucleate microtubules (Bettencourt-Dias and Glover 2007). In higher eukaryotes, the γTuRC complexes are composed of a number of γTuSCs with associated GCP4, GCP5 and GCP6 proteins, and are required to assemble and stabilise tubulin molecules. The γTuRCs mould α- and β-tubulin heterodimers into a

hollow cylinder, restricting the dynamic instability (the dynamic lengthening and shortening of spindle microtubules) at the minus end and keeping microtubules in an aligned position (Lin *et al.* 2015).

Centrosomal microtubules are anchored through the subdistal appendage protein ninein and γ-tubulin-binding protein NEDD1 (Delgehyr *et al.* 2005, Manning *et al.* 2010). Centriolar satellites play a role in supplying microtubule anchorage proteins via the PCM-1 scaffold protein through indirect interaction with the microtubule motor protein attachment factor dynactin, a function which is counteracted by katenin, a microtubule severing protein. The coordination of the activities of these microtubule stabilisation and destruction factors mediates the remodelling of cellular microtubules throughout the cell cycle (Dammermann and Merdes 2002, Quintyne and Schroer 2002, Bettencourt-Dias and Glover 2007). Polo-like kinases (Plks) and Aurora-A promote microtubule nucleation, whereas protein phosphatase 1 (PP1), PP2A and BRCA1 act in an inhibitory manner to regulate recruitment of γ-tubulin and other assembly factors (Tournebize *et al.* 1997, Blagden and Glover 2003, Marumoto *et al.* 2005, Sankaran *et al.* 2007).

Although the centrosome has a high capacity for microtubule nucleation, the Golgi apparatus has also emerged as a microtubule nucleator. The Golgi acts as a microtubule organiser by anchoring γTuRCs at the centrosome via AKAP450 and Cdk5Rap2, which are bound to the Golgi membrane (Takahashi *et al.* 1999, Wang *et al.* 2010). The particular organisation of the microtubule network acts as a highway for protein trafficking as well as cell mobility. Through the sliding action of kinesin microtubule motor proteins and dyneins, cellular cargo is transported in the cytoplasm. In addition, the positioning of the centrosome in coordination with cellular polarity directs cell movement by forcing microtubules to extend in the desired direction in response to stimulatory extracellular signals. This specific localisation pattern is severely hindered by disruption of the Golgi-centrosome association (Hurtado *et al.* 2011).

Furthermore, the centrosomal influence on cell shape facilitates cellular mobility via microtubules that direct vesicles towards the leading edge of the cell (Wade 2007, Petrie *et al.* 2009, Kushner *et al.* 2014, Panic *et al.* 2015). The control of centrosome number has also been shown to be necessary for cellular adhesion. This is supported

by the finding that the formation of supernumerary centrosomes in cancerous cells results in the increased capacity for metastasis, due to changes in normal cell-cell adhesion processes (Godinho *et al.* 2014).

1.6.2 Cell division

Boveri first documented the participation of centrosomes in mitosis. Since that time, it has been established that the centrosomes organise the mitotic spindle apparatus - a subcellular structure comprising microtubules and many proteins - which separates chromosomes at anaphase of the cell cycle. Spindle poles at centrosomes function as anchor points in prophase from which the bipolar spindle can be assembled. The centrosomes organise an array of microtubule asters which extend in radial arrangement from the γTURC complexes anchored in the PCM. Microtubules that grow towards the cell membrane function to position the centrosome relative to the cell membrane and help define the cleavage plane during cytokinesis, whereas the microtubules which extend inwards seek contact with the chromosomes (Khodjakov *et al.* 2000, Kiyomitsu and Cheeseman 2012). Kinetochores act as microtubule attachment sites on sister chromatids and anchor a network of microtubules called k-fibres (kinetochore fibres) which extend into the cytoplasm (Rieder 1981). In addition, microtubule filaments produced by the chromosome arms also stretch outward from the condensed DNA (Rieder *et al.* 1986). The overlap and interaction of these microtubule fibres and associated proteins allow the alignment of the metaphase plate where the chromatin is positioned in the middle of the two spindle poles.

Two models have been proposed for the method by which the mitotic spindle aligns correctly, a ‘search-and-capture’ model and a ‘chromatin stabilisation’ model. The ‘search-and-capture’ model centres on the ability of proteins bound to the plus ends of microtubules, namely CLIPs (cytoplasmic linker proteins), CLASPs (CLIP-associating proteins), dynein/dynactin and EB1 (an APC-interacting protein), which stabilise the microtubules and can facilitate the association of plus ends of different microtubule fibres (Kirschner and Mitchison 1986, Akhmanova *et al.* 2001, Komarova *et al.* 2002, Mimori-Kiyosue and Tsukita 2003).

The ‘chromatin stabilisation’ model utilises Ran GTPase as its main effector. At the onset of mitosis, cyclin B/Cdk1 is activated at the centrosome and can phosphorylate

the guanine nucleotide exchange factor RCC1 (Regulator of Chromosome Condensation 1) (Jackman *et al.* 2003, Hutchins *et al.* 2004). RCC1 catalyses the exchange of GDP for GTP to activate Ran GTPase, allowing microtubule aster growth which promotes microtubule spindle assembly in the cytoplasm (Bischoff and Ponstingl 1991, Kalab *et al.* 1999). Importins also play a role in spindle formation by releasing spindle assembly factors, such as centrosomal protein TPX2, from their importin-α and -β-bound inhibitory complexes (Gruss *et al.* 2001, Wiese *et al.* 2001). Importins also assist in nuclear membrane reassembly following chromosome segregation (Harel *et al.* 2003).

The microtubule network created allows the chromatids to be pulled apart using both lateral attachment of microtubules to the kinetochores and by end-on attachment of plus end microtubules from the kinetochore and the centrosome, where the dynein motor protein facilitates the transport of the chromosome to the spindle poles by a pulling mechanism (Wollman *et al.* 2008, Joglekar *et al.* 2010, Kops *et al.* 2010, Magidson *et al.* 2011). Dynamic instability of the microtubules plays a role in chromosome segregation where the depolymerisation of microtubules comprising the k-fibres causes the kinetochores to be pulled towards the spindle poles, termed the 'Pac-Man' mechanism (Mitchison and Kirschner 1984, Rieder and Salmon 1998). Microtubule flux, where the tubulin heterodimers are shed from the minus end of the microtubule, also contributes to the process of chromosome segregation and is predominantly used by lower eukaryotes (Gorbsky and Borisy 1989, Kline-Smith and Walczak 2004).

The Polo-like kinase, Plk1, is a serine/threonine kinase necessary for this nucleation capacity. Plk1 is required for recruiting γTURC complexes to the centrosome to mediate bipolar spindle assembly (Archambault and Glover 2009). Plk1-dependent phosphorylation of Nlp (ninein-like protein) after centrosome separation, as part of the centrosome maturation process, allows Aurora A and Kizuna recruitment to the spindle poles (Casenghi *et al.* 2003, De Luca *et al.* 2006, Oshimori *et al.* 2006, Barr and Gergely 2007). This directs the nucleation of microtubules and the formation of focused spindle poles by maintaining PCM integrity which is dependent on the Plk1 substrate, Kizuna (Oshimori *et al.* 2006). Later on, during prophase, Plk1 facilitates the removal of cohesin from the chromosomes, but protects centromeric cohesin by regulating the APC/C (anaphase-promoting complex) through inhibition of EMI1

(early mitotic inhibitor 1) (Sumara *et al.* 2002, Hansen *et al.* 2004).

The kinetochores play a role in monitoring the formation of correct chromatin attachments (Cheeseman and Desai 2008). Plk1 also plays a role in the spindle assembly checkpoint (SAC) by interacting with BUBR1 to ensure that sister chromatids are not separated before the formation of stable kinetochore attachments at each chromosome (Elowe *et al.* 2007). The SAC ensures the integrity of the centrosome and bipolar spindle via Mad2-Cdc20 interaction with kinetochores (section 1.2.4) (Luo *et al.* 2002).The cleavage furrow pinches the cell membrane to leave a single interconnecting bridge called the midbody, before being resolved to form two individual daughter cells. It has been reported that the centrosome containing the older of the centrioles plays a role in the resolution of the midbody structure by briefly localising to the microtubule bundles that link the two daughter cells (Piel *et al.* 2000).

The role and necessity of centrosomes has been addressed in various systems. Laser ablation studies of the centrosomes in vertebrates showed that, in the absence of centrosomes, cells were still able to form a bipolar spindle but displayed a higher cytokinesis failure rate (Khodjakov and Rieder 2001). Evidence for the ability of chromosomes and associated microtubule motors to organise a mitotic spindle in different cell types and organisms is also present (Karsenti and Vernos 2001). In chicken DT40 cells, the knockout of *CEP152* and *STIL*, genes essential for centriole assembly, resulted in chromosomal instability and aneuploidy, demonstrating the necessity for centrioles in the maintenance of genomic stability (Sir *et al.* 2013). In contrast, plant cells and adult cells from the *Drosophila melanogaster* fruit fly lacking centrosomes can undergo normal cell division (Basto *et al.* 2006). Recently, the importance of centrosomes in human cells was further confirmed using the Plk4 inhibitor centrinone, which induced an irreversible p53-dependent cell cycle arrest in G1, independently of DNA damage or DNA replication errors (Wong *et al.* 2015).

The most notable evidence for the essential role of centrosomes in mammalian cells comes from *SAS-4* (spindle assembly defective-4) null mouse embryo studies. Embryos survive until the midgestation stage of development without centrosomes. However the cells exhibit defective Hedgehog (Shh) signalling due to the absence of cilia. A prolonged delay in spindle assembly results in the activation of a cell cycle checkpoint, from which a p53-dependent apoptotic cell death pathway ensues (Bazzi

and Anderson 2014). Similarly in mice without the centriole replication protein *STIL*, embryo development is arrested at gastrulation (David *et al.* 2014). Due to the role of centrosomes in maintaining genome integrity, and organising efficient and rapid assembly of microtubules in mitosis, centrosomes are considered to be critical organelles for cell division in mammalian cells.

1.6.3 Cilia formation

Cilia are extensions of the mother centriole which protrude from the cell into the extracellular space and have roles in signal transduction and cellular motility. Two types of cilia have been identified and are formed via slightly different pathways. The primary cilium is a signalling organelle found on most types of human cells. Motile cilia are found on specialised cell types such as the lining of the airways and the oviduct, and are responsible for fluid flow over epithelial layers. Flagella are a type of motile cilium found on motile cells such as spermatozoa, and are necessary for movement of single cells. The structures of cilia differ in that the barrel of microtubule doublets in primary cilia is accompanied by an additional pair of microtubules in the central lumen of motile cilia and flagella, which confers motility to these types of cilia (Nachury 2014). The microtubule-based structures inside cilia and flagella are known as the axoneme. Specialised regions of the ciliary membrane contain receptors for Wnt, Hedgehog and PDGF (platelet derived growth factor) signalling pathways, which are responsible for transmitting signals relating to cell proliferation and differentiation (Schneider *et al.* 2005, Wallingford and Mitchell 2011, Vuolo *et al.* 2015).

The ability of the mother centriole to dock with ciliary vesicles and extend centriolar microtubules at the proximal end of the centriole in the formation of cilia is one of the main reasons centrosomes are critical organelles in eukaryotic cells. Upon exit from the cell cycle through deprivation of nutrients, response to signals from external sources, or serum starvation of cells in culture, the proximal end of the mother centriole can fuse with cellular vesicles and form a cilium by extending into the extracellular space (Sorokin 1968a). The centrosome is now referred to as the basal body, with the subdistal appendages becoming the basal foot that anchors the cilium in the cell. The distal appendages make up the transition fibres between the basal body and the ciliary pockets that are located at the base of the cilium.

The cilium is also anchored in the cell by the striated rootlet, which is comprised of rootletin and other fibrous linker proteins (J. Yang *et al.* 2002, Kim and Dynlacht 2013). Intraflagellar transport (IFT) complexes IFT-A and IFT-B bind tubulin and other cofactors to be transported by the microtubule motor protein kinesin 2 to the tip of the cilium to facilitate their incorporation into the axoneme. This anterograde tubulin transport is counteracted by retrograde transport of IFT complexes mediated by dynein during cilium disassembly (Satir *et al.* 2010). Cilia generally grow to 3-5μm in length, with the basal body remaining just 0.5μm long. Maintenance of cilium length within this range is important for IFT transport rate and for signalling pathways initiated at the cilium (Broekhuis *et al.* 2014).

As mentioned previously, *Drosophila* do not require centrioles in adulthood, but they rely on them to make neuronal axonemes during development, illustrating the importance of cilia in sensory neuron formation (Basto *et al.* 2006). Cilia are produced in bulk via deuterosomes, which are dense gatherings of centrosome proteins, including Cep152, Plk4, and SAS6, necessary for canonical centrosome duplication (Klos Dehring *et al.* 2013). Numerous centrioles cluster at these deuterosomes during growth before they are released into the cytoplasm and dock at the cell membrane (Zhao *et al.* 2013).

Cilia are important for photoreceptor cells, with the ciliary rootlet structure contributing to the function of these cells by increasing in size from its normal length of a few micrometers to span the entire length of the cell (J. Yang *et al.* 2002). Mutations in genes that encode proteins necessary for cilia assembly and function result in human disorders and syndromes such as Bardet-Biedl syndrome, Joubert syndrome and Meckel-Gruber syndrome, and are collectively known as ciliopathies (Nigg and Raff 2009). Centriolar satellite protein depletion results in phenotypes which are indicative of defective cilium structure and in turn affect the signalling pathways stimulated by the cilium (Tayeh *et al.* 2008, Ferrante *et al.* 2009, Baye *et al.* 2011, Chavali *et al.* 2014).

Primary effects of the neurodevelopmental disorder microcephaly result from mutations in centriole duplication genes, including *CPAP*, *Cep152*, *STIL* and *Cep135*, in addition to *MCPH1* mutations which compromise the DNA damage response, DNA repair, and cell cycle checkpoint transitions (Lin *et al.* 2005, Gilmore and Walsh 2013). Efficient formation of the primary cilium also requires these

proteins, and in the case of microcephaly, delay or defects in the formation of the primary cilium could be one of the factors contributing to impaired development of the cerebral cortex, due to the role of the cilium and ciliary proteins in neurogenesis via the Shh and Wnt signalling pathways (Tasouri and Tucker 2011, Wallingford and Mitchell 2011, Paridaen *et al.* 2013).

1.6.4 Cellular signalling

As described above, cilia are a central feature in cellular signal transduction in development and proliferation. Other components of the centrosome are important for intercellular signalling, such as the PCM and various appendage and centriolar structural proteins. The centrosome is the site for Plk1-mediated activation of cyclin B-Cdk1 by phosphorylation and activation of Cdc25 phosphatases, and inhibition of the kinases Wee1 and Myt1 (Watanabe *et al.* 2004, Inoue and Sagata 2005, Archambault and Glover 2009). The Plk1 phosphorylation of Cdc25 is regulated by the upstream activation of Plk1 by Aurora A which has been shown to promote nuclear envelope breakdown (Macurek *et al.* 2008). Centrosome function in the cell cycle also extends to cytokinesis and cell abscission at the end of mitosis, where the centrosome itself, in addition to centrosome proteins centrolin and Cep55, has been reported to localise to the midbody (Piel *et al.* 2001, Arquint *et al.* 2014).

The PCM protein, pericentrin, has most recently been shown to respond to DNA damage-induced Chk1 activation by altering its normally toroidal structure, which may act as a subsequent signal from the centrosome to propagate the DNA damage response (DDR) (Antonczak *et al.* 2015). Other DDR proteins have been reported to localise to the centrosome during mitosis. ATM, ATR, Chk1 and Chk2 all displayed co-localisation with γtubulin during metaphase, which was more pronounced when the cells were treated with an inhibitor of the DDR kinase DNA-PK (Zhang *et al.* 2007). Of particular interest is the Plk1-mediated phosphorylation of Chk2 at the centrosome (Tsvetkov *et al.* 2003). Alluding to the role of centrosomes in the DDR, the theory of a centrosome inactivation checkpoint has been proposed, although compelling evidence for such a checkpoint is lacking (Loffler *et al.* 2006).

Centrin and Cep164 are two centrosomal proteins displaying additional roles, distinct from their function in centrosome organisation. Cep164 is a distal appendage protein involved in ciliogenesis, which has been shown to play a role in the G2/M

checkpoint by localising to the sites of DNA damage via ATM/ATR (Chaki *et al.* 2012). The calcium-binding protein centrin, which localises to the lumen of the centrioles, has been implicated in DNA repair in the nucleus. Acting as a cofactor in stabilising XPC (Xeroderma Pigmentosum C), centrin 2 is involved in detection of bulky DNA lesions in the early steps of the nucleotide excision repair pathway (Araki *et al.* 2001).

Centrosomes also play a role in T lymphocytes, where they are involved in the formation of the immune synapse. The ability of the centrosome to create different cell polarisation states facilitates the generation of a highly polarised region at the cell membrane, and gives rise to the site of the immune synapse (Stinchcombe *et al.* 2011, Yi *et al.* 2013). This facilitates the secretion of cytokines in cytotoxic T-lymphocytes from secretory clefts which are similar to ciliary pockets formed on either side of the primary cilium (Stinchcombe *et al.* 2001, Stinchcombe and Griffiths 2014).

1.7 The centrosome cycle

1.7.1 Overview of the centrosome cycle

The centrosome duplication cycle is a semi-conservative process, much like the replication of DNA (Fig. 1.7). The cell must ensure that the centrioles are duplicated only once per cell cycle to allow faithful segregation of the chromosomes (Mardin and Schiebel 2012). The centrosome cycle can also be divided into four stages that co-ordinate with the stages of the cell cycle: *i)* centriole disengagement (late mitosis/G1), *ii)* centriole duplication (S phase), *iii)* centrosome disjunction (late G2), and *iv)* bipolar spindle assembly (mitosis), depicted in Fig. 1.7. Centriole disengagement occurs after cytokinesis at the end of mitosis and is a relaxing of the tight orthogonal arrangement of the centrosome. The dissolution of an intercentriolar "stalk" by the combined action of Plk1 and the protease separase, and the association of linker proteins C-NAP1 and rootletin with centrioles facilitate a more flexible centrosome structure (Tsou and Stearns 2006b, Nigg 2007, Wang *et al.* 2008). Disengagement is a key licensing step to permit centrosome duplication in the following cell cycle. Plk1 plays a pivotal role in the duplication process by regulating centriole maturation (Lane and Nigg 1996, Wong and Stearns 2003). The

centrosome is then duplicated during S phase to produce two new daughter centrioles (procentrioles) from the pre-existing mother and daughter centrioles (Fong *et al.* 2014).

When the assembly and elongation of procentrioles in a site adjacent to the pre-existing centrioles is complete, the intercentriolar linker is removed (Fig. 1.7) through the phosphorylation of C-Nap1 and rootletin by Nek2 (NIMA-related kinase) (Fry 2002, Mayor *et al.* 2002, Bahe *et al.* 2005). This process is termed disjunction, with the now separated centrosomes free to migrate to opposite poles of the cell through a push-pull mechanism, anchored on the microtubule network of the cell, and directed by the kinesin and dynein microtubule motor proteins (Sawin and Mitchison 1995, Florian and Mayer 2012). Following nuclear envelope breakdown (NEBD), the centrosomes organise the microtubules of the cell into a bipolar spindle by nucleating γTURC complexes embedded in the PCM (Wiese and Zheng 2000, Luders and Stearns 2007). The microtubules then attach to the kinetochores of the chromosomes and force the chromosomes apart, pulling the sister chromatids to opposite ends of the cell (Section 1.6.2).

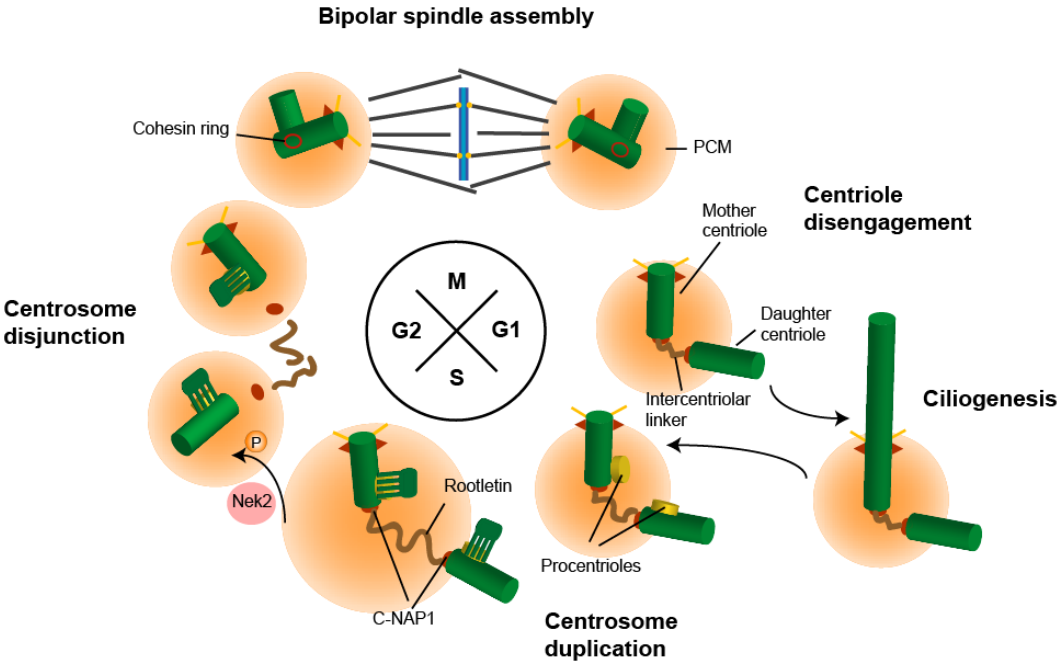

Figure 1.7: The centrosome duplication cycle. Dissolution of the cohesin ring structure at the end of M phase (centriole disengagement) licences procentriole formation. PCM expansion and centriole elongation in centrosome duplication precedes centrosome disjunction (G2 phase) which is mediated by Nek2 phosphorylation facilitates bipolar spindle formation in mitosis. The centrosome can exit the cell cycle to form a primary cilium in G1. Adapted from (Wang *et al.* 2014).

1.7.2 Centriole disengagement

The centrosome is held in position by the bipolar spindle until the later stages of mitosis, but the centrioles are also in a tightly fixed position. The identification of key proteins maintaining this orthogonal structure led to the conclusion that there are two mechanisms by which centrioles can attain a state where the daughter centriole is free to move in the cytoplasm, while still remaining attached to the mother centriole (Piel *et al.* 2000). The first mechanism implicates the chromatid cohesion complex, cohesin, as the interconnecting molecule between the mother and daughter centrioles (Schockel *et al.* 2011). A centrosomal fraction of the cohesin subunit Scc1 was identified by Nakamura *et al.* in fractionation experiments using a sucrose gradient (Nakamura *et al.* 2009). Since it is well known that separase is the protease responsible for cleavage of chromatin-bound cohesin, it was not surprising when separase was also found to localise to the centrosome (Agircan and Schiebel 2014). Securin- and cyclin B-Cdk1-mediated inhibition of separase prevent centrosome disengagement until the activation of APC/C at the end of mitosis. The activated APC/C targets securin and cyclin B for proteasomal degradation via polyubiquitylation, resulting in separase activation (Gorr *et al.* 2005, Peters 2006, Tsou and Stearns 2006b). In addition, other proteins present at centrosomes, including astrin and Aki1 have been shown to regulate separase function (Thein *et al.* 2007, Nakamura *et al.* 2009). Recently the PCM protein kendrin (also known as pericentrin B) was shown to be cleaved by separase at the centrosome and to be involved in centriole disengagement (Lee and Rhee 2012, Matsuo *et al.* 2012).

Plk1 phosphorylation of a centrosomal shugoshin isoform is a second mechanism regulating centriole disengagement (Tsou *et al.* 2009). Plk1 is an important centrosome-localising protein for a spliced version of the chromatid cohesion protein shugoshin, sSgo1 (small shugoshin), which maintains centrosome cohesion in mitosis (Wang *et al.* 2008). Although the exact mechanism by which sSgo1 prevents premature centrosome disengagement is as yet unclear, it was shown that inhibition of Plk1 prevents centriole disengagement by disrupting sSgo1 localisation (Wang *et al.* 2008). Plk1 may also be involved in the separase-mediated cleavage of cohesin by modifying Scc1 to favour separase binding (Sumara *et al.* 2002, Hauf *et al.* 2005, Schockel *et al.* 2011).

Once the centrioles are partially separated, the centriolar linker proteins begin to

accumulate and form a loose tether between the mother and daughter centrioles (Mayor *et al.* 2000). Recent identification of the ASPP1 and ASPP2 tumour suppressor proteins have provided a mechanism by which linker protein C-NAP1 is recruited to the centrosome (Zhang *et al.* 2015). This is a promising start to the task of trying to identify the mechanism by which the linker is re-established in G1. Centriole disengagement is considered a key licensing step to allow the duplication of centrosomes marking an important juncture in the centrosome cycle (Tsou and Stearns 2006a, Tsou *et al.* 2009).

1.7.3 Centrosome duplication

Centrioles are duplicated during S phase using a template created by the oligomerisation of SAS-6 protein, which gives the 9-fold symmetry for the microtubule triplets of the centriole barrel (Fig. 1.8) (Kitagawa *et al.* 2011, van Breugel *et al.* 2011). In order to localise and anchor to this cartwheel structure at the wall of the pre-existing centriole, Plk4 accumulates at the site of procentriole biogenesis via the Cep152 scaffold protein (Kim *et al.* 2013). Plk4 recruits STIL (SAS-5) and stabilises SAS-6 through its interaction with STIL, a mechanism which has been shown also through the STIL analogue Ana2 in *Drosophila* (Dzhindzhev *et al.* 2014, Kratz *et al.* 2015). Cep152 stabilises CPAP (also called SAS-4) at the ends of the SAS-6 cartwheel, thereby stabilising the microtubules of the centriole (Cizmecioglu *et al.* 2010, Sonnen *et al.* 2013).

Initially, Plk4 localises in a ring-like structure on the side of the mother centriole before rearranging into a more discrete dot which precedes binding of SAS-6 and procentriole formation (Kitagawa *et al.* 2011, Kim *et al.* 2013). The ‘hub’ and ‘spokes’ of the SAS-6 cartwheel are formed, with Cep135 linking this structure to CPAP making up the wall of the new centriole (Lin *et al.* 2013). Cep135 has also been shown to stabilise C-NAP1 at the proximal end of the centriole, indicating a dual role for the protein (Kim *et al.* 2008). Both Plk4 and CPAP bind STIL, with Plk4 phosphorylation of STIL being required for centriole duplication (Tang *et al.* 2011). The γTuRCs are then recruited to the end of each SAS-6 spoke, and in cooperation with CPAP, which is recruited by centrobin, they nucleate the A-tubules, the first and innermost microtubule of the triplets (Dammermann *et al.* 2008, Azimzadeh and Marshall 2010, Gudi *et al.* 2014, Gudi *et al.* 2015). The B- and C-tubules are then templated from each other, B-tubules from A-tubules and C-tubules

from B-tubules (Guichard *et al.* 2010).

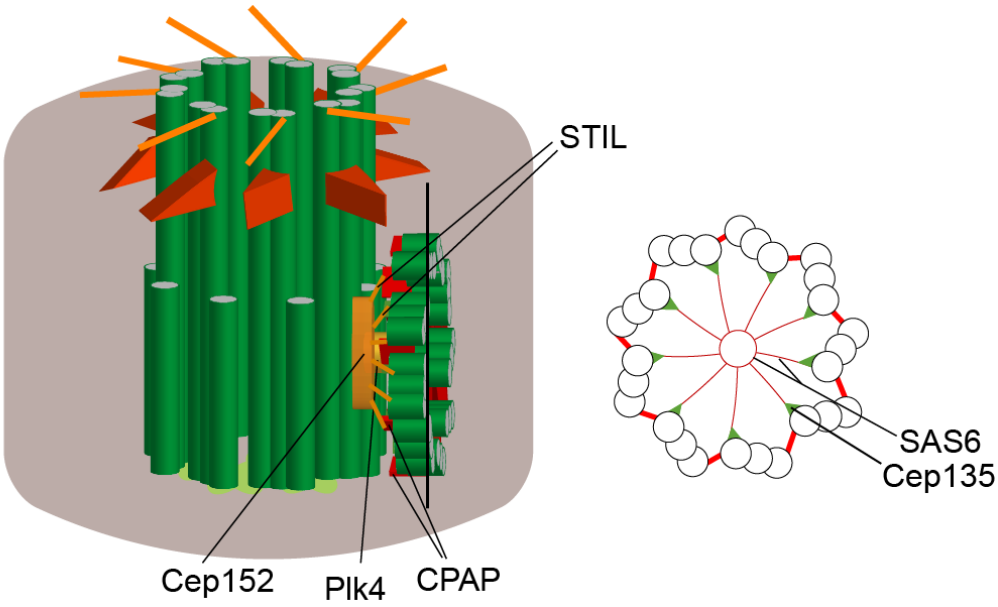

Figure 1.8: Initial stages of centrosome duplication. The cartwheel structure displaying the SAS6 "hub and spokes" is present at the through section indicated by the black line. Adapted from (Kitagawa *et al.* 2011).

As the microtubules elongate, centrin and POC1 occupy the lumen of the microtubule barrel, and cap proteins CP110 and Cep97 restrict centriole length by binding the plus end of the microtubule triplets (Paoletti *et al.* 1996, Pearson *et al.* 2009, Tsang and Dynlacht 2013). While the bulk of the assembly of the centriole occurs during S phase, the centriole must elongate and reach full maturity later in the cell cycle. Odf2 localises to the distal and subdistal appendages and POC5 localises to the lumen of the mother centriole. Both Odf2 and POC5 have regulatory roles in G2 to control the length of the centriole by restricting and facilitating elongation (Azimzadeh *et al.* 2009).

The final maturation event is the acquisition of distal and subdistal appendages in the next cell cycle, in order to organise microtubule nucleation for bipolar spindle assembly and ciliogenesis. Odf2 is required for the recruitment of both distal and subdistal appendages, in addition to Cep164, which localises at the distal appendages, facilitating primary cilia formation. The presence of Odf2 at subdistal appendages is necessary for both anchoring centrosomal microtubules and microtubule nucleation via ninein and Cep170 respectively (Ishikawa *et al.* 2005, Graser *et al.* 2007a).

1.8 Centrosome disjunction and the intercentriolar linker

Centrosome disjunction is the process in which the duplicated centrosomes separate before the onset of NEBD to orchestrate the formation of the bipolar spindle in mitosis. The process of centrosome disjunction entails the dissolution of the intercentriolar linker that connects the centrosomes after centriole disengagement in G1. The result is that the two centrosomes are released and can nucleate microtubules at opposite poles of the cell in mitosis (Lim *et al.* 2009, Tanenbaum and Medema 2010). The factors regulating this separation event are very different to the centriole disengagement factors, with the Hippo signalling pathway being integral in the regulation of disjunction (Fig. 1.9). The mammalian sterile-20 like effector kinase Mst2, Nek2 and protein phosphatase 1 (PP1) are held in a complex via the scaffold protein hSav1. Plk1 has been shown to phosphorylate Mst2 to promote the formation of the Mst2-Nek2-hSav1 complex (Mardin *et al.* 2010). PP1 binds the C terminal region of phosphorylated Nek2, to mediate an inhibitory dephosphorylation of its KVHF motif contained in the non-catalytic region of the protein (Helps *et al.* 2000, Mi *et al.* 2007).

In late G2, Mst2-mediated phosphorylation of Nek2, counteracting PP1 phosphatase activity, leads to phosphorylation of Nek2 targets (Mardin *et al.* 2010). The activated Nek2 phosphorylates the main linker proteins C-NAP1 and rootletin, inducing conformational changes that release both proteins from their respective binding sites on the proximal ends of centrioles and the fibrous linker (Fry *et al.* 1998, Mayor *et al.* 2000, Mayor *et al.* 2002, Bahe *et al.* 2005). Nek2-dependent phosphorylation of serine and threonine residues in the C terminal centriole-interacting region of C-NAP1 results in an overall change in the charge of this protein region, sufficient to dissociate C-NAP1 from the centrioles. Upon release of C-NAP1 from the centrosome, its local concentration is likely to decrease through passive diffusion in the cytoplasm (Hardy *et al.* 2014). This, however, could not explain the marked decrease in protein levels detected by western blot during mitosis, suggesting the existence of an active degradation mechanism (Mayor *et al.* 2002).

Tumour suppressor proteins ASPP1 (apoptosis stimulating protein of p53 1) and ASPP2 have been proposed to bind and sequester C-NAP1 in the cytoplasm until early G1 (Zhang *et al.* 2015). ASPP1 and ASPP2 directly interacted with C-NAP1 in vivo and knockdown of both ASPP1/2 prevented C-NAP1 reaccumulation at

centrosomes in telophase. Interaction of the ASPP1/2-PP1 complex with C-NAP1 promoted C-NAP1 phosphorylation and dissociation from the centrosome at the end of mitosis (Zhang *et al.* 2015). A recent C-NAP1 knockout using zinc finger interference displayed mislocalisation of rootletin and Cep68 at centrosomes in addition to a dramatic increase in inter-centrosomal separation (Panic *et al.* 2015). More striking defects in cell migration speed and Golgi apparatus disorganisation suggest C-NAP1 loss impacts microtubule nucleation and disrupts of the centrosome-Golgi network (Hurtado *et al.* 2011, Panic *et al.* 2015). *C-NAP1* mutations have been implicated in an atypical form of Usher syndrome, an inherited disorder characterised by retinal degeneration and sensorineural hearing loss (Khateb *et al.* 2014). The loss of C-NAP1 binding partner rootletin and its function in photoreceptor cells is a plausible cause of the retinal degeneration observed in these patients (J. Yang *et al.* 2002).

C-NAP1 and rootletin are regulated by Nek2 which phosphorylates both proteins and releases them from the centrosome (Fry *et al.* 1998, Bahe *et al.* 2005). Nek2 is a highly regulated kinase which induces premature centrosome separation when overexpressed (Faragher and Fry 2003). Overexpression of Nek2 also reduced the formation and length of primary cilia, while depletion of Nek2 compromised the resorption of cilia before mitosis (Spalluto *et al.* 2012). Nek2 has been proposed to play a role in the control of centrosome separation following a DNA damage-induced G2 arrest (Fletcher *et al.* 2004). Exposure to ionising radiation reduced Nek2 activation and prevented centrosome separation, thus suggesting a mechanism to hindering centrosome amplification in the presence of DSBs. Rootletin interacts with C-NAP1 and is a major component of the fibres that connect the centrosomes from G1 to G2/M (Bahe *et al.* 2005, Yang *et al.* 2006). As previously mentioned, rootletin forms the ciliary rootlet in ciliated cells, a structure which is particularly well developed in photoreceptor cells (J. Yang *et al.* 2002). Depletion of rootletin increases centrosome splitting, whereas cells that overexpress rootletin displayed an increased frequency of nuclear defects such as multinucleation, micronucleation, and irregular nuclear size and shape (Yang *et al.* 2006).

More recently, a number of proteins have been identified that play a role in centrosome cohesion, by either forming part of the centrosomal linker or localising to the proximal ends of the centrioles to exert an influence on linker integrity.

Centlein has been identified as a C-NAP1 interactor and localises at proximal ends of the centrioles (Fang *et al.* 2014). Cep68 and Cep215 (also known as Cdk5Rap2) were described as centrosome cohesion proteins and co-localise with rootletin and pericentrin (PCNT), respectively (Graser *et al.* 2007b). Cep68 interacts with centlein, which connects Cep68 fibres to C-NAP1 at the proximal ends of the centrioles (Fang *et al.* 2014). Rootletin and Cep68 display similar localisation pattern in the intercentriolar space, as do C-NAP1 and centlein (the only non-Nek2 substrate), which localise to the proximal end of the centrioles (Man *et al.* 2015). Cep215 is a PCM protein and causes an increase in separated centrosomes when depleted. Cep215 requires the removal of Cep68 combined with PCNT cleavage to facilitate mother and daughter centrioles physically separating from each other's PCM and distancing themselves from one another after centrosome disengagement (Pagan *et al.* 2015). Cep85 has been identified through its interaction with Nek2 and has a role in opposing the effects of Nek2. Overexpression of Cep85 resulted in maintenance of centrosome cohesion which was comparable to centrosome cohesion percentages following knockdown of Nek2 by siRNA (Chen *et al.* 2015). Finally, LRRC45, a protein which has a high sequence identity to rootletin, localises similarly to rootletin by spanning the intercentriolar space (He *et al.* 2013).

β-catenin is an effector in the Wnt signalling pathway (Dierick and Bejsovec 1999). β-catenin also localises to the proximal ends of centrioles and associates with linker protein rootletin (Bahmanyar *et al.* 2008). Upon depletion of the C-NAP1 linker docking protein, β-catenin displays a scattered localisation pattern between the centrioles and co-localises with rootletin fibres. In mitosis, Nek2 binds and phosphorylates β-catenin, thus stabilising the protein at the centrosome. β-catenin is a negative regulator of centrosome cohesion, through its accumulation and stabilisation at sites independent of C-NAP1 and rootletin in mitosis (Bahmanyar *et al.* 2008). After linker dissolution and through a combination of Eg5 kinesin and dynein motor proteins, the two centrosomes are forced apart and migrate along the nuclear envelope via the microtubule network by binding the nuclear envelope directly and through interaction with proteins that comprise the nuclear pore complexes (reviewed by Guttinger *et al.* 2009, (Mardin and Schiebel 2012). Eventually the centrosomes detach from the nuclear envelope and position themselves using solely the microtubule motor proteins to 'push and pull' the

centrosomes to the opposite ends of the cell (Florian and Mayer 2012).

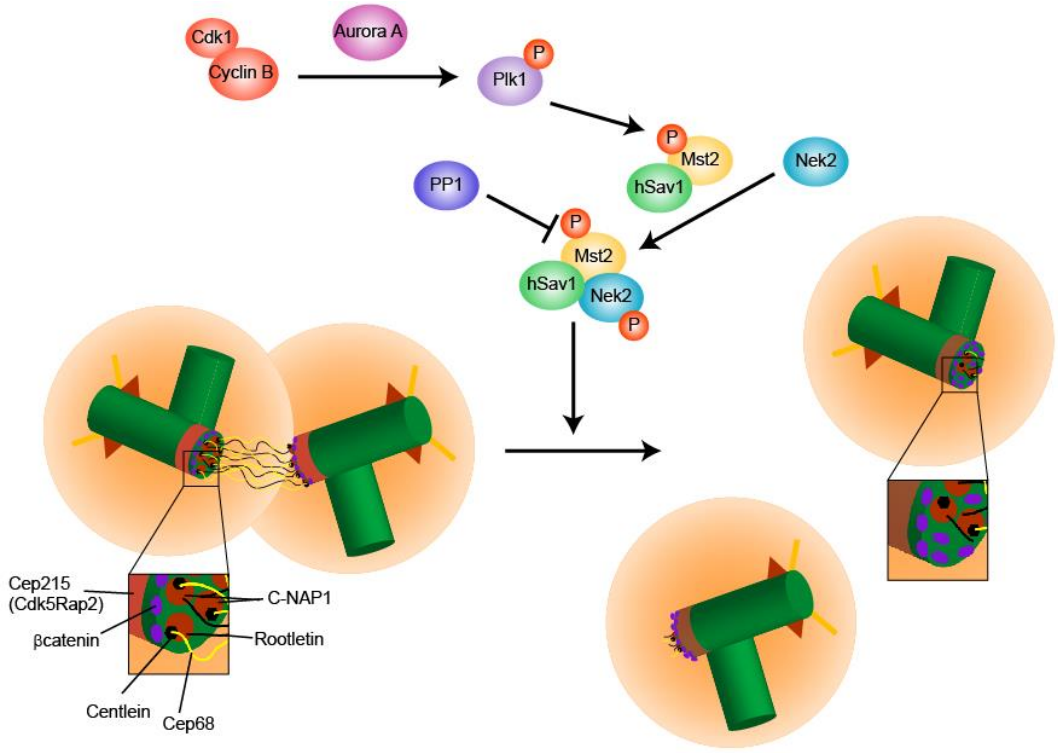

Figure 1.9: Intercentriolar linker composition and dissolution in G2/M. Preceding mitotic entry, cyclin B/Cdk1 activates Plk1 via Aurora A. Active Plk1 then phosphorylates the Mst2-hSav1 complex, which recruits and activates Nek2 by phosphorylating the kinase, counteracting the inhibitory activity of protein phosphatase 1 (PP1). Nek2 phosphorylates C-NAP1 and rootletin to dissolve the intercentriolar linker. Centlein and Cep68 are also displaced and βcatenin is recruited to the proximal ends of the centrioles. Adapted from (Agircan *et al.* 2014, Fang *et al.* 2014).

1.9 Centriolar satellites

1.9.1 Structure and cell cycle distribution

Centriolar satellites are small electron-dense granules, approximately 70-100μm in diameter, that are concentrated at the centrosome but also display a more dispersed localisation pattern throughout the cell (Bowers and Korn 1968, Fais *et al.* 1986, Kubo *et al.* 1999). Centriolar satellites (also called pericentriolar satellites) have been observed in most cell types but descriptions of their size, composition, abundance and relative localisation vary greatly (Tollenaere *et al.* 2015). Centriolar satellites have been described in many different species, however in the last 2 decades more details about the composition of satellites has been discovered.

The identification of PCM1 as a centriolar satellite protein was based in part on the discovery of its centrosomal and peri-centriolar localisation (Balczon *et al.* 1994).

The dynamics of the protein in the different cell cycle stages changed from a concentrated state at the centrosome and surrounding region in G1 and S phases of the cell cycle, to a more diffuse staining pattern in late G2. The signal was almost completely non-centrosomal in mitosis,s although the amount of the protein in the cell remained constant (Balczon *et al.* 1994, Dammermann and Merdes 2002). This is a common characteristic of the proteins now classified as satellite proteins. Discovery of other proteins that constitute centriolar satellites include OFD1 (oral-facial-digital syndrome type 1), Cep290, Cep72 and AZI1/Cep131, all of which display a similar localisation pattern (J. Kim *et al.* 2008, Lopes *et al.* 2011, Staples *et al.* 2012, Stowe *et al.* 2012).

In addition to being the first protein to shed light on centriolar satellite dynamics, PCM1 is the only satellite component discovered to date that does not have a defined role at the centrosome or in ciliogenesis. PCM1 functions solely as a scaffold protein for centriolar satellites without having a distinct role at the centrosome and is therefore considered a true satellite protein (Fig. 1.10) (G. Wang *et al.* 2013). Ninein, pericentrin and centrin co-localise with PCM1 at sites other than the centrosome, with ninein and pericentrin requiring PCM1 for centrosomal recruitment (Dammermann and Merdes 2002). Ninein functions to stabilise microtubules at the mother centriole by localising to subdistal appendages, whereas pericentrin localises to the PCM and organises centrosomal microtubule nucleation (Zimmerman *et al.* 2004, Delgehyr *et al.* 2005). Just as PCM-1 is dependent on the dynein-dynactin microtubule motor complex for its cellular localisation, the loss of dynein activity, and therefore PCM-1 localisation, caused ninein and pericentrin depletion at the centrosome resulting in failure to anchor microtubules (Kubo *et al.* 1999, Dammermann and Merdes 2002, Tollenaere *et al.* 2015). PCM1 is therefore necessary for microtubule nucleation and anchoring through its protein localisation function.

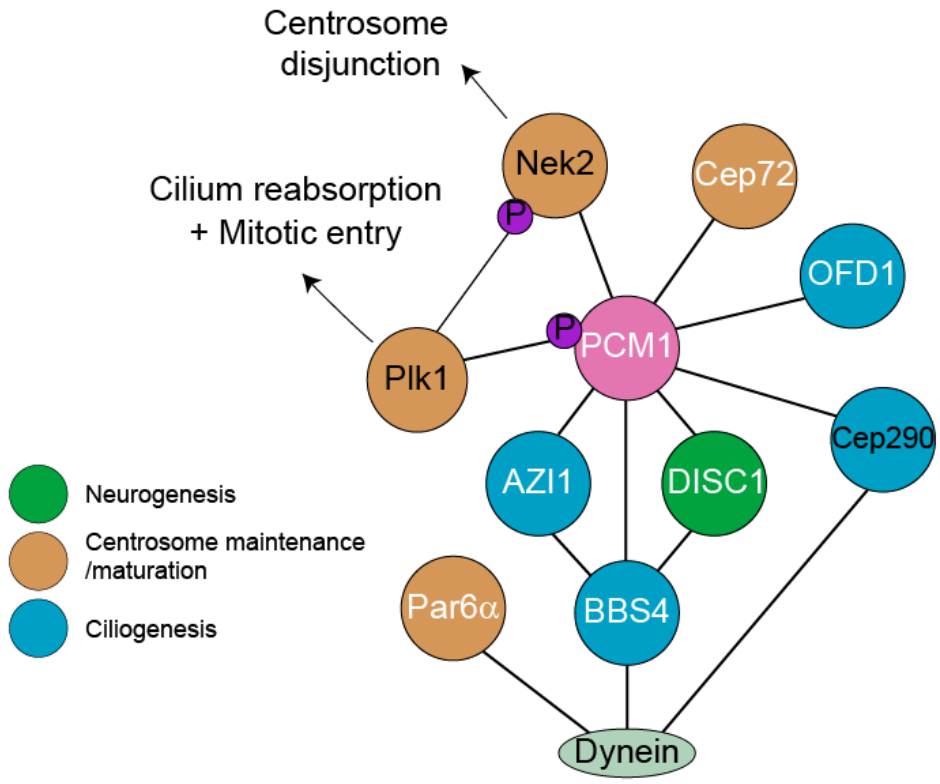

Figure 1.10: Schematic of interactions of centriolar satellites in interphase. PCM1 is a central scaffold protein, binding to microtubules through BBS4 and dynein. Cep72, OFD1, Cep290, AZL1 and DISC1 are associated with the satellites throughout the cell cycle. Par6α, Plk1 and Nek2 are bound to the satellites in a more transient manner. Protein names in white are important for maintenance of satellite structure. Adapted from (Barenz *et al.* 2011, Tollenaere *et al.* 2015)**.**

1.9.2 Centriolar satellites and ciliation

In ciliated cells, the centriolar satellite complex clusters around the basal body, which prompted the investigation of centriolar satellite protein function in primary cilium formation (Sorokin 1968a, Kubo *et al.* 1999). The identification of OFD1 as a component of centriolar satellites creates a link between these complexes and primary cilium formation. A role for OFD1 in the cilium assembly process has been described, but OFD1 also functions in the maintenance of centrosome structure by controlling centriole length (Singla *et al.* 2010). Localisation of OFD1 also varies throughout the cell cycle, with the protein associating with PCM1 at the centriolar satellites but dissociating from the satellites and relocating to the distal ends of both centrioles during ciliogenesis in G0 (Singla *et al.* 2010, Lopes *et al.* 2011, Tang *et al.* 2013).

OFD1 recruits IFT88 to distal appendages of the mother centriole and is required for the docking of the mother centriole to vesicle membranes during cilium formation

(Singla *et al.* 2010). Depletion of OFD1 is necessary for cilium resorption through an autophagy-dependent pathway, which is a mechanism by which ciliogenesis can be regulated in the cell: centriolar satellite-bound OFD1 is removed by the autophagosome, thus relieving inhibition of OFD1 mediated cilium elongation (Tang *et al.* 2013). OFD1 dynamics provide strong evidence for the role of centriolar satellites in cilium formation, in addition to the idea of there being a cytoplasmic pool of centrosomal proteins which is regulated by the interaction of these proteins with the satellites (Tollenaere *et al.* 2015).

Cep290 is another protein which associates with PCM-1 and also associates with BBS4 (Bardet-Biedl syndrome 4) of the BBSome (Bardet-Biedl syndrome protein complex) at centriolar satellites. Cep290 is important in cilium function, transporting Rab8 to the cilium transition zone to mediate trafficking of ciliary vesicles via interaction with the $p150^{glued}$ subunit of dynein (J. Kim *et al.* 2008, Stowe *et al.* 2012). Like OFD1, Cep290 mediates cilium resorption through association with distal appendage proteins in the presence of Rab8, where CP110 is the Cep290-interacting partner (Tsang *et al.* 2008). Cep72 has been identified as a centriolar satellite protein which interacts with Cep290 to recruit the BBS8 subunit of the BBSome to the cilium transition zone. PCM-1 interaction localises Cep72 to satellites and depletion of PCM-1 results in centrosome-only localisation of Cep72 (Stowe *et al.* 2012). Cep72 is required for the centrosomal targeting of Kizuna, which stabilises γTURC complexes and associated microtubules at the centrosome during bipolar spindle formation (Oshimori *et al.* 2009).

Plk1 is another binding partner of the PCM-1 scaffold protein. PCM-1 interaction with Plk1 requires Cdk1 phosphorylation of PCM-1 and results in cilium disassembly through Plk1 activation of deacetylase complexes at the basal body that remove acetyl-modifications from the ciliary axoneme (G. Wang *et al.* 2013).

1.9.3 Anchoring and transportation functions of centriolar satellites

As mentioned above, proteins of the BBSome, such as BBS4, are also found at centriolar satellites (Kim *et al.* 2004). The BBSome is a complex of BBS proteins BS1, BBS2, BBS4, BBS5, BBS7, BBS8 and BBS9 and localises to the cilium transition zone (Nachury *et al.* 2007, Jin *et al.* 2010). It is thought that BBS4 (with bound BBSome) acts as a link between the microtubules and PCM1 by association

with the microtubule network of the cell via the microtubule binding protein dynein, specifically the $p150^{glued}$ subunit. The transportation of cellular and possibly centrosomal cargo is thought to be mediated by the BBS proteins in the centriolar satellites, with disruption of the microtubule network and PCM-1 delocalisation arising from depletion of BBS4 (Kim *et al.* 2004).

AZI1 (Cep131) is a binding partner of BBS4 and inhibits the localisation of BBS4 at the basal body during the cell cycle (Chamling *et al.* 2014). DISC1 (disrupted in schizophrenia 1) has also been described as a BBS4 binding partner at centriolar satellites and is involved in neurogenesis. Similar to the function of BBS4, DISC1 has been implicated in the microtubule-dependent trafficking of proteins via interaction with BBS4 and PCM1 to and from the centrosome (Kamiya *et al.* 2008). In addition to Cep290 and BBS4, Par6α is a dynein-interacting protein which binds $p150^{glued}$ and localises to centriolar satellites, leading to the idea of dynein-mediated organisation of centriolar satellites via the interaction of these three proteins with $p150^{glued}$ (Kodani *et al.* 2010).

1.9.4 Centriolar satellites and the cell cycle

The roles of the individual centriolar satellite proteins described above provide strong evidence for the theory that the satellite complexes are a type of scaffold for many centrosomal proteins. The ability of the satellites to traffic centrosomal proteins from a cytoplasmic pool along the microtubule network to the centrosome allows centrosomal duplication, but also facilitates the modification of the centrosome when the cell is exposed to stress such as DNA damage. Centrin has been shown to associate with centriolar satellites and has been exploited in the analysis of centrosome duplication, but also in the cellular dynamics of centriolar satellites (White *et al.* 2000, Dammermann and Merdes 2002, Wong and Stearns 2003, La Terra *et al.* 2005, Kuriyama *et al.* 2007).The accumulation of centrin-containing granules surrounding the centrosome after DNA damage or checkpoint mediated cell cycle arrest has been linked to the formation of extra centrioles through a *de novo* centriole assembly pathway (Kuriyama *et al.* 2007, Prosser *et al.* 2009, Loffler *et al.* 2013).

A cellular microtubule network is necessary for the assembly of core centrosome proteins for centrosome formation by either regular centriole duplication or centriole

overduplication events (Balczon *et al.* 1999). In a process dependent on dynein, centrin-containing cytoplasmic granules converge on the centrosome in checkpoint arrested cells and the formation of new mature centrioles can be observed after 48 hours (Prosser *et al.* 2009). Cdk2 is required for centrosome overduplication and in cells which have been arrested in G1 phase. This overduplication can be induced prematurely by the ectopic expression of cyclin A (Meraldi *et al.* 1999, Duensing *et al.* 2006, Prosser *et al.* 2009). The overduplication of centrioles during cell cycle arrest indicates a dissociation of the centrosome cycle from the DNA replication cycle and may provide a route to cancer or cell death through chromosomal instability (Balczon *et al.* 1995, Nigg 2006).

Centriole amplification after DNA damage is also preceded by the formation of centrin granules close to the centrosome (Loffler *et al.* 2013). Amplification of centrosomes can occur independently of the cell cycle stage and relies on the activation of Chk1 (Bourke *et al.* 2007). After exposure to DNA damaging agents such as ionising radiation and bleomycin, the appearance of large centrin-containing granules, which co-localised with centriolar satellites in human cells, preceded centrosome amplification (Loffler *et al.* 2013). Initially, the centrin granules formed large lattice-like structures in the vicinity of the centrosome and could be observed by IF and displayed an electron dense appearance by EM. After 96 hours the large centrin granules became more discrete and now contained a number of other centriolar proteins such as γtubulin (Loffler *et al.* 2013). These observations further the notion of the role of centriolar satellites as assembly points for centrosomal proteins.

Centriolar satellites are necessary for the duplication of centrioles in S phase and play important roles in cytoplasmic protein storage and also protein trafficking upon induction of ciliogenesis (Tollenaere *et al.* 2015). Centriolar satellite accumulation evidently plays a role in the overduplication of centrosomes after cell cycle arrest via DNA damaging agents. However, it is not yet clear whether the mechanisms for satellite assembly are also responsible for centriolar satellite biogenesis in a regular cell cycle. The upstream regulators of satellite biogenesis and accumulation after cell cycle arrest are not detailed at present, although Cdk2 and Chk1 signalling have been shown to influence satellite structure and could form part of a more intricate cell cycle regulation pathway governing centriolar satellite structure and composition.

Cytoplasmic Nek2 particles co-localize in part with PCM1-containing centriolar satellites and depletion of PCM1 interferes with centrosomal recruitment of Nek2 and its substrate C-NAP1 (Hames *et al.* 2005). This represents another function of centriolar satellites, by assisting centrosome disjunction in G2 via Nek2 localisation.

1.10 Centrosome amplification

Centrosome amplification is the synthesis of extra centrioles and associated PCM which can occur in response to particular external stimuli or as a result of internal cellular abnormalities. There exist a number of pathways and mechanisms by which cells can induce the formation of extra centrosomes. Centrosome amplification can arise from internal failures such as failure in cytokinesis at the end of mitosis and mitotic slippage, where in both cases the result is that the cell retains both centrosomes (Nigg 2002, Musacchio and Salmon 2007). Other causes of aberrations in centrosome number include tetraploidy and cell-cell fusion, overexpression of centrosomal proteins and assembly of centrioles via a *de novo* pathway (Godinho and Pellman 2014).

1.10.1 Tetraploidy and Polyploidy

Tetraploid cells have twice the typical amount of DNA in a single cell, and with that, they carry extra centrosomes from centrosome duplication in the previous cell cycle. Cytokinesis failure is one of the main causes of tetraploidy and defects in any one of a large number of proteins involved in cytokinesis can result in the retention of two nuclei and the associated four centrioles in the same cell (Eggert *et al.* 2006). Tetraploid cells can also arise from the chromosome segregation process in mitosis where large amounts of DNA between the two nuclei block cell abscission, thus preventing cytokinesis (Mullins and Biesele 1973). The incorrect segregation of DNA, where both chromosomes are directed to a single cell can also cause tetraploidy via cytokinesis failure (Ganem *et al.* 2007).

A prolonged spindle assembly checkpoint is the origin of mitotic slippage and arises mainly from the inability to resolve abnormal kinetochore-microtubule attachments. The mechanism behind stalling the normal progression through anaphase and telophase relies on the presence of high levels of cyclin B which holds the cell in the metaphase stage of mitosis (Brito and Rieder 2006). Gradual slippage from mitosis is

the product of cyclin B degradation by the proteasome resulting in tetraploidy and the presence of more than one centrosome.

Aurora A kinase localises to the centrosome in interphase but binds to and stabilises microtubule spindle attachments to kinetochores during mitosis (Andrews 2005). Increased expression of Aurora A correlates with elevated centrin and γtubulin levels and induces centrosome amplification in cancer cells through tetraploidy. Accumulation of the protein at kinetochores and on microtubule spindles in cytokinesis resulted in an increase in chromosome aberrations such as DNA bridges causing cytokinesis failure and multinucleation (Meraldi *et al.* 2002).

Cell-cell fusion is an event that occurs as part of normal development in certain tissues of the body and manipulation of this event can facilitate generation of cells with extra centrosomes (Ganem *et al.* 2007). Certain viruses can induce cell-cell fusion, as observed by the effects of the Sendai virus on human cells (Duelli *et al.* 2005). Multinucleation and centrosome amplification, among other effects impeded cell proliferation in normal cells after fusion, however aberrant expression of p53 by either of the fused cells allowed cell survival thus highlighting a path to tumorigenesis. Rad6 is a ubiquitin-conjugating enzyme which localises to the centrosomes and also induces cell-cell fusion by a similar method, resulting in multinucleation and centrosome amplification upon overexpression (Shekhar *et al.* 2002).

1.10.2 Centrosome protein overexpression

Plk4 is a protein critical for centriole duplication in its role in marking the site on the mother centriole from which a new daughter centriole can by synthesised (Kleylein-Sohn *et al.* 2007, Dzhindzhev *et al.* 2014). The overexpression of Plk4 in human cells induced the formation of numerous centrioles around mother centrioles (Kleylein-Sohn *et al.* 2007). Hindering the $SCF^{cyclinF}$/ubiquitin-dependent proteolysis and dysregulation of Plk4 autophosphorylation also triggers the assembly of extra centrosomes by a similar mechanism (Cunha-Ferreira *et al.* 2009, Holland *et al.* 2010). Centriole duplication protein SAS-6 also regulates centriole formation through its degradation via activated Cdh1-APC/C complex and its overexpression can induce the formation of cartwheel templates for centriole assembly (Strnad *et al.* 2007).

Centriolar cap proteins Cep97 and CP110 are important for the regulation of cilia assembly, with Cep97 necessary for CP110 recruitment and prevention of spindle defects in mitosis and polyploidy possibly caused by premature centrosome splitting (Spektor *et al.* 2007). Recent studies have found that over expression of USP33, a deubiquitinating enzyme controlling CP110 in S and G2/M phases, results in centrosome amplification due to an increase in CP110 levels (Li *et al.* 2013). Ninein-like protein (Nlp) localises to the centrosome and regulates the stabilisation of γTURC complexes after its phosphorylation by Plk1 (Casenghi *et al.* 2003). Overexpression of Nlp results in the formation of centrosomal patches with a high capacity to organise centrosomal microtubule nucleation. Nlp has been shown to be overexpressed in cancer cells and mediates microtubule organisation at the centrosome, creating a dense microtubule network facilitated by an enrichment of centrin and γtubulin (Shao *et al.* 2010, Schnerch and Nigg 2015). In addition to centriolar protein overexpression, the overexpression of pericentriolar material proteins can also induce centrosome overduplication. Overexpression of the PCM component, pericentrin, was shown to drive the formation of extra daughter centrioles which were not always found in close proximity to existing centrioles (Loncarek *et al.* 2008).The strong capacity for microtubule nucleation by pericentrin overrides the need for a template as the mother centriole can organise microtubules sufficiently to facilitate centriole assembly.

Templated centriole duplication seems a favourable avenue by which cancer cells can gain extra centrioles with increased expression of centrosomal proteins regularly seen in cancer cells. The theory that a high concentration of centriole duplication or PCM proteins will allow the formation of supernumerary centrosomes, whether the cartwheel is templated or not, is a compelling one. Cells which can overcome the centrosome reduplication block have an even greater advantage, as the assembly of duplication proteins into extra centrioles is not physically hindered by a tight centrosome configuration (Wong and Stearns 2003).

1.10.3 *De novo* centriole formation

Aside from the canonical duplication pathway, the centrosome has the ability to form centrioles *de novo* in the case where the existing centrioles are removed or ablated. The number of centrioles present in the cell is restricted to two in G1, which can each form one procentriole during S phase. The biogenesis of centrioles *de novo* is

not a feature regularly seen in human cells, although the phenomenon has been previously observed in sea urchin eggs, rabbit blastomere cells and clam zygotes (Kallenbach and Mazia 1982, Szollosi and Ozil 1991, Palazzo *et al.* 1992). *De novo* centriole formation is a process held under tight control as the presence of supernumerary centrosomes causes such defects as apoptosis resulting from multipolar spindles in mitosis and also tumorigenesis as a consequence of alterations in cell migration (Ganem *et al.* 2009, Leber *et al.* 2010, Godinho *et al.* 2014).

Human HeLa cells have displayed the ability to reassemble their centrosomes after dispersion of centrosomal γtubulin by overpowering the cells with anti polyglutamylated tubulin antibodies (Bobinnec *et al.* 1998). This is in contrast to laser ablation experiments performed by Khodjakov *et al,* in which the centrosome structure was completely destroyed with no recovery of the centrioles as the cells progressed into mitosis (Khodjakov and Rieder 2001). Subsequent experiments showed that centriole biogenesis factors transcribed during S phase are necessary for the synthesis of new centrioles after laser ablation (Khodjakov *et al.* 2002). In cells arrested in S phase, the initial gathering of PCM proteins was followed by the assembly of radial microtubules that resembled centrioles by EM. This *de novo* assembly of centrioles was highly sophisticated as the new centrioles were assembled and matured into true centrosomes. However, the number of centrioles generated varied greatly, with a random number between 2 and 14 centrioles observed in cells after ablation (Khodjakov *et al.* 2002).

Cell progression into the early stages of mitosis after centrosome ablation demonstrated that the cell cycle was not dependent on the presence of centrosomes (Khodjakov and Rieder 2001). Further laser ablation studies went on to demonstrate the fate of cells after one or both centrioles are removed (La Terra *et al.* 2005). Centrioles reformed in S phase through the formation and accumulation of centrin at a number of spots in the cell before their assembly into a number of centrioles, which cluster in G2 and M phase to organise the mitotic spindle (Khodjakov *et al.* 2002). The clustering of centrioles formed by the *de novo* pathway allowed cell proliferation through organisation of a bipolar spindle to facilitate faithful chromosome segregation (Quintyne and Schroer 2002).

1.11 DNA damage and centrosome amplification

There are many checkpoints to monitor the integrity of DNA and chromosome segregation, regulation of centrosomes can become desynchronised with replication of the genetic material. Prolonged periods in interphase caused by cell cycle arrest after DNA damage, in S phase in particular, can allow the duplication of centrosomes while the DNA is being repaired (Balczon *et al.* 1995). The availability of centrosome duplication proteins in S phase facilitates the assembly of additional procentrioles which can result in multipolar spindles and uneven chromosome segregation in mitosis. DNA damage response and repair proteins have often showed a correlation with the presence of extra centrosomes, although the question remains as to whether centrosome amplification is a cause or consequence of DNA damage (D'Assoro *et al.* 2002b, Nigg 2002).

Linking the DNA damage response to centrosome amplification, loss of the *p53* gene has also been implicated in centrosome amplification. *p53* is a tumour suppressor which is the most commonly mutated gene in cancer, and is responsible for cell cycle arrest during cytokinesis failure, triggering cell death pathways in a p53-dependent manner (Uetake and Sluder 2004). p53 mediates cell cycle arrest in response to DNA damage, scanning the genome to maintain DNA integrity (Kuerbitz *et al.* 1992). In the absence of p53, tetraploid cells which manage to begin a new cell cycle can continue to proliferate and bypass p53 induced apoptosis at the end of G1, a checkpoint controlled by regulation of cyclin E-Cdk2. P53 activates the transcription of p21 which is an inhibitor of Cdk2 and thus inhibits S phase initiation (Harper *et al.* 1995). The inhibition of E2F-mediated transcription via p53 also prevents S phase entry in the event of DNA damage (Meraldi *et al.* 1999). Progression to S phase allows further amplification of centrosomes from the already tetraploid cell state (Fukasawa *et al.* 1996, Hinchcliffe *et al.* 1999).

It is thought that chromosomal instability is high in the early stages of tumour development in order to find an oncogenic state where the extra copies of particular chromosomes, and associated extra centrosomes, confer a growth advantage to the cells (Fukasawa 2008). Once this is established, chromosomal instability declines and cancer cells which are p53-deficient acquire mutations that result in high expression of BubR1, a spindle checkpoint kinase which enhances the potency of the spindle assembly checkpoint, despite the presence of extra centrosomes (Oikawa *et*

al. 2005).

Other proteins involved in the DNA damage response have been implicated to play a role in centrosome duplication, with their loss or mutation resulting in amplification in cancer cells. BRCA1 and BRCA2 are breast cancer susceptibility genes and activate the G2/M checkpoint via ATM-mediated activation of p53 (H. Yang *et al.* 2002, Fabbro *et al.* 2004). Loss of function of either of these proteins results in centrosome amplification (Tutt *et al.* 1999, Xu *et al.* 1999). Loss of Rad51 or the Rad51 paralogues have also been associated with the formation of extra centrosome through a prolonged G2 arrest (Dodson *et al.* 2004, Date *et al.* 2006). Absence of BRCA1, BRCA2, Rad51 or RAD51 paralogues in homologous recombination DNA repair pathway triggers the G2/M checkpoint, during which centrosomes can reduplicate. The reduplication of centrioles requires centriole disengagement as a licensing signal for DNA damage-induced amplification in G2 (Inanc *et al.* 2010). The G2/M checkpoint is mediated by Chk1 signalling via ATM activation and cells deficient of Chk1 or ATM displayed loss of both proteins abrogated radiation-induced centrosome amplification (Dodson *et al.* 2004, Bourke *et al.* 2007).

1.12 Centrosomes and cancer

Cancer cells often display a greater than normal number of centrosomes, yet it is still undecided if this is an advantage for the cell or not (Nigg 2002). The presence of increased numbers of centrosomes can result in the formation of multipolar spindles or merotelic attachment of microtubules to kinetochores, where more than one centrosome of a bipolar spindle forms an attachment with a single kinetochore (Ganem *et al.* 2009, Kops *et al.* 2010). The resulting aneuploidy can be an advantage to cells if the cell can cope with the accompanying genomic instability, however if the cell lacks genes that are critical for cell function then cell death soon follows. An interesting observation made by Godinho *et al.* revealed that, in the case of tetraploid cells generated by cytokinesis failure, the presence of extra centrosomes promoted the specific invasive behaviour of the cells whereas cells that had lost their extra centrosomes spontaneously did not exhibit metastatic properties (Godinho *et al.* 2014). However, cancer derived cells do not necessarily require centrosomes for their proliferation, but their presence increases mitotic fidelity as demonstrated by

addition of the PLK4 inhibitor centrinone (Wong *et al.* 2015).

In many cancers, increased centrosome numbers accompanied by changes in the structure of the PCM and additional extra-centriolar structures resulting from changes in protein expression can drive the formation of tumours and their metastatic capabilities (Lingle *et al.* 2002, Basto *et al.* 2008, Godinho *et al.* 2014). Overexpression of key proteins such as Plk4 and SAS-6 that are necessary for the duplication of the centrosome display the ease with which the centrosome duplication pathway can be hijacked and used to drive cancer progression through generation of extra centrioles (Duensing *et al.* 2007, Holland *et al.* 2010). Other structural changes include the alteration in centriole structure which is observed in cancer cells that overexpress CPAP, a protein that regulates centriole length (Kohlmaier *et al.* 2009). Although PCM abnormalities have been characterised in some cancers by analysing the volume of PCM markers at the centrosome (D'Assoro *et al.* 2002a, Guo *et al.* 2007), the evidence for these changes being PCM-specific abnormalities which are unrelated to the centrioles themselves is still under question (Godinho and Pellman 2014).

Although centrosome clustering appears to be beneficial for driving cancer, the separation of centrosomes is also a factor that contributes to tumorigenic behaviour. Premature centrosome separation seen in cancer, where cancer cells have upregulated signalling via their own EGF receptor pathway to increase the concentration of Mst2 and Nek2 kinases at cell cycle stages earlier than G2, facilitates cell cycle progression in these cells (Mardin *et al.* 2013). Separated centrosomes are frequently observed in cancer cells which no longer require the Eg5 motor protein to mediate the assembly of the bipolar spindle.

Cell shape and adhesion patterns can influence the propensity of cells to form multipolar spindles. In cells that contain extra chromosomes and with the potential to cluster these centrosomes, the shape, based on the adhesion pattern the cell displays, correlates to the extent to which the cell forms multipolar spindles (Kwon *et al.* 2008). Multipolar spindles were more commonly found in cells that conform to a circular shape in interphase compared to either elongated or polarised cells which mainly formed a bipolar spindle. Manipulation of cell adhesion to control bipolar spindle formation also reduced the number of multipolar cells in the population, thus echoing the idea that cell adhesion and shape can reduce the formation of multipolar

mitoses.

Decreases in the expression of centrosome proteins have also been correlated with tumorigenic behaviour. C-NAP1 has recently been implicated in cell mobility, where ablation of the gene resulted in the separation of the centrosomes and a resulting decrease in the rate of cell motility, possibly due to the disruption of microtubules and loss of cell polarity (Panic *et al.* 2015). Similar to C-NAP1 loss, centrosome splitting appears to licence duplication, signalling for the disengagement of centrioles to allow reduplication (Saladino *et al.* 2009, Inanc *et al.* 2010).

1.13 Aims of this study, model systems and targeting methods

Centrosome amplification requires centriole disengagement in order to facilitate the reduplication of centrioles. C-NAP1 regulates centrosome cohesion in human cells, forming an attachment point at the centrioles for the intercentriolar linker. Knockdown of *C-NAP1* results in loss of intercentriolar cohesion and centrosome splitting. Our goal in this Thesis was to discern whether centrioles were capable of amplifying in a scenario where the centrosomes are already split. To address this question we decided to create chicken and human cell lines which were depleted of the C-NAP1 protein using the following approaches:

1. We generate a stable C-NAP1 conditional knockdown cell line by combining an in-frame auxin inducible degron (AID) sequence with the endogenous *C-NAP1* locus using reverse genetic techniques in the chicken DT40 cell line, a B lymphocyte cell line with a genome highly proficient in recombination (Baba *et al.* 1985, Buerstedde and Takeda 1991, Nishimura *et al.* 2009). In addition, fusion of a green fluorescent protein (GFP) sequence to *C-NAP1* will allow investigation of C-NAP1 dynamics in chicken cells. By exposure of cells depleted of C-NAP1 to γ-irradiation, this will create conditions which promote centrosome amplification via induction of a DNA damage response.

2. Following on from our studies in chicken cells, we explore the functions of C-NAP1 in human cells. We aim to dissect the role of C-NAP1 by disrupting the *C-NAP1* locus in the hTERT-RPE1 cell line. Retina pigmented epithelial (RPE) cells immortalised by telomerase integration are karyotypically normal which facilitates analysis of centrosome structure and function (Bodnar *et al.* 1998, Jiang *et al.* 1999). Introduction of a frame shift in the *C-NAP1* coding region will be generated using CRISPR (clustered regularly interspaced short palindromic repeat)/Cas9 endonuclease technology (Cho *et al.* 2013, Cong *et al.* 2013, Mali *et al.* 2013, H. Wang *et al.* 2013). We investigate the impact of DNA damage on centrosome amplification in human *C-NAP1* deficient cells following exposure to γ–irradiation. We study the impact that loss of centrosome cohesion may have on cilia structure and centriolar satellites.

2. Materials and methods

2.1 Reagents and materials

2.1.1 Materials

Most analytical grade chemicals used were obtained from Sigma-Aldrich (Arklow, Ireland). For reagents supplementary to those supplied by Sigma-Aldrich, Fisher (Dublin, Ireland), Life Technologies (Carlsbad, CA, USA) and GE Healthcare (Little Chalfont, Buckinghamshire, UK) were employed. Buffers and common reagents were prepared using double distilled water (ddH_2O) or Milli-Q purified water obtained using the ELGA Purelab flex 3 (ELGA LabWater, Veolia Water Systems, Kildare, Ireland) and are listed in Table 1. Kits used in this study are listed in Table 2. TRIzol reagent was obtained from Ambion (Life Technologies), restriction endonucleases, T4 ligase, DNA Polymerase I, Large (Klenow) Fragment and T4 Polynucleotide Kinase were obtained from New England Biolabs (NEB, Ipswich, MA, USA). Shrimp Alkaline Phosphatase was purchased from United States Biochemical (USB, Affymetrix, Santa Clara, CA, USA) or Promega (Madison, WI, USA). Invitrogen (Life Technologies) supplied the 1Kb Plus DNA ladder and KOD polymerase was obtained from Novagen (Merck Millipore, Darmstadt, Germany). The PageRuler Plus prestained protein ladder (Fermentas, Life Technologies) or the Colour protein standard, broad range marker (NEB) were used. Whatman paper was supplied by Hartenstein (Würzburg, Germany). All sterile plasticware used for cell culture was obtained from Sarstedt (Numbrecht, Germany), Greiner (Kremsmünster, Austria) and Corning (Riverfront Plaza, NY, USA).

Table 1: Common reagents and buffers.

Solution/Reagent	Composition	Notes and use
Blocking solution (IF)	1% Bovine Serum Albumin in 1xPBS	for immunofluorescence
Blocking solution (WB)	5% dried semi-skimmed milk powder in 1x PBS, 0.05% Tween-20	for blocking nitrocellulose membranes during Western blot
Cacodylate wash buffer	0.1M Sodium Cacodylate-HCl pH 7.2	for washing cell pellets for electron microscopy
Cytoskeleton buffer	137mM NaCl, 5mM KCl, 1.1mM Na_2HPO_4, 0.4mM	for fixing and staining IF slides to visualise microtubules, filter

	KH_2PO_4, 2mM $MgCl_2$, 2mM EGTA, 5mM PIPES, 5.5mM glucose, pH 6.1	sterilised
6x DNA binding dye	0.25% Bromophenol blue, 0.25% Xylene cyanol FF, 40% sucrose	for binding DNA during agarose gel electrophoresis
DEPC-treated H_2O	0.1% DEPC in ddH_2O	for preparing RNA
Detection buffer	0.1M Tris-HCl, 0.1M NaCl, pH 9.5	to equilibrate membrane for probe detection during Southern blot
Fixation solution (IF)	4% Paraformaldehyde (PFA) in 1x PBS or 1x CB, or methanol with 5mM EGTA	for fixation of cells before immunofluorescence microscopy
High stringency buffer (HSB)	0.5x SSC, 0.1% SDS	for hybridisation of probe to nylon membrane during Southern Blot
Low stringency buffer (LSB)	2x SSC, 0.1% SDS	for hybridisation of probe to nylon membrane during Southern Blot
Luria-Bertani (LB) medium	1% Tryptone, 0.5% Yeast extract, 1% NaCl, pH 7.0	For growth of bacterial (*E. coli*) cultures
Maleic acid wash buffer	0.1M Maleic acid, 0.15M NaCl, pH 7.5, 0.3% Tween-20	for washes and blocking and antibody dilution for Southern blot
Mounting medium	0.3% N-propyl gallate, 80% Glycerol	for mounting slides after IF staining
1x Phosphate buffered saline (PBS)	137mM NaCl, 2.7mM KCl, 1.4mM NaH_2PO_4, 4.3mM Na_2HPO_4, pH 7.4	for washes, blocking and antibody dilution during IF and WB
1x PBST	1x PBS, 0.025% Tween-20	for washes, blocking and antibody dilution during IF and WB
Permeabilisation buffer	0.15% Triton X-100 in 1x PBS or 1x CB	to permeabilise cells after fixation with PFA
Ponceau S	0.5% w/v Ponceau S, 5% acetic acid	for staining nitrocellulose membranes during Western blotting
Primary fixative	2% Glutaraldehyde, 2%	primary fixation of samples for

(Electron Microscopy)	Paraformaldehyde, 0.1M Sodium cacodylate-HCl, pH 7.2	electron microscopy
Primary antibody dilution buffer	1x PBST, 1% milk, or 1x TBST	for dilution and incubation of primary antibodies for Western blot
RIPA Buffer	50mM Tris, 150mM NaCl, 0.25% Sodium deoxychlorate, 1% IGEPAL, 1mM EDTA	for lysis of human cells for protein extraction, supplemented with protease inhibitor mix (Roche) and phosphatase inhibitors (Sigma-Aldrich)
SDS-PAGE running buffer	24mM Tris, 192mM glycine, 0.1% SDS	for running SDS-PAGE gels
20x Salt-sodium citrate (SSC)	3M NaCl, 300mM Sodium citrate, pH 7.0	for transfer of DNA to nylon membranes during Southern blot
6x Sample buffer	440mM Tris, 12% SDS, 30% Glycerol, 0.1% Bromophenol blue, 30% β-Mercaptoethanol	for binding protein for SDS-PAGE gels
Secondary fixative (EM)	1% Osmium tetroxide, 0.1M Sodium cacodylate-HCl, pH 7.2	secondary fixation of samples for electron microscopy
Semi-Dry transfer buffer	1x Tris-Glycine, 20% Methanol, 0.0375% SDS	for semi-dry transfer of proteins to nitrocellulose membrane during Western Blot
1 x TAE	40mM Tris, 20mM Acetic acid, 1mM EDTA	for agarose DNA gels
1x Tail buffer	50mM Tris-HCl (pH 8.8), 100mM EDTA (pH 8.0), 100mM NaCl, 1% SDS	for lysis of mammalian cells to extract genomic DNA
1x Tris-buffered saline (TBS)	137mM NaCl, 2.7mM KCl, 19mM Tris	for wash and blocking solutions while using phospho-antibodies during Western blot
1x TBST	1x TBS with 0.025% Tween-20	for wash and blocking solutions while using phospho-antibodies during Western blot
1x TG Transfer buffer	24mM Tris, 192mM glycine,	for wet transfer of proteins for

	15% methanol, 0.1% SDS	Western blot
Wash Buffer	1x PBS, 0.05% Tween-20	for Western blot

Table 2: Kits Used in this study.

Name	Use	Supplier
GenElute plasmid miniprep kit	Small scale plasmid DNA extraction	Sigma-Aldrich
High Capacity RNA-to-cDNA kit	cDNA synthesis	Applied Biosystems (Life Technologies)
NucleoBond Xtra midi (EF)	Large scale (endotoxin-free) plasmid DNA extraction	Macherey-Nagel (Düren, Germany)
PCR DIG probe synthesis kit	DIG labelling of probes for southern blot	Roche (Mannheim, Germany)
QIAquick gel extraction kit	Extraction and purification of DNA fragments from agarose gel	Qiagen (Crawley, UK)
QIAquick PCR purification kit	Purification of DNA fragments	Qiagen
5'/3' RACE kit, 2nd generation	Amplification of 5' cDNA ends	Roche

A list of the plasmids used in this study is detailed in Table 3.

Table 3: Plasmids used in this study.

Plasmid name	Use	Source/ Reference
pGEM-t easy	General cloning, DT40 targeting vector	Promega
pCMV-3Tag2A-hsPlk4	For Plk4 overexpression	Helen Dodson, Centre for Chromosome Biology (CCB)
pEGFP-C1/N1	For general expression of various genes	Clontech
pANMerCreMer	Cre recombinase encoding plasmid for floxing	(Arakawa *et al.*, 2001)
pJE108	OsTIR1-9Myc containing plasmid for degron system	(Eykelenboom *et al.*, 2013)
pGEM-t Easy-AID-GFP	AIDGFP fusion tag for DT40	Tiago Dantas, CCB,

	targeting	unpublished
pX330	Cas9 nuclease plasmid for CRISPR system	Nishimura *et al*,2009, (Obtained from Addgene, Cambridge, MA, USA)
pTS1681 (PCM1-mycHAHis)	For centriolar satellite overexpression	(Stowe *et al*., 2012)
pTS1919 (Cep72-GFP)	For centriolar satellite overexpression	(Stowe *et al*., 2012)

Primary antibodies used for Western blot (WB) and immunofluorescence (IF) during this study are listed in Table 4.

Table 4: Primary antibodies used in this study.

Reactivity/ Antigen	**Ref. no/ Clone no.**	**Host species**	**Dilution for WB**	**Dilution for IF**	**Source**
α-Tubulin	B512	Mouse	1:5000	1:5000	Sigma-Aldrich
Acetylated Tubulin	T 6793	Mouse		1:2000	Sigma-Aldrich
Arl13B	17711-1-AP	Rabbit		1:1000	Proteintech (Chicago, IL,USA)
ATM	Ab78	Mouse	1:1000		Abcam (Cambridge, UK)
Centrin	20H5	Mouse		1:1000	Millipore (Darmstadt, Germany)
Centrin 3	M01 3E6	Mouse		1:1000	Abnova (Taipei, Taiwan)
Centrobin	6D4 F4	Mouse		1:10000	David Gaboriau, CCB
Cep72	A301-297A	Rabbit	1:500		Bethyl Laboratories, Inc. Montgomery, TX, USA
Cep135	ab75005	Rabbit		1:750	Abcam
Cep135	1457 748	Rabbit		1:1000	Alex Bird (Bird and Hyman, 2008)
Cep164	1C3 A10	Mouse		1:200000	David Gaboriau, CCB
Cep290	1C3 G10	Mouse	1:500	1:200	David Gaboriau, CCB
CHK1	DCS-310	Mouse	1:1000	1:1000	Sigma-Aldrich
C-Nap1	6F2 C8	Mouse	1:2	1:2	David Gaboriau, CCB
Detyrosinated	Ab48389	Rabbit		1:500	Abcam

Tubulin					
ɣ-Tubulin	GTU88	Mouse		1:600	Sigma-Aldrich
ɣ-Tubulin	T3559	Rabbit		1:600	Sigma-Aldrich
GAPDH	14C10 2118	Rabbit	1:5000		Cell Signalling
GFP	7.1+13.1	Mouse	1:500	1:500	Roche
GFP		Rabbit		1:500	Abcam
Myc	9E10	Mouse	1:500	1:500	Ciaran Morrison, CCB
Nek2	20	Mouse	1:250	1:100	BD Transduction (San Jose, CA, USA)
Ninein	Ab4447	Rabbit		1:200	Abcam
OFD1	NBP1-32843	Rabbit	1:500	1:500	Novus Biologicals (Littleton, CO, USA)
pATM Ser 1981	Ab81292	Rabbit	1:1000		Abcam
pCHK1 Ser 345	2348S 133D3	Rabbit	1:500		Cell Signalling
PCM1	817	Rabbit	1:10,000	1:10,000	A. Merdes, (Dammermann and Merdes, 2002)
Rootletin	NBP1-80820	Rabbit		1:750	Novus Biologicals
Rootletin	C20 Sc 67824 C0408	Goat	1:250	1:100	Santa Cruz

All secondary antibodies (listed in Table 5) were obtained from Jackson Immunoresearch (Bar Harbour, ME, USA). Unconjugated antibodies had been affinity-purified and sterile filtered at source. With the exception of horseradish peroxidase conjugates, conjugated affinity-purified antibodies were freeze-dried in phosphate buffer with stabilizers and sodium azide.

Table 5: Secondary antibodies used in this study.

Reactivity	Conjugation	Host species	Dilution for WB	Dilution for IF
Mouse IgG	FITC	Goat		1:1000
Goat IgG	FITC	Donkey		1:200
Mouse IgG	Alexa 488	Donkey		1:750
Mouse IgG	Alexa 594	Donkey		1:750

Rabbit IgG	Alexa 488	Donkey		1:750
Rabbit IgG	Alexa 594	Donkey		1:750
Mouse IgG	Horseradish Peroxidase (HRP)	Goat	1:10000	
Rabbit IgG	HRP	Goat	1:10000	
Goat IgG	HRP	Donkey	1:1000	

2.1.2 Biological materials

2.1.2.1 Bacterial strains

Top 10 *Escherichia coli* (*F- mcrA Δ(mrr-hsdRMS-mcrBC) φ80lacZΔM15 ΔlacX74 nupG recA1 araD139 Δ(ara-leu)7697 galE15 galK16 rpsL(StrR) endA1 λ-*) were obtained from Invitrogen and used for all cloning throughout this study. Ampicillin or kanamycin were obtained from Sigma-Aldrich.

2.1.2.2 Cell lines

DT40 cells were obtained from Shunichi Takeda (Kyoto University, Japan). hTERT-immortalized retinal pigment epithelial cells (hTERT-RPE1) human cells were acquired from American Type Culture Collection (ATCC), Manassas, VA, USA. U2OS are an osteosarcoma cell line that were also acquired from ATCC.

2.2 Bacterial culture methods

2.2.1 Preparation of *E. coli* for transformation

An inoculation of 500 ml of LB with *E. coli* from an overnight mini culture was incubated at 37°C with shaking until an OD 600 between 0.4 and 0.6 was reached. The bacteria were then pelleted at 6000g for 10 minutes at 4°C. The pellet was resuspended in 250 ml of cold 0.1 M $CaCl_2$ and incubated on ice for 30 minutes. The cells were then spun again under the above conditions and the pellet was resuspended in 50 ml of cold 0.1M CaCl2 containing 15% glycerol before aliquoting and storage at -80°C.

2.2.2 Transformation of chemically competent *E. coli*

For transformation, an aliquot of the *E. coli* was thawed on ice and either 5 µl of a ligation reaction or 1 µl of plasmid DNA were mixed in sterile conditions. The cells were placed on ice for 20 minutes before heat shock for 90s at 42°C, followed by 2

minutes on ice. LB was added before the bacteria were placed in a shaking thermoblock at 37°C for 30 minutes. For ligation transformations, the bacteria were pelleted at top speed for 1 minute and all transformants were spread on agar containing the appropriate antibiotic. Ampicillin or kanamycin were used as selection antibiotics at 50µg/ml or 30µg/ml respectively. For plasmid transformations, 50 µl of the transformation was spread on an agar plate. The plates were then inverted and incubated in a 37°C incubator overnight.

2.3 Nucleic acid methods

2.3.1 RNA isolation and cDNA synthesis

1x 10^6 cells were resuspended in 1ml of TRIzol and incubated for 5 min at room temperature. Then 0.2ml of chloroform was added, the tube was mixed by inversion and incubated at room temperature for 2 minutes. The sample was then centrifuged at 4°C for 15 minutes at 12000g and the upper layer transferred to a new tube. An equal volume of isopropanol was added, the tube was mixed by inversion and after 10 min incubation at room temperature the RNA was pelleted at 12000g for 10 minutes in a 4°C centrifuge. A wash in 75% ethanol in DEPC-treated water was followed by spinning at 7500g for 5 minutes at 4°C. A 5-minute drying period at 42°C preceded RNA resuspension in 30µl of DEPC-treated water. cDNA synthesis was carried out using the RNA-to-cDNA kit from Applied Biosystems as per manufacturer's instructions.

2.3.2 Extraction of genomic DNA

Suspension cells ($5x10^6$) and adherent cells ($1x10^6$) were harvested from a confluent 6 well dish and incubated with 500 µl of Tail buffer containing 0.5 mg/ml Proteinase K (Sigma-Aldrich) overnight at 37°C. The next day, the tubes were mixed vigorously in a thermomixer at 1400 rpm for 5 minutes. 200µl of 6M NaCl was added and tubes were mixed for an additional 5 minutes before being centrifuged at 13000 rpm for 10 minutes. The supernatant was transferred into a new tube, to which 750 µl of isopropanol was added and mixed by inversion to precipitate the DNA. Centrifugation was followed by a wash in 70% ethanol and after air drying the pellet for 1-2 minutes at 37°C the DNA was resuspended in 70 µl of dH_2O. Incubation of the DNA in dH_2O for 1h at 37°C allowed DNA solubilisation before subsequent use.

2.3.3 Polymerase chain reaction

Polymerase chain reaction (PCR) was carried out using KOD polymerase as per the conditions below (Table 6). Annealing temperature and $MgSO_4$ concentration were initially optimised as directed in the manufacturers' instruction book, and cycling was carried out in an Eppendorf Mastercycler Nexus Gradient (Hamburg, Germany) or Biometra T3000 or T-gradient (Göttingen, Germany) PCR machine. Denaturation, annealing and extension steps were performed for between 20 and 30 cycles.

Table 6: PCR reagents and cycling conditions for KOD polymerase.

Reagent	**Final Concentration**	**Program Cycling**	
Primers	200µM	Initial denaturation	95°C – 2 minutes
PCR Buffer	1x	Denaturation	95°C – 20 seconds
MgSO4	1.5mM	Annealing	50°C to 65°C – 10 seconds
dNTPs	200nM	Extension	70°C – 25 seconds/kb
Plasmid/ genomic DNA/ RT reaction (template)	10ng/ 100ng/ 2ul	Final extension	70°C – 5 minutes
Enzyme	0.02U/µl		

2.3.4 DNA cloning methods

DNA digestion was carried out using restriction endonucleases (NEB) for either 2 hours or overnight. Ligations using T4 Ligase (NEB) were performed at 16°C overnight, blunting reactions using DNA Polymerase I, Large (Klenow) Fragment and DNA phosphorylation by T4 Polynucleotide Kinase were carried out using enzymes obtained from NEB as per the manufacturer's instructions. Dephosphorylation was carried out using Shrimp Alkaline Phosphatase from USB (Affymetrix, Santa Clara, CA, USA) or Promega (Madison, WI, USA) as per the manufacturer's instructions. A list of primers and siRNA sequences is detailed in Table 7.

Table 7: DNA and RNA oligos used in this project.

Oligo name	Sequence	Use
RACE Primer 3 (SP3)	CGCTGCTCCAGCTCACGACACC	5'RACE
RACE Primer 2 (SP2)	GCTGTGGTCTTCAGT	
RACE Primer 1 (SP3)	TCACTGCGCCATTC	
AID-GFP fwd	GTTTAAACATGCTAGCCCGCGGATGATG GGCAGTGTCGAG	Targeting ggC-NAP1 locus
AID-GFP rev	GATATCAGATCTGCAGTGAAAAAATGCT TT	
5' arm fwd	CCGCGGATAGAAAAGCTGTCATCAAAAG CT	
5' arm rev	GCTAGCCCTCAGACCATCCCTTGTGGTGG A	
3' arm fwd	GATATCCAGGAGCAGCATGCAGCTGGAG CT	
3' arm rev	GTCGACCAGCTCTGGGCAGCAGTACCGG GG	
Probe fwd	GATAACTCTTGAGCAGGTAAAAAA	Targeting probe
Probe rev	TTCTAGAAGCAGGCATCTTGTCCT	
CRISPR targ. 1	CACCGACATTCCGACGCCACTTCC	CRISPR targeting
CRISPR targ. 2	AAACGGAAGTGGCGTCGGAATGTC	
CRISPR screen fwd	TGTGCTCAGTGGTTTATG	CRISPR screening
CRISPR screen rev	CCTCACATGCTCAGCTTT	
C-NAP1 1	GAGGCTCTTAAGATGGAGACAAGAAGCC CT	Cloning hsC-NAP1
C-NAP1 2	AGTAGTCGACCTGCAAAGCATTTCTCGC CT	
C-NAP1 3	AGTAGTCGACCTGGCGGAGGCAGAGAAG AG	
C-NAP1 4	AGTAAAGCTTGTGGAGGGCAGATGCTAC TG	
C-NAP1 5	AGTAAAGCTTCATCAAGACCTGTGGAAG	

	AC	
C-NAP1 6	GATACCATGGGCAGATGCTCTAAAACAG AC	
C-NAP1 7	GATACCATGGCCGTCCAGGAGCGAGAGC AG	
C-NAP1 8	GATACATATGGGCTTGCTCCAGAGCTCC CT	
C-NAP1 9	AGGACATATGACACTGAAGGAGCGTCAT GG	
C-NAP1 10	GCGGCCGCCTACCTGGAGGCGGCTTG	
CEP250 siRNA 1	GAGCAGAGCUACAGCGAAU	Knockdown of C-NAP1
CEP250 siRNA 2	GGACCUCGCUGAACAACUA	
CEP250 siRNA 3	AAGCUGACGUGGUGAAUAA	
CEP250 siRNA 4	GAGAAUAUGAUCCAAGAGA	

2.3.5 Assembly of target CRISPR plasmids

Oligos were annealed by heating to 95°C for 5 minutes then cooling slowly. The oligos were then phosphorylated with T4 Polynucleotide Kinase (New England Biolabs, MA, USA) as per manufacturer's instructions. pX330 plasmid was obtained from Addgene (MA, USA), digested with BbsI and dephosphorylated with Calf Intestinal Phosphatase (NEB). Annealed oligos were then ligated to the digested pX330 plasmid and successful cloning was verified by BbsI digest and direct sequencing.

2.3.6 Analysis of cloned DNA and sequencing

Plasmid DNA was analysed by restriction digest (as described for Southern blot) and sequencing reactions were performed by Source BioScience (Waterford, Ireland).

2.3.7 DIG labelling of DNA probes

DNA probes for Southern blotting were generated according to the manufacturer's instructions using the DIG DNA labelling kit (Roche, Basel, Switzerland). PCR reaction to generate probes was carried out as in section XXX. Template plasmid was used at 10ng per reaction.

2.3.8 Southern blot

2.3.8.1 Digestion, separation and transfer of genomic DNA

For digestion, 10-15 µl of genomic DNA was incubated overnight with 10 units of StuI. The digestions were supplemented with 0.5 µg/ml RNase A. A 0.7% agarose/TAE gel containing 15 µl of ethidium bromide was used to separate the digested samples with added 1x DNA binding dye for 4 hours at 100 V. The gel was then depurinated using 0.25 N HCl for 20 minutes on a rocker, followed by a brief wash in dH_2O and incubation with denaturing solution for 30 minutes, again with rocking. The gel was rinsed once in ddH_2O then soaked briefly in transfer buffer. Capillary transfer of the DNA to a nylon membrane (Hybond N+, GE Healthcare, Buckinghamshire, UK) was carried out overnight using 10x SSC buffer.

2.3.8.2 Hybridisation of DIG labelled *C-NAP1* probe

After transfer the membrane was air dried for 5 minutes before crosslinking the DNA with 3000 J/m^2 UV. Prehybridization with DIG Easy Hyb Granules (Roche) for 30 mins at 44°C was carried out while the DIG labelled probe (60µl) was denatured by boiling in 300 µl of MilliQ H_2O for 5 minutes before cooling on ice. The denatured probe was added to 10 ml of the Easy Hyb hybridisation solution and incubated at 44°C for 14 – 18 hours. The next day the membrane was washed 2x 5 minutes in LSB at room temperature, then 2x 15 minutes in HSB at 65°C. The membrane was washed at room temperature in SB wash buffer for 2 minutes. Blocking solution was applied for 30 minutes at room temperature after which the Anti-Digoxigenin-AP antibody (Roche) was diluted 1:10000 in 20 ml of the blocking solution and incubated for an additional 30 minutes. SB wash buffer was applied 2 times for 15 minutes each to wash off unbound antibody and the membrane pH was equilibrated with 20 ml of detection buffer for 3 minutes to allow for probe detection. The membrane was then immersed with CSPD substrate between two sheets of PE foil for 5 minutes before the excess was removed and the foil was

sealed air tight around the membrane. The membrane was incubated at 37°C for 10 minutes before exposure to x-ray film (Hartenstein, Germany) for 4-16 hours.

2.4 Protein Methods

2.4.1 Extraction of protein from cells

For suspension cells, $2x10^6$ cells were pelleted at 200g for 5 minutes, washed with 1x PBS, re-pelleted and lysed in an appropriate amount of lysis buffer (usually 40 µl). Lysis was performed on ice for 30 minutes. For adherent cells, $2x10^6$ cells were trypsinised and pelleted as above. The pellet was then washed with 1x PBS before being re-pelleted and lysed in 40 µl of RIPA buffer for an hour on ice with regular vortexing. Samples were then centrifuged at 4°C in a desktop centrifuge at 15,000g for 20 minutes. The supernatant was then transferred to a fresh pre-chilled 1.5 ml eppendorf tube, Bradford assay was performed and the lysate was then stored at -80°C for up to one month. For loading on SDS-PAGE gel, 40µg of total cell lysate was transferred to a fresh tube to which sample buffer to a concentration of 1x was added. The sample was then boiled in a thermoblock at 95°C for 5 minutes before spinning in a desktop centrifuge at 15,000g for 5 minutes. The supernatant was then loaded on the gel or stored at -20°C for 2-3 days maximum.

2.4.2 Protein quantification

A standard curve for protein concentration was prepared using BSA standards before estimation of the concentration of protein samples to be used for SDS-PAGE gel. Bradford Reagent (Sigma-Aldrich) was mixed in a 1:1 ratio with MilliQ H_2O and 1µl of the standard or sample was added before vortexing and analysis at 595 nm using an Eppendorf BioPhotometer or Nanodrop 2000c. The absorbance obtained was interpolated to calculate protein concentration.

2.4.3 SDS Polyacrylamide Gel Electrophoresis (SDS-PAGE)

Based on the size of the protein of interest, a 8% or a 12% SDS-PAGE gel was assembled according to Table 8 in a mini or large Hoefer electrophoresis unit (GE Healthcare). The samples were subjected to 40 mA (mini) or 70 mA (large) for between 50-90 minutes.

Table 8: Reagent concentrations used for assembly of SDS-PAGE gels.

Reagent	Running gel		Stacking gel
30% Acrylamide mix (37.5:1)	8%	12%	4%
Tris-HCl pH 8.8 (Running) / 6.8 (Stacking)	375mM	375mM	125mM
Sodium dodecyl sulfate (SDS)	0.1%	0.1%	0.1%
Ammonium persulfate (APS)	0.1%	0.1%	0.1%
Tetramethylethylenediamine (TEMED)	0.04%	0.04%	0.1%

2.4.4 Western Blot

After separation by SDS-PAGE gel, protein samples were transferred to a nitrocellulose membrane (Hybond-ECL, GE Healthcare). Three sheets of Whatman paper soaked in transfer buffer sandwiched the gel and membrane. For semi-dry transfer, the membrane was pre-soaked in semi-dry transfer buffer for 5 minutes before transfer assembly. The transfer was carried out at room temperature for 2h at 200 V and an amperage equivalent to the area of the membrane; 1 mA per cm^2, using a Hoefer Semi-Phor TE70 transfer unit. For wet transfer, proteins were transferred at 4°C for 3h at 100 V, 350 mA in a TE22 Mighty Small transfer tank from Hoefer or the larger Bio-Rad Trans-Blot Cell transfer unit. After transfer the membrane was washed 3 times with dH_2O, stained with Ponceau S for 10 minutes on a rocker at room temperature, then blocked in 5% milk for 1 hour, again on the rocker at room temperature. For primary antibody incubation, antibodies were diluted in 1% milk (or 1x TBST) according to Table 4. The incubation was carried out at room temperature for 1 hour or overnight at 4°C. The membrane was then washed 3 times in 1x PBST (or 1x TBST for phospho-antibodies). Secondary antibodies were diluted in 1% milk as per Table 5 and incubated with the membrane for 40 minutes on the rocker at room temperature. The membrane was washed 3 times for 5 minutes with either 1x PBST or 1x TBST before detection of the signal with ECL Detection kit (GE Healthcare) and exposure to x-ray film (Hartenstein, Germany). The film was fixed and developed by passing it through a developing machine (CP 1000, AGFA, Brentford, UK).

2.5 Cell biology methods

2.5.1 Cell maintenance

DT40 chicken B lymphocytes have a doubling time of 8 to 10 hours and were cultured in Roswell Park Memorial Institute (RPMI) 1640 media (Gibco, MA, USA) supplemented with 10% Fetal Bovine Serum (FBS, Sigma-Aldrich), 5% chicken serum (Sigma-Aldrich) and 1% Penicillin/Streptomycin (P/S, Sigma-Aldrich) at 39°C with 5% CO_2. They were maintained at a confluency of between 0.2 $x10^6$ and 1.0 $x10^6$ cells/ml. hTERT-RPE1 cells were cultured in Dulbecco's Modified Eagle Medium (DMEM) F12 (Lonza), supplemented with 10% FBS and 1% P/S. They have a doubling time of 24 hours, and were maintained at a confluency of between 20% and 80%. U2OS cells are grown in DMEM supplemented with 10% FBS and 1% P/S. U2OS have a doubling time of 24 hours and were maintained at a confluency of between 20% and 80%. All human cell lines used in this study were grown at 37°C with 5% CO_2. Cells were trypsinised in 1x PBS containing 0.05% trypsin and 0.02% EDTA at 37°C for 5 minutes before being reseeded into plates containing fresh media. For long term storage, cells were spun down directly or trypsinised first, then spun down before the removal of the media and resuspension in FBS containing 10% DMSO. This was performed for both human and chicken cells; however chicken cells were placed directly at -80°C or into liquid nitrogen, whereas human cells were placed in a Mr. Frosty Freezing Container (Thermo Scientific, Wilmington, DE, USA) overnight before storing at -80°C or in liquid nitrogen. To thaw cells, the tubes were warmed in a 37°C water bath and transferred to a dish containing fresh media. The media was replaced the next day. Selection drugs for the generation of stable cell lines were obtained from Sigma-Aldrich or Invivogen and are listed along with their working concentrations in Table 9.

Table 9: Drugs used for the selection of stable cell lines in human and DT40 cells.

	Final Concentration	
Drug	**Chicken**	**Human**
Blasticidin S (Sigma-Aldrich)	25µg/ml	10µg/ml
Geneticin (Invivogen)	2mg/ml	1mg/ml

Other pharmacological drugs used in this study are listed in Table 10.

Table 10: Drugs used throughout the project (all obtained from Sigma-Aldrich).

Drug	Stock concentration	Working concentration	Solvent	Application
Hydroxyurea (HU)	2M	2mM (DT40) 4mM (hTERT-RPE1)	ddH_2O	Induction of S phase arrest resulting in centrosome overduplication
Indole-3-acetic acid (Auxin)	500mM	500µM	100% ethanol	Depletion of Auxin-Inducible Degron (AID) tagged proteins in cells expressing TIR1
Nocodazole	6M	2µM	DMSO	Depolymerisation of microtubules/ M phase cell arrest

2.5.2 Transient transfection

2.5.2.1 Plasmid DNA overexpression

For DT40 cells, $5x10^6$ cells were spun down and resuspended in 100µl of solution T from the Amaxa Cell Line Nucleofector Kit (Lonza) and mixed with 15-30µg of circular, endotoxin-free DNA. The mix was transferred to a cuvette and electroporated using program B-23 on the Nucleofector 2b device. Cells were then placed in 10 ml of growth media for 24 hours before fixation for immunofluorescence or plating by limiting dilution for clone generation.

hTERT-RPE1 and U2OS cells were plated for transient DNA transfection at $0.6x\ 10^6$ cells per well of a 6 well plate the day before transfection. The next day they were transfected with 9µl Lipofectamine 2000 Reagent (Invivogen) diluted in in Opti-MEM serum-free medium (Invitrogen, Life Technologies) combined with between 0.5 and 4µg of circular, endotoxin-free DNA (also diluted in Opti-MEM). The cells and transfection mixture were then incubated for 48 hours at 37°C.

2.5.2.2 RNAi mediated interference

hTERT-RPE1 cells were plated at 30-40% confluency the day before transfection. The next day, the cells were transfected using 3µl of Oligofectamine Transfection Reagent (Invitrogen) diluted in Opti-MEM serum-free medium (Invitrogen). siRNA oligos were obtained from Ambion (Life Technologies, MA, USA) for GAPDH and Dharmacon (GE healthcare Life Sciences, Buckinghamshire, UK) for Human

CEP250 ON-TARGET plus SMART pool siRNA (Table 7). Cells were transfected at concentrations of 50nM and 100nM for 5 hours at 37°C in Optimem medium. The medium was then supplemented with DMEM-F12 containing 30% FBS and incubated for 48 hours before harvesting for Western blot or fixing for immunofluorescence.

2.5.3 Stable cell line generation

For generation of stable cell lines in DT40 cells, 10 x10^6 cells were pelleted and washed with 1x PBS before spinning at 250g and resuspension in 500 µl of 1x PBS. The cells were incubated with 15 µg of linearised plasmid DNA on ice for 10 minutes. Transfection using a Bio Rad Gene Pulser (Bio-Rad, CA, USA) at 300V/600µF was followed by 10 minute incubation on ice before the cells were transferred to 10 ml of pre-warmed media and placed at 39°C for 24 hours. Selection drug was then added before the cells were diluted 1 in 4 with media and seeded in 96 well plates. The plates were incubated at 39°C for 1 week after which single colonies were expanded.

hTERT-RPE1 cells were plated to be 70-80% confluent the following day in antibiotic free media. The next day, cells were transfected using Lipofectamine (Invivogen, CA, USA) as per the manufacturer's instructions with 3µg of pX330-Ex8 and 2µg of pLOX-Neo for 24 hours at 37°C. Cells were then trypsinised and serial dilutions were performed into media containing 1 mg/ml G418 (Invitrogen, CA, USA). Cells were placed under selection for 48 hours, after which the media was replaced with normal growth media, and then incubated at 37°C for 10 days. Colonies were then lifted using cloning discs (Sigma-Aldrich) and transferred to 48 well plates (Sarstedt, Numbrecht, Germany). Cells were expanded and screened by Western blot, immunofluorescence and DNA sequencing (SourceBioscience, Waterford, Ireland).

For generation of the *C-NAP1* rescue cell line in hTERT-RPE1, 9µl of Lipofectamine combined with 4µg of linearised plasmid DNA was transfected for 48h to 0.5 x10^6 cells in a 35mm dish. The media was then replaced with a 1:1 mix of fresh media to conditioned media containing 10µg/ml of Blasticidin S. Selection was carried out for 10-14 days with media replacement every 3 days. Colonies were then expanded and analysed by IF and Western blot.

2.5.4 Auxin mediated protein depletion

Depletion of AID tagged proteins in chicken DT40 cells was carried out overnight using Auxin (IAA). A 500mM solution of the hormone was prepared in 100% ethanol before being diluted to a 5mM solution in growth media and adding to the cells.

2.5.5 Microtubule regrowth assay

hTERT-RPE1 cells were plated on coverslips in a 6 well plate to be 50% confluent the next day. The cells were treated with 2µM nocadazole for 1 hour at 37°C before being placed on ice for 30 minutes to completely depolymerise cytoskeletal microtubules. The cells were then rinsed 3 times with ice cold 1x PBS before warm media was added and the plates were floated on a waterbath at 37°C. Immediately, a depolymerisation control slide was fixed in ice cold methanol and placed on ice. After specified times (between 1 minute and 1.5 minutes) coverslips were lifted from the plate and placed in plates containing cold methanol on ice. The samples were placed at -20°C for at least 10 minutes before staining with antibodies to α-tubulin (B512) and Cep135 (1457 748).

2.5.6 Serum starvation

Cells were plated to be 70-80% confluent the next day, then were washed twice with 1x PBS and once with reduced serum media. Cells were incubated for 48h in 0.1% FBS 5% Pen/Strep DMEM-F12 media to induce ciliation. For microscopy analysis, cells were incubated on ice for 30 minutes to depolymerise the microtubule cytoskeleton before fixation in methanol at -20°C.

2.5.7 Flow cytometry

Suspension cells were harvested when reaching a confluency of 0.7 $x10^6$ cells/ml, adherent cells were trypsinised and resuspended by pipetting and vortexing. They were then counted and 5 $x10^6$ cells were pelleted at 250g for 5 minutes in a Hettich 460 centrifuge. The mediumwas aspirated and the cells were resuspended by vortexing in 1x PBS and pelleted again. Resuspension in 300 µl of 1x PBS was followed by a fixation procedure where 100% ethanol (pre-chilled to 4°C) was added dropwise to the suspension while vortexing on a medium setting, bringing the ethanol up to a final concentration of 70%. The samples were then stored at -20°C

for at least 2 hours. For cell cycle analysis, cells were washed in 1x PBS 3 times and pelleted as above. The samples were then resuspended in 1x PBS containing 200 µg/ml of RNase A and 20 µg/ml of propidium iodide (PI) and left in the dark at 4°C for at least 30 minutes. Samples were vortexed before running through a BD Accuri C6 Flow Cytometer (BD Biosciences, Franklin Lakes, NJ, USA).

2.5.8 Microscopy methods

2.5.8.1 Fixation and staining of cells for immunofluorescence

Adherent hTERT-RPE1 cells were plated (generally $2x10^5$ cells) on UV sterilised coverslips (Menzel- Gläser, Braunschweig, Germany) and allowed to adhere for 12h. The medium was aspirated and a wash in 1x PBS was performed before fixation in ice-cold methanol containing 5mM EGTA (Sigma-Aldrich). Coverslips were placed at -20°C for 10 minutes then washed again with 1x PBS before blocking in 1% bovine serum albumin (BSA, Sigma-Aldrich) for 40 minutes at room temperature. Incubation with primary antibodies diluted in 1% BSA was carried out for 1 hour at room temperature, followed by 3 washes of 5 minutes in 1x PBS before incubation for 40 minutes at room temperature in flourophore conjugated secondary antibody, which was also diluted in 1% BSA. Washes with 1x PBS (3 times for 5 minutes) combined with a wash in distilled water preceded mounting of the coverslips in DAPI diluted 1:1000 in either DABCO or propyl gallate on Superfrost glass slides (Menzel- Gläser). Coverslips were then sealed with nail varnish and allowed to set before viewing under the microscope.

For suspension cells, $1x10^6$ cells were spun down and resuspended in 100µl of media before placing on poly-D-lysine coated slides (Menzel- Gläser) to adhere the cells for 20 minutes at room temperature. Staining was carried out as per adherent cells thereafter. Imaging and counts were performed using an Olympus BX51 microscope (with a Hamamatsu C10600 camera) or IX81 microscope (Hamamatsu C4742-80-12AG camera), using a 100x oil (NA 1.35) objective. Serial z-sections were taken, merged and saved as Photoshop (Adobe Systems, Mountain View, CA, USA) TIFF files. Volocity analysis software (Perkin-Elmer, Waltham, MA, USA) was used for measurement of intercentriolar distances using the ‘line’ tool and for centriolar satellite signal intensity measurements.

2.5.8.2 Electron microscopy

Cells were first treated with 5 Gy of irradiation or serum starved for 48 hours before being harvested by trypsinisation (adherent cells) and pelleting at 200g for 5 minutes along with their untreated controls. 10 $x10^6$ cells were first washed with 1x PBS for 5 minutes followed by 2 washes with cacodylate wash buffer. The samples were fixed overnight in primary fixative. The next day the cells were pelleted and fixed with secondary fixative for a minimum of 2 hours on the dark until the pellet turned black. The pellets were then washed 3 times in cacodylate wash buffer, before being subjected to an increasing ethanol gradient (30% to 90%) of 15 minutes each. The pellets were then placed in 100% ethanol which was refreshed 3 times, with incubations lasting 30 minutes. The pellets were then covered with propylene oxide for 30 minutes to remove the alcohol. The pellets were then placed in a 50:50 resin (TAAB, England, UK) to propylene oxide mixture for 4 hours, followed by a 75:25 resin to propylene oxide mix overnight. The next day the samples were embedded in 100% resin for 3 hour intervals for the first 6 hours and after 24 hours, before placing at 37°C for 48h to polymerise. The blocks were then cut into sections, placed on copper grids and contrasted before viewing with a Hitachi H7000 transmission electron microscope.

2.5.9 Computer programmes

Immunofluorescence microscopy images were saved as Adobe Photoshop CS2 version 8.0 files and combined using Adobe Illustrator C2 (Adobe Systems). DNA subcloning and plasmid maps were designed with the pDRAW32 software (Acaclone, www.acaclone.com). GraphPad Prism 5 (La Jolla, USA) was used to perform statistical analysis. The following databases and programmes were used for bioinformatics:

- NCBI gene database (http://www.ncbi.nlm.nih.gov/gene/);
- ENSEMBLchicken database (http://www.ensembl.org/Gallus_gallus/Info/Index);
- ESTs database (expressed sequence tags) (http://www.ncbi.nlm.nih.gov/dbEST/);
- Blast (http://www.ncbi.nlm.nih.gov/BLAST);
- ExPASy Translate (http://web.expasy.org/translate/)
- ExPASY Compute pI/Mw tool (http://web.expasy.org/cgi-bin/compute_pi/pi_tool)
- ClustalW2 (http://www.ebi.ac.uk/Tools/msa/clustalw2/).

- Phylogeny (http://www.ebi.ac.uk/Tools/phylogeny/clustalw2_phylogeny/)

3. Results: Reverse genetic analysis of C-NAP1 in the DT40 cell line

3.1 Identification of the *Gallus gallus C-NAP1* locus

C-NAP1 is a centrosome linker protein and is important for centrosome cohesion at from late mitosis through to G2 phases of the cell cycle. With reference to the gene, *C-NAP1* is the alias used most frequently for the description and analysis of the gene and the protein in the literature, although for the bioinformatics resources available on both the NCBI and the ENSEMBL databases it is defined using the *CEP250* gene symbol. For the bioinformatic analyses in this project, I will refer to the official gene and protein names *C-NAP1* and C-NAP1, respectively.

To investigate the *C-NAP1* gene we examined the NCBI database and located the locus of the chicken *C-NAP1* gene through the gene search function. The locus of *C-NAP1* in the chicken genome was similar to the human locus, with both genes being flanked on their 5' side by *MMP24, EIF6, FAM83C, UQCC1*, and *GDF5*. 3'of the locus in both species there are genes encoding ERGIC3, FER1L4, CPNE1, RBM12 and NFS1 (Fig. 3.1). The surrounding genes are transcribed in the same direction relative to *C-NAP1* in both species, although their sizes differ slightly. The loci of *C-NAP1* are different lengths between the species; spanning 34 kb in chicken and 62 kb in human. This is due to the presence of an extended 5' UTR region at the human *C-NAP1* locus and also there are larger intronic spaces between the exons in comparison to the chicken locus.

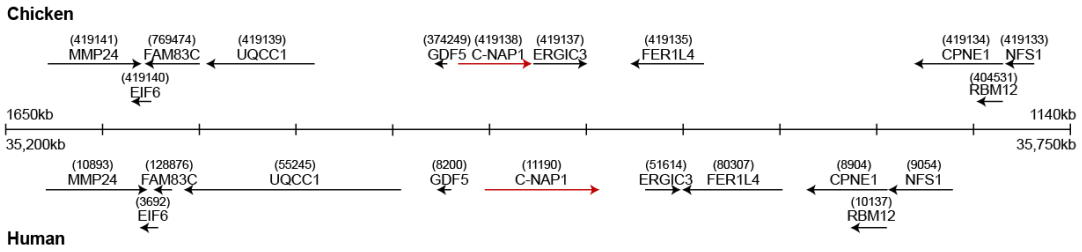

Figure 3.1: Schematic representation of the synteny between chicken and human C-NAP1 loci. The chicken locus is shown above the scale (in the middle) and the human below. C-NAP1 loci are shown in red and 5' and 3' genes are in black with the arrowheads indicating the direction of transcription. The location on the chromosome as per the NCBI database is also shown for each gene along with their respective GeneID numbers. Total length of sequence shown is 550kb, the units on the scale correspond to 50kb.

The *C-NAP1* gene is found on chromosome 20 in both chicken and human. The genomic locus of chicken *C-NAP1* spans 34.3 kb and the transcript is spliced around 31 exons (Fig. 3.2). The 31 exons are distributed at varying intervals and most are

between 100 and 350 bp in length. The exception is exon 28 which is much larger (almost 3kb). This is similar to the human exon arrangement, where there are 32 exons but it is exon 27 that is much larger than the other exons (2.6kb).

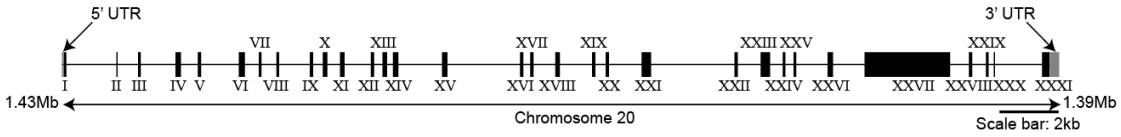

Figure 3.2: Schematic of the genomic locus of *Gallus gallus C-NAP1*. Exons (black) and introns (space) and the 5' and 3' UTR regions (grey) are indicated. Exon number is indicated with Roman numerals. 1.39Mb to 1.43Mb on chromosome 20 is the site in the chicken genome assigned by the NCBI database for the *C-NAP1* locus.

To relate the protein to its function in human and other vertebrate cells we next looked at the homology of the protein between various vertebrate species. Interestingly, the C-NAP1 protein was highly conserved among *Homo sapiens* (human), *Mus musculus* (mouse), *Rattus norvegicus* (rat), *Canis lupus familiaris* (dog), *Macaca mulatta* (monkey) and *Bos taurus* (cow), showing between 78% and 96% identity to the human protein (Table 11). However, *Gallus gallus* (chicken) and *Meleagris gallopavo* (turkey) C-NAP1 showed high identity to one another but not to the other species analysed, showing an average 39.48% sequence identity (±0.44%). All of the sequences were obtained from the NCBI gene database.

Table 11: Comparative analysis of the listed species shows divergence of avian and mammalian *C-NAP1* protein sequences. *C-NAP1* chromosome location and number of isoforms described in the NCBI database are listed. For most of the species there are a number of isoforms of the *C-NAP1* gene, 'x' on the selected isoform denotes if the isoform selected for analysis is a predicted sequence. The percentage identity was calculated using ClustalW.

Species	Chr. no.	Total no. of isoforms confirmed/ predicted	Isoform selected for analysis	Sequence ID	Predicted protein sequence length (aa)	% identity to human	% identity to chicken
Human	20	1/13	1	NP_009117.2	2442	100.00	38.92
Monkey	10	0/1	2	XP_001099508.1	2441	96.52	40.43
Dog	24	0/7	x7	XP_542975.3	2439	81.96	39.52
Cow	13	0/4	x1	XP_005215062.1	2434	82.13	40.06
Mouse	2	4/5	2	NP_001123471.1	2434	79.58	39.48
Rat	3	0/1	x2	XP_008760671.1	2390	79.34	40.0

Chicken	20	0/8	x8	XP_417323.4	2555	42.45	100.00
Turkey	22	0/1	1	XP_010720560.1	2664	42.03	91.49

Coincidently, there are a large number of isoforms detailed in the NCBI database for the human C-NAP1 protein (14), but just one verified sequence. The chicken and dog data have the next highest number of predicted isoforms, both containing 7 each, although these species have no confirmed protein sequence. As one would expect, the human protein shares most sequence identity with the monkey sequence. This makes sense as the monkey is the closest relative of the human from the species listed. Similarly, a high percentage identity is observed between the chicken protein and the one found for the turkey. The rat and mouse sequences are almost equi-distant from the human protein, to which they share 90% sequence identity. The chromosome on which the *C-NAP1* gene is found is somewhat comparable between the mammals studied. Although no *C-NAP1* loci could be found in *Drosophila melanogaster* (fruit fly) or *Danio rerio* (zebrafish), rootletin (which is highly similar to C-NAP1) protein sequences shared low identity with human rootletin (52% and 43% respectively) and less homology with each other (27%).

Based on the protein sequence of C-NAP1 from the species listed in Table 11, we can create a phylogenetic tree to visualise the divergence between these species (Fig. 3.3).

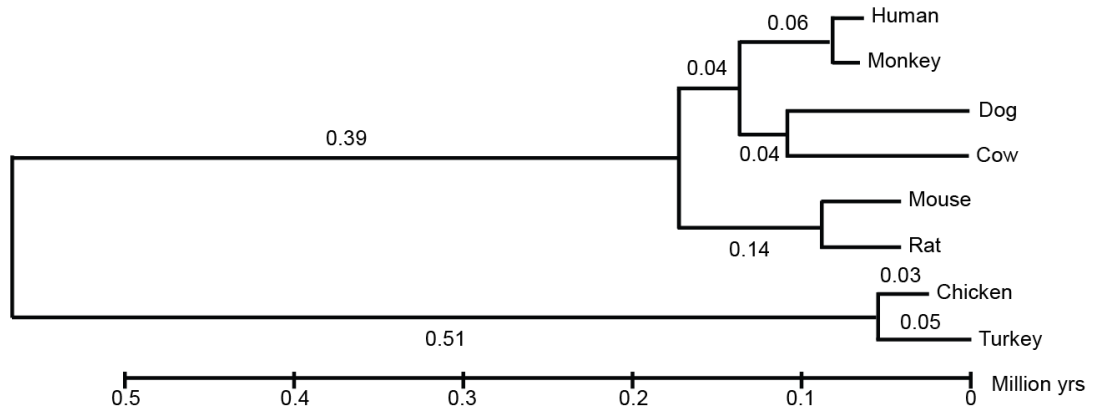

Figure 3.3: Molecular Phylogenetic analysis by Maximum Likelihood method. The evolutionary history was inferred by using the Maximum Likelihood method based on the JTT matrix-based model. The tree with the highest log likelihood (-19325.6075) is shown. Initial tree(s) for the heuristic search were obtained automatically by applying Neighbor-Join and BioNJ algorithms to a matrix of pairwise distances estimated using a JTT model, and then selecting the topology with superior log likelihood value. The tree is drawn to scale, with branch lengths measured in the number of substitutions per site (next to the branches). The analysis involved 8 amino acid sequences. All positions containing gaps and missing data were eliminated. There were a total of 2323 positions in the final dataset. Evolutionary analyses were conducted in MEGA6(Tamura *et al.* 2013).

Figure 3.3 depicts the homology of the C-NAP1 protein between species by grouping the more closely related species; mouse and rat, chicken and turkey, human and monkey; in the same subgroup. This allows us to see the homology of the nearer relatives of each species more clearly. Displayed in this way, we can see the 'real' divergence between species, with the chicken and turkey *C-NAP1* genes being separated by over 3 million years from the other species.

3.2 Analysis of the chicken *C-NAP1* transcript

The first chicken *C-NAP1* transcript identified (X8) is 8003 bp in length and is denoted with a shorter ID number (XM_417323.4) than the other transcripts found in the NCBI database. This contains 7667 bp of coding DNA sequence (CDS) plus an extended 3' untranslated region (UTR). At the beginning of the project this was the only transcript sequence to be found for chicken *C-NAP1* in the NCBI database. Of the 8 predicted transcripts now found in the NCBI database for chicken *C-NAP1* (analysed in Table 12), five of the sequences share the same start site (X8, X11, X12, X13, X14) with the other four each having different methionine residues initiating the transcript. These five share a common 5' UTR of just 4-6 base pairs, but have very different 3'UTR regions, varying in length from 150 bp to 1.6 kb.

Four of the variants (X8, X9, X10 and X15) share high 3' UTR sequence identity; they have the same stop codon ending the translation. However these are not the same sequences that have a highly homologous 5' UTR. The XM_417323.4 transcript is among the subset with similar 5' UTR regions and the subset with similar stop codon site and also shares the highest protein identity with the human protein. For these reasons it is favoured above the others by the NCBI and here for further analysis.

Table 12: *C-NAP1* transcripts are variable in UTR regions but less variable in their CDS. Analysis of the 8 chicken *C-NAP1* isoforms transcript length, CDS length and UTR length. % sequence identity to isoform X8 was calculated using ClustalW2.

Isoform name	NCBI accession number	Transcript length	CDS length (bp)	5' UTR sequence length (bp)	3' UTR sequence length (bp)	% Identity to isoform X8
X8	XM_417323.4	8003	7667	5	330	100
X9	XM_004946944.1	7950	7620	0	330	99.47
X10	XM_004946945.1	8044	7571	142	330	99.34
X11	XM_004946946.1	9117	7457	5	1654	98.3
X12	XM_004946947.1	7605	7457	5	182	98.39
X13	XM_004946948.1	7604	7448	6	149	98.21
X14	XM_004946949.1	7599	7364	6	228	98.97
X15	XM_004946950.1	7654	7163	160	330	100

To clone the entire *C-NAP1* cDNA, primers to the beginning and the end of the XM_417323.4 transcript were designed (red arrows - a and b, Fig. 3.44A). However RT-PCR reactions with these primers did not produce any product. After analysis of the human and chicken protein sequences, we observed regions of high homology toward the N terminus of C-NAP1. We then tried to amplify the *C-NAP1* cDNA in sections of 2.7 kb and 4.6 kb using the primers indicated by the blue arrows (c and d) in Figure 3.4 in combination with the original 3' primer (red, b) and a new primer at the 5' terminus (green, e). The sequence of the new 5' primer corresponds to the region which has strong identity to the human protein and is highly conserved between vertebrate species studied.

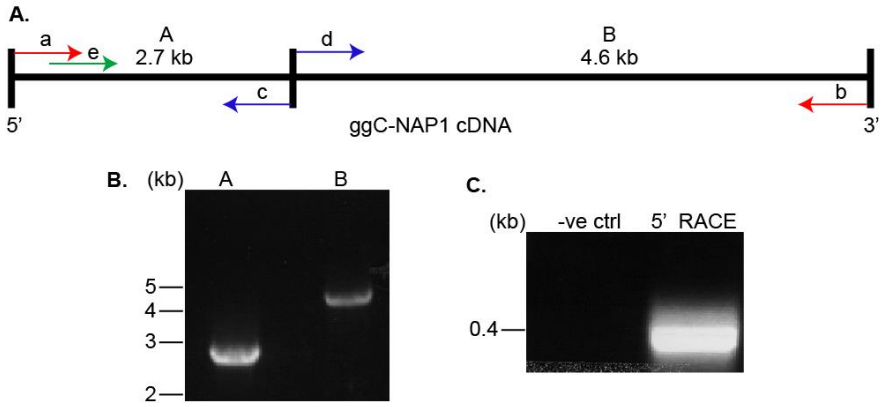

Figure 3.4: Amplification of *C-NAP1* from chicken cDNA. A. Schematic of the chicken *C-NAP1* cDNA. Red arrows a and b indicate primers to amplify to predicted full length cDNA. The green primer e was synthesised to amplify the *C-NAP1* sequence from the highly similar sequence between human and chicken (displayed in Figure 3.5). **B.** *C-NAP1* sections A and B amplification by PCR. C. 5' RACE product (350 bp approx.) amplified using kit anchor primer and RACE primer 3 (SP3).

The new strategy proved successful in amplifying the cDNA (Fig. 3.4B) and the two fragments were sequenced in their entirety (data not shown) and aligned to the main sequence in the NCBI database (XM_417323.4) confirming the transcription of the gene. This proved that the homologous 5' sequence was present in chicken DT40 cells and more importantly, it verified the stop codon of the transcript which gave confidence to the strategy to fuse the C terminus of C-NAP1 with an AID-GFP sequence (Section 3.2.1).

The question of whether the predicted sequence for chicken *C-NAP1* corresponded to the NCBI sequence at the 5' end still remained. We performed a 5' RACE experiment in an attempt to verify the starting methionine of the coding sequence (Fig. 3.4C). Using the 5'/3' RACE kit from Roche, the 5' RACE allowed us to verify more of the cDNA sequence. Reverse primers were designed as directed in the manufacturer's instructions and are indicated in Figure 3.5: the first primer, SP1 - green arrow, second primer, SP2, in blue and the final amplification step was carried out using the most 5' primer (red, SP3).

Figure 3.5: Human and chicken C-NAP1 share high protein sequence identity at their N termini. Highlighted sections indicate regions of particularly high similarity in the first 300 amino acids of the human and chicken sequences. Light grey sequence is the region that was not verified by either cloning or 5'RACE in this project. The green, blue and red arrows are the sequences to which primers SP1, SP2 and SP3 for the 5' RACE were designed. Denotation; *, the same amino acid; :, amino acids with similar side chains; ., amino acids with similar charge.

The alignment above (Fig. 3.5) shows the homology of the chicken protein to the human protein by individual amino acid for the first 300 residues of both proteins. For the chicken sequence, the dark text is the sequence that has been confirmed by cloning and 5' RACE experiments. The light grey sequence corresponds to the amino acids predicted by computational analysis on the NCBI website. The gaps that appear in the chicken sequence are in the middle of predicted exons 1 and 6 respectively. In this figure we can see that there is high sequence identity between the N terminal regions of the human and chicken sequences, with stretches of protein that are exactly the same in both. It is after this region that the homology between the species weakens.

The DNA obtained from the 5' RACE experiment (350 bp, Fig 3.4C) was cloned and sequenced. However the sequence did not extend to the 5' end of the NCBI predicted sequence. There are still 14 amino acids that have not been confirmed at the 5' end sequence of the C-NAP1 protein. We conclude that there is an exon 5' of the chicken sequence confirmed in Figure 3.5 that contains the start codon for the chicken C-NAP1 protein, due to the presence of this highly similar QQQQ region and our inability to clone the predicted start site.

3.3 C-NAP1 localisation and function in DT40 cells

3.3.1 Generation of C-NAP1-AIDGFP cell line

After confirmation of the existence of the *C-NAP1* transcript in the chicken DT40 cell line, we aimed to tag the endogenous locus of the *C-NAP1* gene with an Auxin Inducible Degron (AID) sequence fused to a Green Fluorescent Protein (GFP) tag. The AID system was recently described in Nishimura *et al*, 2009 where they exploited the proteosomal degradation pathway to remove specific proteins from DT40 cells upon the addition of auxin (Nishimura *et al.* 2009). This method would allow us to deplete the protein as desired via addition of indoleacetic acid (auxin), which is a plant hormone present in many eukaryotes. The tag we created fuses the AID tag to a GFP sequence which facilitates the visualisation of the protein during a regular cell cycle. For the design of the targeting strategy, the gene locus of *C-NAP1* (NC_006107.3) from the NCBI database was analysed. A targeting strategy was designed, as depicted in Figure 3.6 and a 5' probe was optimised to verify targeted clones by Southern blot.

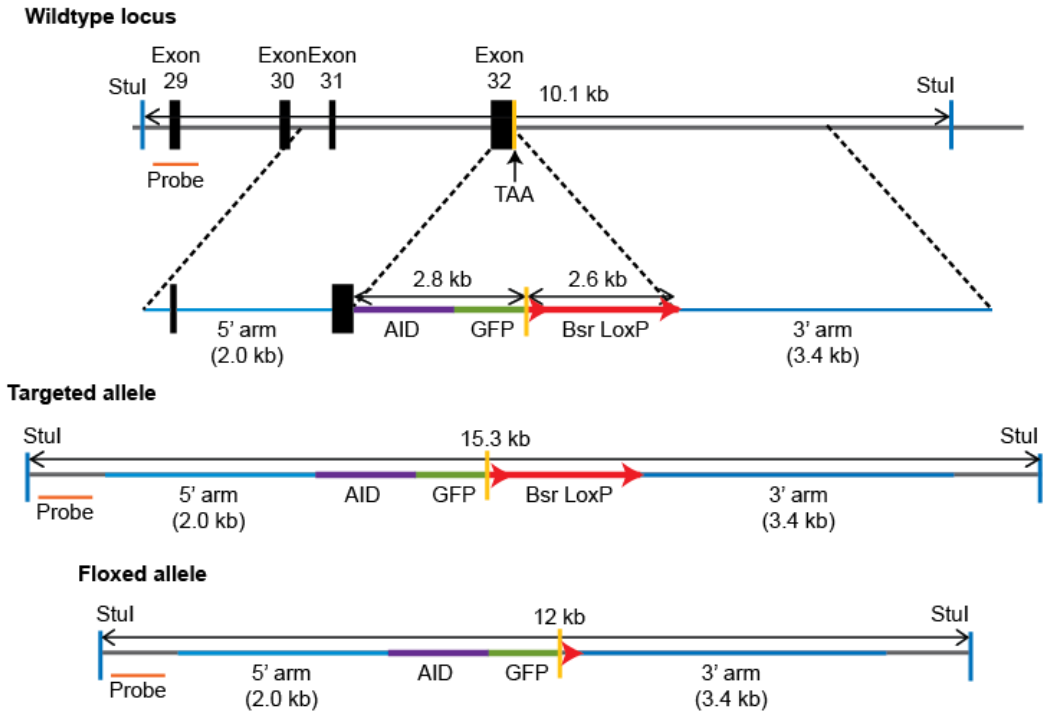

Figure 3.6: Schematic of the *ggC-NAP1* targeting strategy to knock-in AIDGFP. The strategy of targeting *C-NAP1* involved the integration of an AID sequence (purple) fused to GFP (green) in place of the existing stop codon (yellow) for the protein. A resistance cassette, Blasticidin (Bsr, red) was used as selection for correct integration. 5' and 3' arms amplified as part of the targeting vector are indicated in blue, as are StuI restriction sites used for screening clones, the subsequently floxed using the LoxP sites on either end. Clones were screened using a 5' probe (orange). Wild-type alleles were 10.1 kb, targeted alleles were 15.3 kb and floxed alleles were 12 kb.

The 5' and 3' arms of the targeting vector were generated by PCR and the AIDGFP coding sequence was incorporated such that it became continuous with the end of the *C-NAP1* coding sequence when cloned. The stop codon was removed by excluding the bases from the primers for PCR. The targeting arms, AID-GFP coding sequence (generated by cloning in our lab using the AID plasmid from Nishimura *et al*, 2009 and eGFP-N1 (from Clontech) and resistance cassette were assembled by restriction digest and ligation. The sequence of the targeting vector was verified by digestion and by direct sequencing.

3.3.2 Verification of *C-NAP1-AIDGFP* cell line

5' and 3' probes were amplified from genomic DNA by PCR and were labelled using the DIG probe labelling kit (Fig. 3.7A). Analysis of the *C-NAP1* genomic locus by Southern blot using the 5' probe was carried out by digestion of wild-type genomic DNA with AflII, StuI, KpnI and PsiI to verify the location of these sites

(Fig. 3.7B). The use of a number of different enzymes during probe testing allowed us to verify the sequence we had based the targeting vector on was accurate. As expected for AflII, StuI and KpnI, we obtained bands at 10.5 kb, 10.1 kb and 12.1 kb respectively. However, for PsiI, we observed a band above 10kb in addition to the expected size of 6.7 kb. StuI was chosen due to its clean digest and we were able to identify wild-type alleles (10.1kb), targeted alleles (15.3kb) and floxed alleles (12.4kb) (Fig. 3.7C).

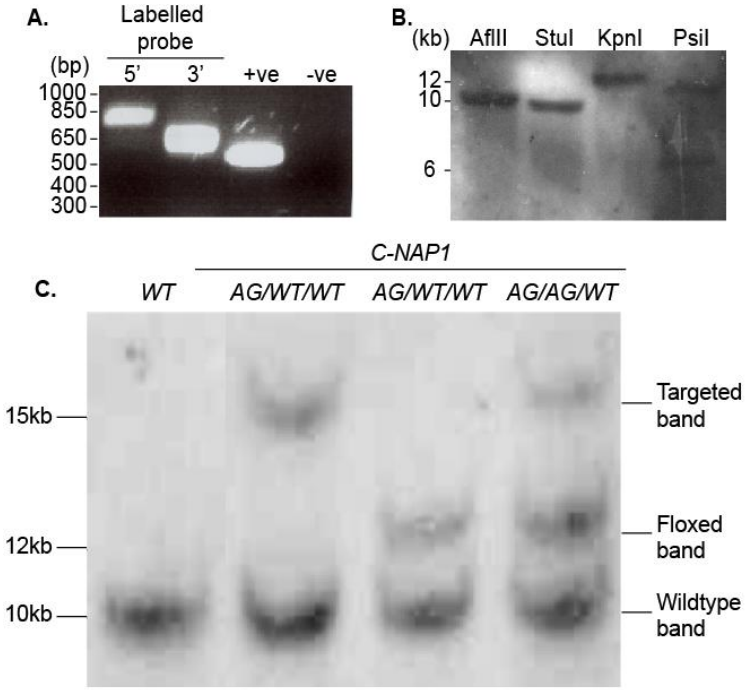

Figure 3.7: *C-NAP1* can be successfully targeted with AIDGFP. A. Gel image of 5' and 3' probe labelling, with positive and negative controls. **B.** Southern blot of 5' probe test using wild-type genomic DNA digested with AflII, StuI, KpnI and PsiI. **C.** Southern blot of wild-type and heterozygote AIDGFP (AG) clones after StuI digest showing wild-type (10.1 kb), targeted (15.3 kb) and floxed (12 kb) alleles detected using a 5' probe.

To avoid disrupting the 3'end of the *C-NAP1* locus, floxing between the LoxP sites on the selection cassette allowed multiple rounds of targeting with the same vector. Probability analysis indicates that retargeting of alleles would reduce *C-NAP1* targeting efficiency but enough targeted clones were obtained in order to continue with the strategy. After two rounds of targeting we observed the continued presence of a wild-type allele in all of the clones that already had one targeted and one floxed allele. We speculated that the *C-NAP1* locus had three copies in chicken cells and proceeded to target the third allele. This speculation turned out to be accurate and the third allele was successfully targeted, despite a low efficiency of the targeting event.

Southern blot analysis of clones obtained after transfection revealed targeted alleles, with the efficiency using the Blasticidin cassette indicated in Table 13. There was a high efficiency in targeting the *C-NAP1* locus when targeting the first of the alleles (82%). However, as one would expect, this frequency declined with targeting the second and third alleles, to 47% and 13% respectively. The floxing efficiency was similar for both rounds, at approx. 33%.

Table 13: Targeting efficiencies of C-NAP1^{AIDGFP} cell line generation.

Targeting Event	Selection	No. of clones targeted	No. of clones screened	Targeting Efficiency
***C-NAP1* 1st Allele**	Blasticidin	14	17	82%
1st Allele Floxing	(Limiting dilution)	6	17	35%
***C-NAP1* 2nd Allele**	Blasticidin	37	78	47%
2nd Allele Floxing	(Limiting dilution)	11	34	32%
***C-NAP1* 3rd Allele**	Blasticidin	8	60	13%

Before we can knock-down the protein in the *C-NAP1-AIDGFP* protein in the targeted cells TIR1 (Transport inhibitor response 1) must be present to form the link between the auxin molecule and the SCF (Skp, Cullin, F-box containing complex) protein complex which is necessary to polyubiquitinate the C-NAP1, marking it for degradation by the proteasome. Integration of the TIR1 coding sequence by random integration was highly efficient (83%) with 7 of the 17 positive clones exhibiting high TIR1 expression by Western blot. Of the *C-NAP1-AIDGFP::TIR1* positive clones, two were selected for further analysis. First, western blot to detect a band of the correct size and to verify the functionality of the AID and GFP tags was carried out. The GFP tagged C-NAP1 was expressed and migrated at a rate slower than the 250 kDa marker (Fig. 3.8). Immunoblotting for C-NAP1-GFP required the loading of 100 µg of cell lysate per lane due to its low abundance in cells, hence there is an overloading and overexposure of the α-tubulin loading control at 55 kDa. The addition of auxin at 0 minutes was followed by the rapid depletion of the GFP tagged form of the C-NAP1 protein.

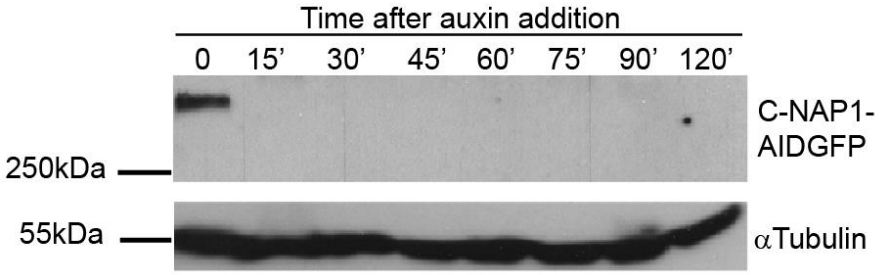

Figure 3.8: C-NAP1-AIDGFP can be detected by Western blot and is degraded within 15 minutes after the addition of 0.5 mM auxin. C-NAP1-AIDGFP is recognised using a mouse anti-GFP antibody and migrates at a size above 250 kDa on a SDS-PAGE gel. α-Tubulin is blotted as a loading control.

We then examined the proliferation capacity of the cells when placed under auxin compared to the untreated C-NAP1-AIDGFP control cell line and wild-type cells for 2 independent clones (Fig. 3.9). Cell proliferation was unaffected by the auxin-mediated C-NAP1-AIDGFP depletion. Cells where C-NAP1 has been depleted via AID tag are given the nomenclature "C-NAP1^{off}", cells with C-NAP1-AIDGFP intact are named "C-NAP1^{on}".

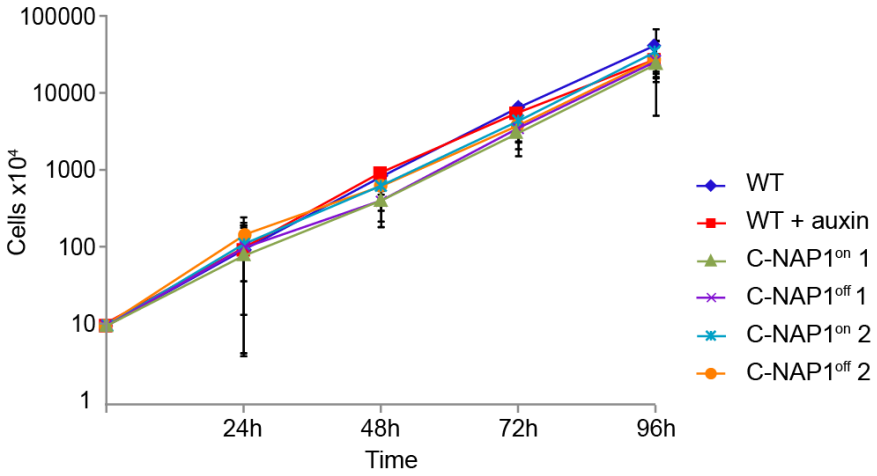

Figure 3.9: Auxin mediated depletion of C-NAP1-AIDGFP has no effect on cell proliferation. Cells were plated on day 0 at 5 x10^4/ml in auxin containing media (where required) for wild-type (WT) and C-NAP1^{on} clones 1 and 2. The cells were counted and split 1 in 3 every day for 4 days, for which the graph was corrected. N=3, error bars indicate s.d.

Next, immunofluorescence microscopy was performed to visualise the localisation of the tagged protein in the cell (Figure 3.10). The GFP tagged protein co-localised with a number of centrosomal proteins, as indicated in the panels on the left side of Figure 3.10. Centrin 3 staining of the lumen of the centrioles in both cases shows the

distal centriole structure is intact (Paoletti *et al.* 1996). Cep135 staining for the proximal ends of the microtubule barrels shows the centrioles have maintained their structure at the ends normally tethered by C-NAP1 (K. Kim *et al.* 2008). γ-Tubulin constitutes part of the pericentriolar material (PCM) and is located around the proximal regions of both centrioles (Bobinnec *et al.* 1998). Figure 3.10 shows that γ-tubulin maintains its pericentriolar localisation in both the knockout clone and in the AIDGFP tagged controls. The mother centriole is identified using antibodies to the appendage protein ninein and in both C-NAP1^{on} and C-NAP1^{off} cells; the mother centriole can be clearly identified (Ou *et al.* 2002). Centriolar satellites in DT40 cells are clustered quite tightly around the centrosome and, in the absence of C-NAP1, this distribution is maintained as seen by staining cells with antibodies to the satellite protein PCM1 (Dammermann and Merdes 2002). We can conclude from this data that the structure of the centrosome and localisation of the core centrosomal proteins is unaffected by the tagging and removal of C-NAP1.

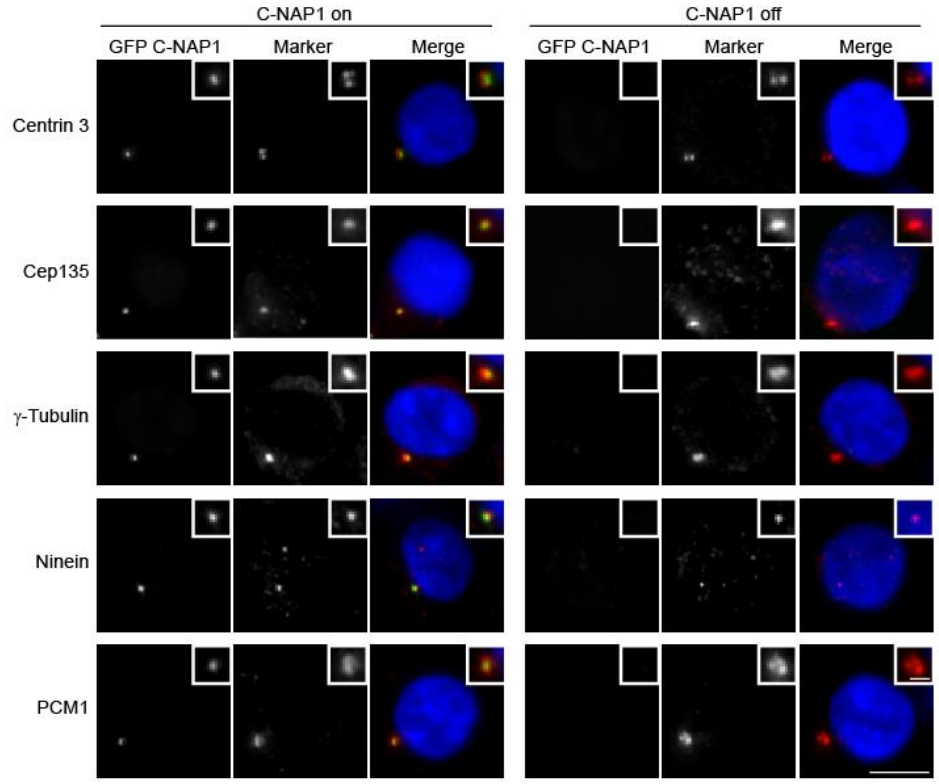

Figure 3.10: Auxin mediated depletion has no detectable effect on centrosome composition or structure by IF microscopy. C-NAP1^{on} and C-NAP1^{off} homozygote clones were stained with antibodies to the centriolar markers centrin3 and Cep135, the PCM marker γ-tubulin, the mature centriole marker, ninein, and PCM1, which localises to the centriolar satellites. (Scale bar: 5μm. Inset scale: 1 μm).

3.3.3 Centrosome cohesion in C-NAP1^{off} cells

We can see in Figure 3.7 that the centrioles remained in close proximity even in the absence of C-NAP1. It has been previously shown that the centrioles can be prematurely separated through microinjection of anti-C-NAP1 antibodies or RNA interference (Mayor *et al.* 2000, Bahe *et al.* 2005). We set out to explore centriolar cohesion in the C-NAP1-depleted DT40 cells. Using centrin 3 as a marker for the centrioles, we measured the difference in intercentriolar distance between C-NAP1^{on} and C-NAP1^{off} cells. Analysis of 30 C-NAP1^{on} cells and 30 C-NAP1^{off} cells showed no difference in the number of separated centrosomes between the populations (Figure 3.11). The centrioles remained on average 0.5µm apart, with the distance ranging from 0.3µm to 0.7µm.

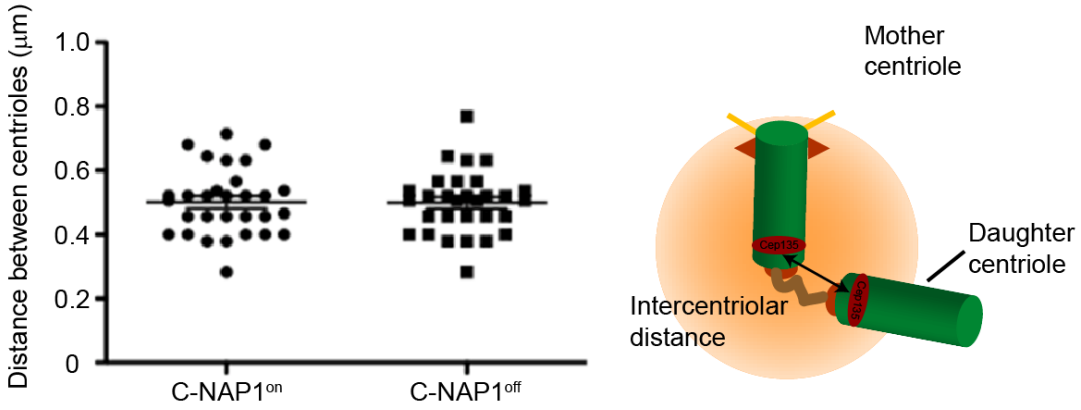

Figure 3.11: Centriole separation is unaffected in C-NAP1^{off} cells. 24 hr after the addition of auxin, 30 cells were measured for both C-NAP1^{on} and C-NAP1^{off} conditions using the line tool on Volocity analysis software. As illustrated in the schematic on the right, centrioles were identified using centrin3 to stain the centriolar lumen of both centrioles. n=3 separate experiments in which 10 cells were examined, error bars indicate s.d.

This result was unexpected, given the strong splitting phenotype observed previously (Mayor *et al.* 2000, Bahe *et al.* 2005). We thought it could be possible that the centrosomes in DT40 cells are smaller and the structure of the whole centrosome could be more compact, and that this would mask our ability to analyse the centriole separation distance. We then looked to electron microscopy (EM) to provide higher resolution in order to perform intercentriolar distance measurements.

EM analysis of the ultrastructure of the centrosome 24 hours after C-NAP1 depletion (Figure 3.12) confirms the cartwheel structure of the centrioles is not disrupted in the

absence of C-NAP1. Analysis of the 4 cases where both centrioles were present in the same section showed that these centrosomes held their centrioles within 2 μm of each other. This observation confirmed that centrosome cohesion is maintained, despite the loss of C-NAP1-AIDGFP.

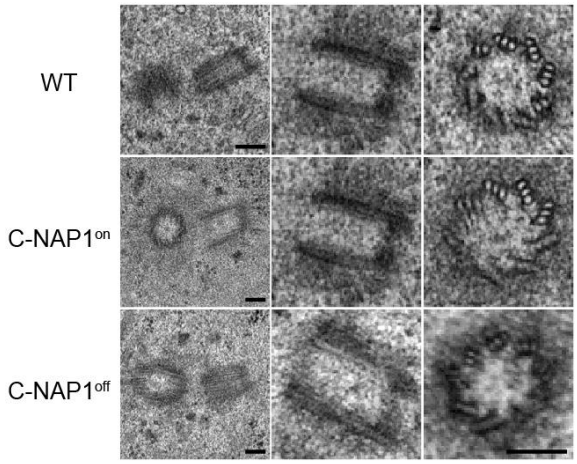

Figure 3.12: No ultrastructural difference is observed between C-NAP1^{on} and C-NAP1^{off} cells. Wild-type, C-NAP1^{on} and C-NAP1^{off} cells (24h after auxin addition where necessary) were fixed and embedded for transmission electron microscopy. Sections were analysed for centrosome, centriolar barrel and microtubule triplet structure integrity. Scale bars: 200 μm.

3.3.4 Centrosomal responses to DNA damage after C-NAP1 depletion

Genomic stability is necessary for continued cell proliferation. Much like DNA must be segregated equally into daughter cells, centrosomes must also be divided in a specific manner. Double strand breaks (DSBs) are the most serious form of DNA damage and must be repaired as quickly and accurately as possible. In addition to mediating DNA repair, the DNA damage response (DDR) in cells can either cause structural changes or unwanted amplification of centrioles (Fletcher and Muschel 2006).

Examination of the DNA damage response in C-NAP1^{on} and C-NAP1^{off} cells displayed a slight difference in relation to their ability to amplify centrioles in response to ionising radiation (IR) or hydroxyurea (HU) treatment (Figure 3.13). For analysis of centrosome amplification after ionising radiation, wild-type, C-NAP1^{on} and C-NAP1^{off} cells were subjected to 5 Gy IR and stained with antibodies to centrosomal proteins and the number of centrosomes per cell then counted (Fig. 3.14). There was also no change in the centrosome amplification capacity of the C-NAP1^{off} cells compared to C-NAP1^{on} cells. Hydroxyurea treatment did not significantly affect the ability of C-NAP1^{off} cells to amplify their centrosomes after

18 hours, but there is a slight decrease in the number of cells with amplified centrosomes on C-NAP1^{off} cells after 21 and 24 hours (Fig. 3.13B). The number of cells with greater than 2 centrosomes was slightly reduced after both treatments however since the experiment was only performed once it is difficult to know if there is any significant difference between the samples. The fact that centrosome cohesion was intact which made it difficult to draw conclusions about the function of C-NAP1 in DT40 cells.

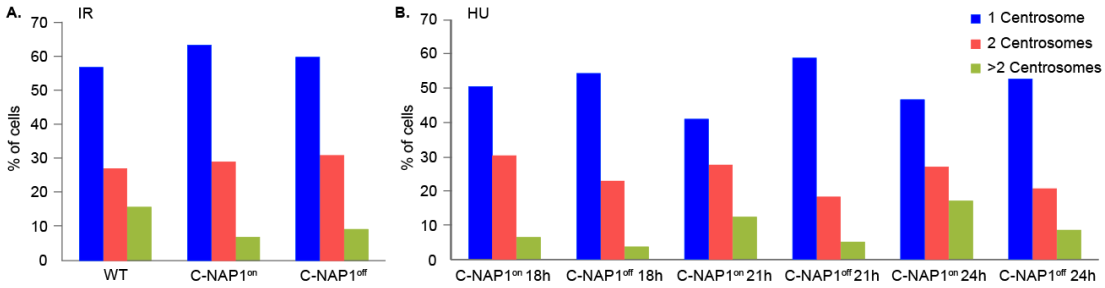

Figure 3.13: C-NAP1 deficient centrosomes are not significantly amplified after exposure to DNA damaging agents. A. Cells were treated with 0.5 mM auxin for 2h before exposure to 5Gy IR. Cells were harvested for IF after 8h and stained with antibodies to centrin3 and PCM1 to count centrosomes. **B.** Cells were treated with 0.5 mM auxin for 2h before incubation with 2 mM hydroxyurea. Cells were harvested for IF at the indicated times and stained with antibodies to Cep135 and γ-tubulin and the number of centrosomes counted. n=1 for both experiments, where 200 cells were examined in each case.

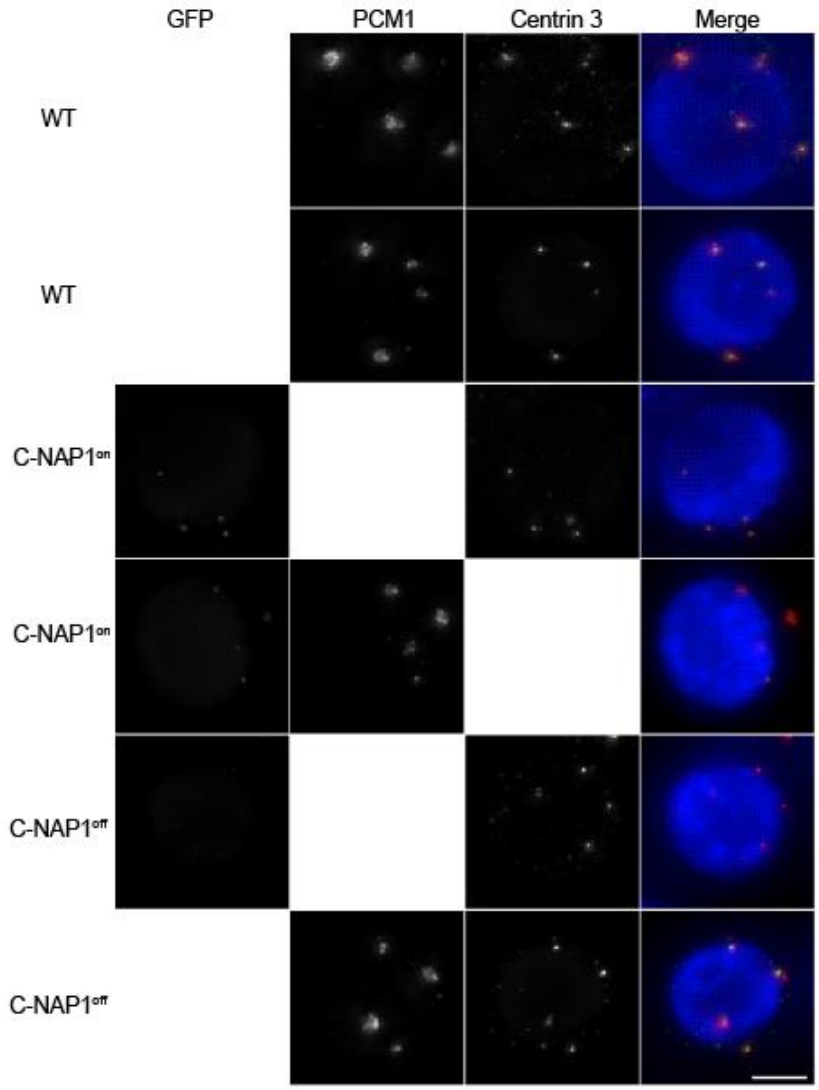

Figure 3.14: IF of wild-type (WT), C-NAP1^{on} and C-NAP1^{off} DT40 cells after 5Gy IR. Wild-type cells are stained with antibodies to PCM1 and centrin3. C-NAP1^{on} cells express C-NAP1-AIDGFP combined with Centrin 3 and PCM1 staining. C-NAP1^{off} cells are stained for centrin3 only and PCM1 and centrin3. Scale bar: 5µm.

In summary, investigation of the *C*-NAP1 locus allowed the identification and cloning of the C-NAP1 CDS and this was then verified by sequencing. For the purpose of investigating the function of C-NAP1 in chicken cells, use of the AIDGFP tag system to degrade the protein did not have an effect on centrosome cohesion. Unfortunately there is no antibody available that can detect chicken C-NAP1 by IF or Western blot. If this were possible then we could determine if the entire protein was degraded or if it was just the tag that somehow became detached and degraded. Analysis of the centrosomal response to DNA damage in these cells did not reveal a difference between C-NAP1^{on} and C-NAP1^{off} cells.

4. Results: Disruption of human C-NAP1

4. Disruption of human C-NAP1

To assess the functional importance of the of C-NAP1in human cells, we generated C-NAP1 knockout cells using CRISPR/Cas9 genome editing. Analysis of centrosome cohesion defects in hTERT-RPE1 cells verified a previously described role for C-NAP1, which were not present in the DT40 model system after C-NAP1 depletion.

4.1 Analysis of the *HsC-NAP1* locus

Identification of the *C-NAP1* locus in the human genome was carried out using the NCBI database. Chromosome 20 was found to be the site of the gene and we have already seen that the surrounding genes are the same as the chicken locus (Fig. 3.1). As was the case with the chicken locus, the human *C-NAP1* analysis described a number of predicted isoforms of the protein. One of these isoforms has been verified by a number of groups, including the Nigg lab where the protein was first characterised (Fry *et al.* 1998). This isoform has a spliced mRNA sequence of 8341 bp in length and is divided into 32 coding exons and 4 exons forming the 5' and 3' UTR regions on a locus of 62 kb. The 5' UTR region of 647 bp makes the first 3 exons and the 3' UTR of 365 bp is comprised of a single exon with the coding sequence spanning 7328 bp. Figure 4.1 shows the layout of these exons in the gene and of note is exon 27 which, as with exon 28 in the chicken gene, is much larger than the other exons.

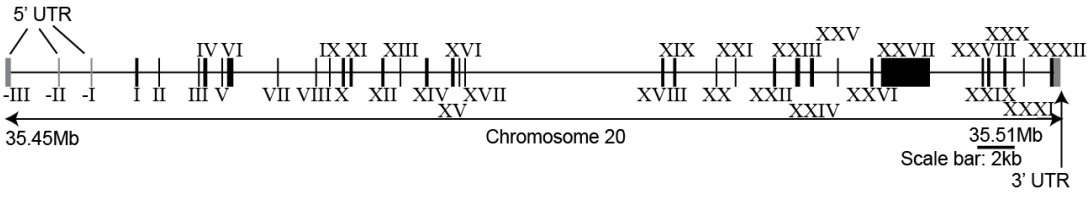

Figure 4.1: Schematic of the human *C-NAP1* genomic locus. Exons (black boxes) and introns (connecting lines) and the 5' and 3' UTR regions (grey) are indicated. Exon numbers are indicated with Roman numerals.

All the isoforms for human C-NAP1 are listed in Table 14 and share between 95 and 100% sequence identity. We can see that for most of the isoforms, a C-NAP1 protein which is similar in length to the verified isoform is predicted. The X2 and X3 isoforms are the most similar, with X4 and X5 next in line due to changes in their 5' UTR regions, which contain only 2 of the 3 5' UTR exons. The X6 isoform is

missing coding exons 18 and 28, and isoforms X8 and X10 have extended 3' UTR regions as predicted by automated computational analysis. X11, X12 and X13 have extra coding sequence, 5 bp, 32 bp and 3 bp respectively and also use alternative translation initiation sites (further 3' of the starting methionine for the more similar isoforms) causing them to differ even more from the verified sequence as a result. The X14 isoform is much shorter than the other isoforms, where the starting methionine is further downstream of the consensus methionine and a stop codon is located just prior to the sequence coding for the large exon 27. From this analysis we can see the differences in the predicted *C-NAP1* transcripts, but due to the large size of the protein it is unlikely that the minor discrepencies which result in the slightly lower sequence identity of some transcripts would cause a change in the functional capacbilities of the protein.

Table 14: Comparative analysis of the predicted *C-NAP1* isoforms in the human genome. Analysis of the 14 human *C-NAP1* isoforms transcript length, CDS length and UTR length.

Isoform name	NCBI accession number	Transcript length	CDS length (bp)	5' UTR sequence length (bp)	3' UTR sequence length (bp)
1 (verified)	NM_007186.4	8341	7328	648	365
X2	XM_006723690.2	8073	7328	397	348
X3	XM_006723691.1	8290	7328	614	348
X4	XM_006723692.2	7997	7328	321	348
X5	XM_006723693.2	7985	7328	309	348
X6	XM_006723694.2	7962	7214	400	348
X8	XM_005260263.3	8014	7112	400	502
X9	XM_005260264.3	7844	7097	399	348
X10	XM_011528517.1	10411	7067	400	2944
X11	XM_011528518.1	8080	6959	773	348
X12	XM_011528519.1	7202	6722	132	348
X13	XM_005260265.2	7626	5432	1846	348
X14	XM_011528520.1	4297	3812	401	84

4.2 Cloning and overexpression of C-NAP1

Once the *C-NAP1* locus had been identified and the verified transcript analysed we designed primers in order to clone the entire cDNA. For fidelity and ease of handling reasons, the *C-NAP1* cDNA sequence was divided into 5 sections that could be

easily amplified and ligated together based on restriction endnoclease sites that were already present in the sequence. The entire length of the cDNA is 7.3 kb with the length of the fragments ranging from 700 bp to 1.9 kb. Figure 4.2A indicates the length of the respective fragments A to E and their location on the full length cDNA. RNA was extracted from hTERT-RPE1 cells and converted to cDNA. The fragments were amplified using primers listed in Table 7, named C-NAP1 1 to C-NAP1 10, with primers 1 and 2 amplifying fragment A, 3 and 4 amplifying fragment B and so on (Fig. 4.2B). The full length sequence was then cloned into the pcDNA 3.1 (+) vector that had been modified to include a sequence encoding blasticidin resistance in the site of the neomycin cassette in the original plasmid (Fig. 4.2C). The plasmid sequence was then verified by sequencing.

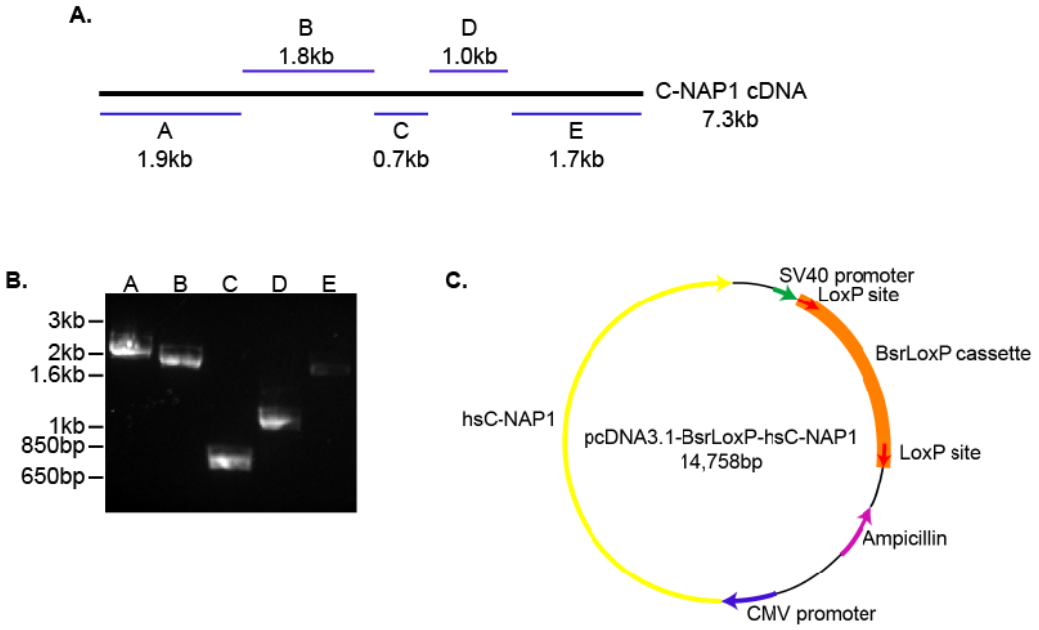

Figure 4.2: *C-NAP1* amplification and cloning into pcDNA 3.1(+)-BsrLoxP. A. *C-NAP1* fragments A to E and their sizes and location relative to the full length C-NAP1 cDNA sequence. **B.** Agarose gel separation of the amplified *C-NAP1* fragments from **A. C.** Schematic of the final pcDNA3.1-BsrLoxP-hsC-NAP1 plasmid indicating the CMV promoter, ampicillin resistance marker for bacterial propagation and the blasticidin resistance cassette for mammalian selection.

4.3 Novel C-NAP1 antibody and RNA interference of *C-NAP1*

To detect C-NAP1, a novel monoclonal antibody (named 6F2 C8) generated in our lab was used. The antibody was raised against a region towards the C terminal of the protein (Fig. 4.3A). 6F2 C8 can detect C-NAP1 at the centrosome by immunofluorescence. siRNA-mediated depletion of C-NAP1 confirmed the

specificity of the antibody, as there was no antibody signal found to co-localisation with centriole marker Cep135 after transfection of RPE1 cells with 100nM siC-NAP1 (Fig. 4.3B).

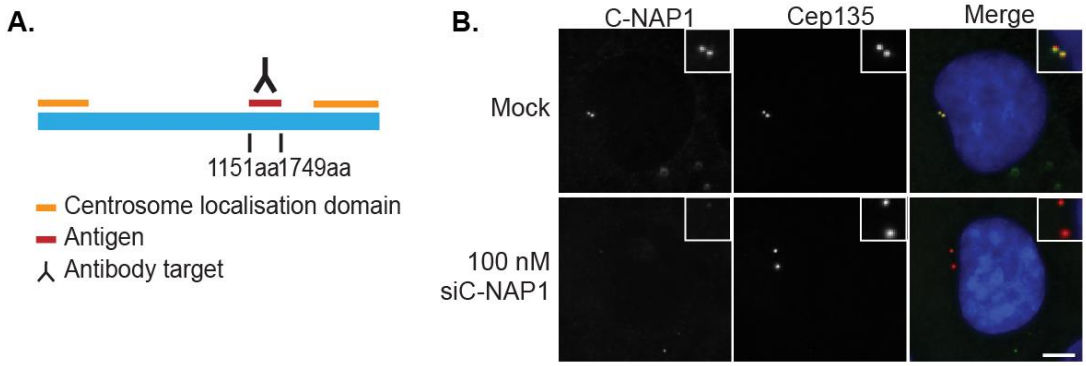

Figure 4.3: A novel monoclonal antibody (6F2 C8) is specific for C-NAP1. A. Schematic of the antigen site on full length C-NAP1 sequence (blue bar) which is recognised by the 6F2 C8 antibody. **B.** 6F2 C8 anti-C-NAP1 specifically detects C-NAP1 at the centrosome (top panels). 100nM siRNA depletion of C-NAP1 diminishes C-NAP1 visualisation at the centrosome using 6F2 C8. Scale bar: 5μm.

In order to verify the specific depletion of C-NAP1 and to confirm the specificity of the 6F2 C8 antibody, western blot following transfection of 50 and 100 nM concentrations of siRNA duplexes that inhibit C-NAP1 was performed. C-NAP1 was no longer detectable by western blot when probed with 6F2 C8 (Fig. 4.4A). GAPDH knockdown verified the transfection; α-tubulin was used as a loading control. Centrosome splitting was increased in the case of C-NAP1 knockdown cells compared to mock-transfected RPE1 cells (Fig. 4.4B). The presence and absence of the a high molecular weight band before and after C-NAP1 knockdown by IF and western blot, combined with the observed increase in centrosome splitting verified the specificity of the 6F2 C8 C-NAP1 antibody.

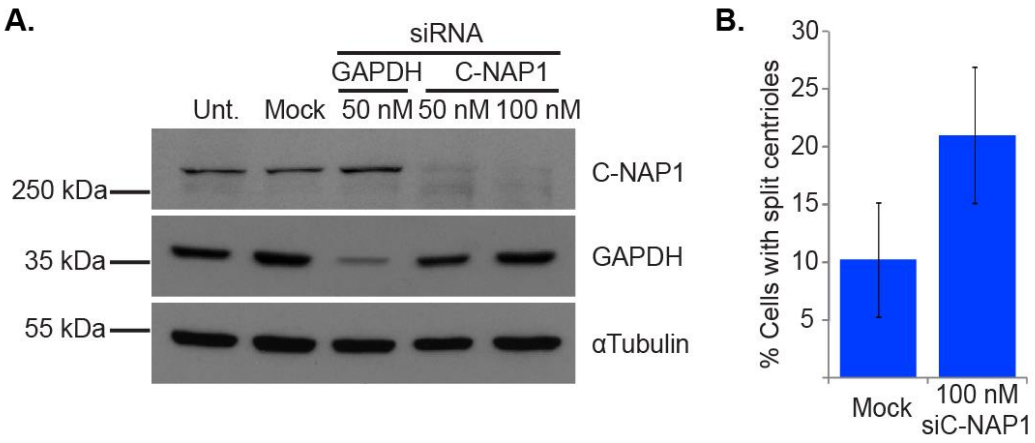

Figure 4.4: siRNA depletion of C-NAP1 is detectable by western blot using anti-C-NAP1 6F2 C8 antibody in RPE1 cells, with depletion resulting in an increase in the percentage of cells with split centrosomes. A. Western blot of siRNA transfection shows depletion of C-NAP1 and GAPDH using 50 and 100nM concentration of *C-NAP1* siRNA. αtubulin is used as a loading control. **B.** Split centrosomes were counted in 200 cells using Cep135 staining for mock and 100nM C-NAP1 depletion. N=3.

4.4 C-NAP1 detection and overexpression in hTERT-RPE1 cells

To test the functionality of the C-NAP1 in the pcDNA3.1-BsrLoxP-hsC-NAP1 plasmid, the DNA was transfected into wild-type hTERT-RPE1 cells (Fig. 4.5). Transient overexpression of the protein resulted in the formation of cytosolic aggregates that stained positive for C-NAP1 using the monoclonal 6F2 C8 anti-C-NAP1 antibody generated in our lab. The C-NAP1 signal co-localised with γ-tubulin at the centrosome, indicating a previously documented cellular localisation pattern of C-NAP1 in RPE1 cells (Fry *et al.* 1998, Mayor *et al.* 2000). While localisation to the centrosome was observed, there is also a high level of aggregation of the overexpressed protein in the cytoplasm. C-NAP1 overexpression was also detected at the expected size by Western blot using α-tubulin as a loading control. It has been previously shown that centrosome cohesion and cell cycle progression are unaffected by C-NAP1 overexpression, indicating that the plasmid encodes a functional C-NAP1 protein (Mayor *et al.* 2002).

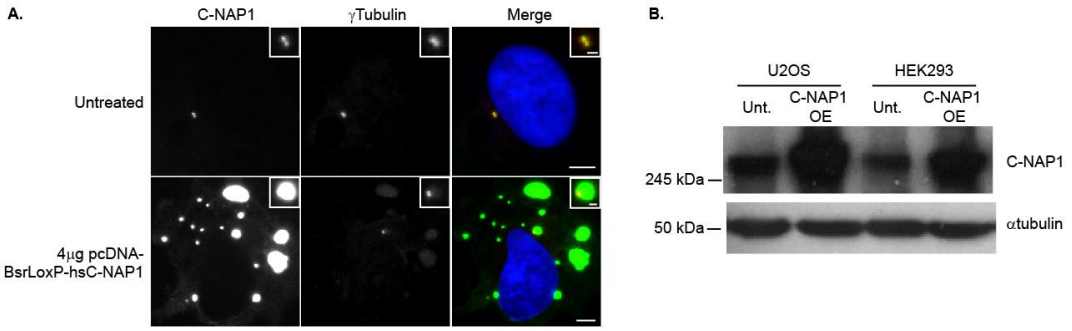

Figure 4.5: *C-NAP1* can be overexpressed in hTERT-RPE1, U2Os and HEK293 cells. A. WT RPE1 cells ($0.5x10^6$) were transfected with 4μg pcDNA3.1-BsrLoxP-hsC-NAP1for 48 hours before fixation and staining with 6F2 C8 (green) and γ-tubulin (red). Scale bar: 5μm. Insets show the two-fold enlargement of the centrosome in each cell, scale bar: 1μm. **B.** U2OS and HEK293 cells were transfected with pcDNA3.1-BsrLoxP-hsC-NAP1 then lysed for western blot after 48 hours.

4.5 Targeting *C-NAP1* using CRISPR/Cas9 in hTERT-RPE1 cells

As described previously, CRISPR/Cas9 genome editing technology has allowed the manipulation of DNA in order to investigate gene function. We employed this method in order to examine the function of C-NAP1 and also the consequences of its removal. Using the http://arep.med.harvard.edu/human_crispr/ website, forward and reverse oligos were designed in order to target exon 8 of the *C-NAP1* transcript (exon 5 of the protein) for editing (Fig. 4.6). The sequence of the oligos (CRISPR targ. 1 and 2) are listed in Table 7 (materials and methods section) and their assembly into the pX330 plasmid is described in section 2.3.5. The plasmid was co-transfected with a neomycin resistance cassette and stable clones were obtained. Cell lysate, genomic DNA and samples for immunofluorescence microscopy were harvested from three of the clones and analysed.

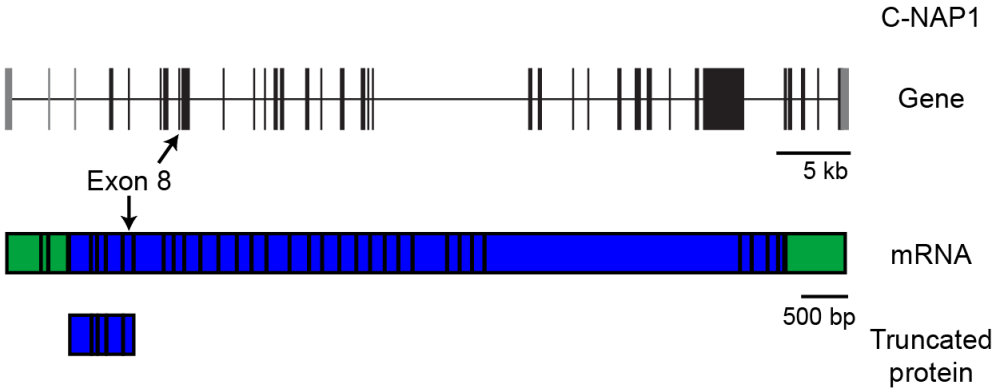

Figure 4.6: Targeting *C-NAP1* using CRISPR/Cas9 editing. Schematic of the *C-NAP1* genomic locus and spliced mRNA sequence showning the location of the CRISPR/Cas9 target site. The length of the truncated protein in relation to the mRNA sequence length shows a large region of the protein will not be expressed after targeting.

As we can see from the Western blot in Figure 4.7A, C-NAP1 is no longer expressed in its full form, which can be seen clearly in the lane containing wild-type cell lysate. Unfortunately the 6F2 C8 monoclonal antibody cannot be used to detect the truncated C-NAP1 protein due as the antigen used to generate the antibody is outside the region of the shorter protein. IF staining using the same anti-C-NAP1 antibody also indicates that the protein can no longer be detected at centrosomes (identified using an anti Cep135 antibody) (Fig. 4.7B).

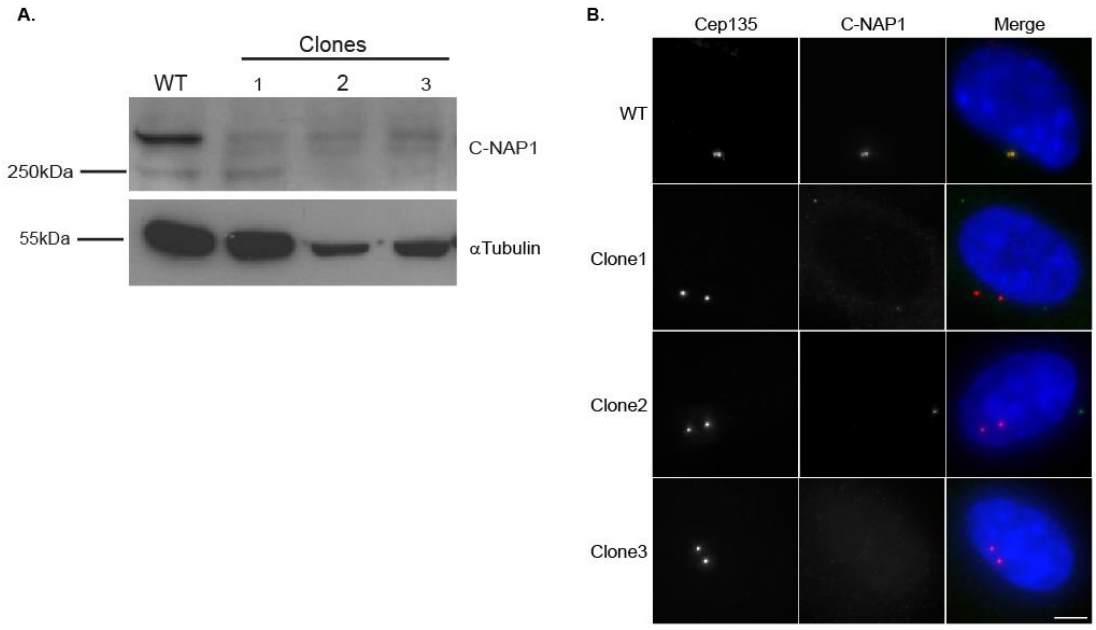

Figure 4.7: Generation of C-NAP1 deficient hTERT-RPE1 cells. A. Western blot for C-NAP1 in WT and C-NAP1 null clones 1, 2 and 3. **B.** IF micrographs of wildtype RPE1 cells and *C-NAP1* disrupted clones 1, 2 and 3 stained for C-NAP1 and Cep135. Scale bar: 5μm.

We then analysed the exact genomic site of the Cas9 mediated DNA alteration by amplifying a 500 bp section of the *C-NAP1* locus by PCR surrounding the exon 8 (in relation to the mRNA sequence) target site using CRISPR screen forward and reverse (fwd and rev) primers. The purified PCR product was then sequenced using the CRISPR screen fwd and rev primers (Table 7) to analyse the sequence of *C-NAP1* after Cas9 activity. The sequencing traces of the total PCR products for wild-type cells and the three clones deemed positive by Western blot and IF reveal the exact modifications that occurred after the Cas9 cleavage (Fig. 4.8).

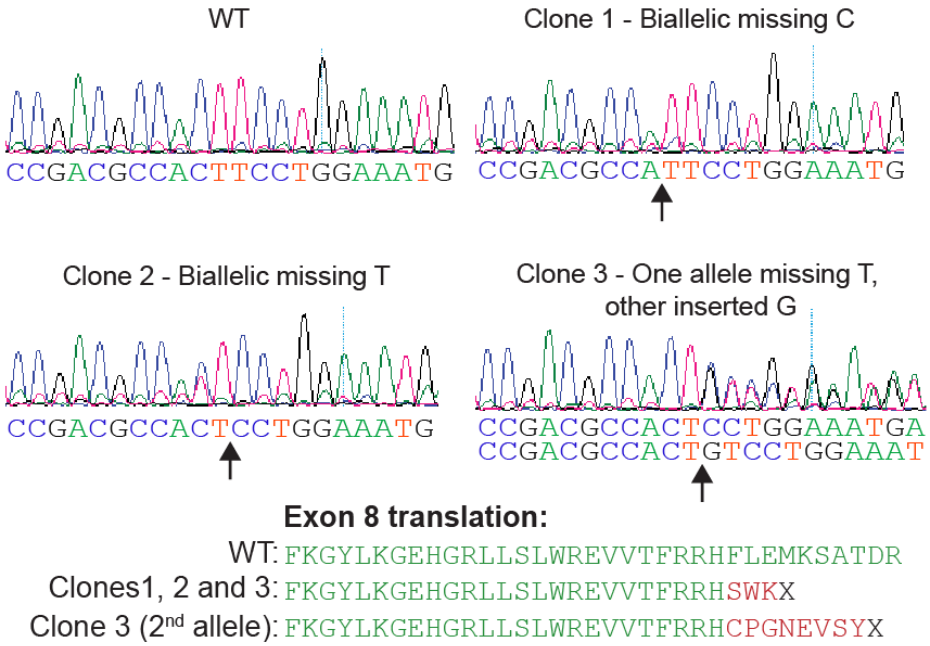

Figure 4.8: Sequence traces of RPE1 clones with depleted C-NAP1 indicate the frameshift resulting from insertions/deletions after CRISPR/Cas9 endonuclease reaction. Insertion/deletion sites are indicated with a black arrow below the sequence traces for each clone. Nucleotide sequences for each PCR product corresponding to the trace peaks are positioned beneath each peak. Translation of exon 8 of C-NAP1 in WT RPE1 cells and C-NAP1 depleted clones reveals the location of premature stop codons. Green text indicates database sequence, red text shows the sequence translated after CRISPR targeting, X indicates a stop codon.

The traces from the total PCR product for clones 1 and 2 show single peaks all the way throughout the section displayed. This indicates that the same alteration in the DNA occurred on both alleles, making them homozygous. Clone 1 has a missing cytosine and clone 2 has a missing thymine. The third clone has double peaks after the Cas9 target site, which indicates a heterozygous mutation. DNA amplified from the three clones and the wild-type cells was also cloned into pGEM-t Easy and sent for sequencing using the T7 and SP6 primers which flank the vector multiple cloning site (MCS) on 5' and 3' sides of the insert respectively. This allowed us to ascertain the individual mutations on each allele. 5 individual samples for each cell line were analysed and these confirmed the results observed for clones 1 and 2, with all 5 samples returning the same sequence. For the third clone, the sequencing clarified the modifications that had taken place on the individual alleles. For 3 of the 5 samples, there was a missing thymine and for the other 2 there was an extra guanine residue. To see what this resulted in for the C-NAP1 protein in these cells the DNA sequence for exon 8 from these clones was translated using the ExPASy Translate tool (Fig. 4.8).

For all clones, there arises a stop codon before the end of exon 8, resulting in the production of a truncated C-NAP protein 190 amino acids in length with a predicted weight of 22kDa. Clones 1 and 2 and one of the alleles of clone 3 have an extra 3 non-C-NAP1 amino acids before reaching a stop codon, whereas the other allele of the third clone has 8 extra amino acids that add another 1 kDa to the predicted weight of the protein. The length and weight of the shortened C-NAP1 protein is less than a tenth of the wild-type protein and is unlikely to be sufficient to carry out the functions of the full-length protein to any great extent.

Proliferative analysis of clones 1 and 2 (referred to as Clone1 and Clone2 from this point forward) indicated no harmful effect of C-NAP1 deficiency on cell doubling times when compared to wild-type cells (Fig. 4.9). Clone 1 has a doubling time of 26 hours 50 minutes, which is very close to the wild-type doubling time of 26 hours 28 minutes. Clone 2 has a slightly longer cell cycle, of 29 hours 7 minutes.

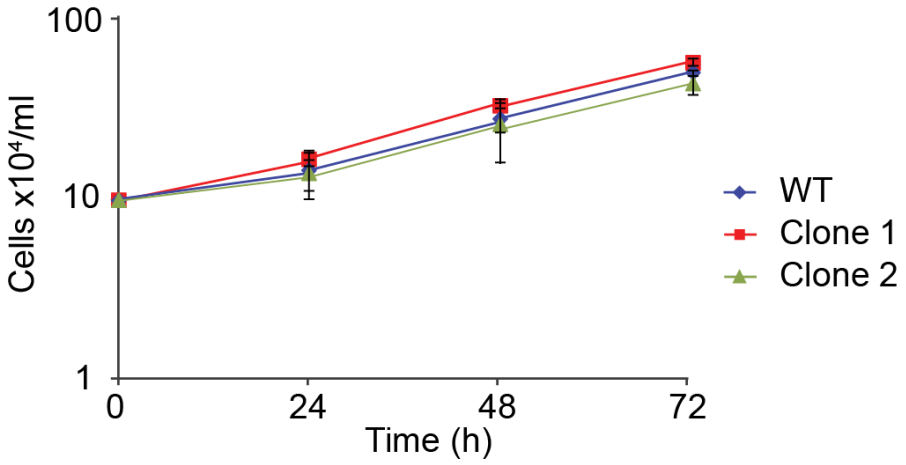

Figure 4.9: C-NAP1 deficient cells have no defect in cell proliferation. Cells were plated at 10 x104/ml and counted every 24 hours for 72 hours. N=3, error bars indicate s.d.

Analysis of the cell cycle profiles of the 3 clones by FACS using PI staining revealed no difference between the DNA content and the percentage of cells in the different stages of the cell cycle (Fig. 4.10). Figure 4.10B is a quantification of the percentage of cells in G1, S and G2/M phases of the cell cycle for each of the C-NAP1 disrupted clones. The number of cells in G1 is slightly higher in the Clone 1 population and there are a greater percentage of Clone 2 cells in G2/M. Clone 3 cells show the same percentage of cells in S and G2/M. Although the experiment was only preformed once, we can see that in both cases, the cell cycle profile differences are not radically

different from the wild-type sample, indicating no significant change in cell cycle in C-NAP1 deficient cells.

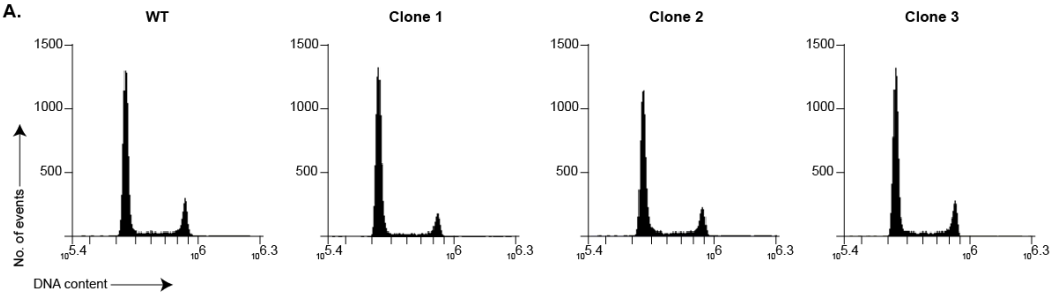

B.

Cell line	Cell cycle stage		
	G1	S	G2/M
WT	69.3%	16.4%	14.7%
Clone 1	75.7%	11%	13.7%
Clone 2	65.9%	14.6%	20.9%
Clone 3	68.4%	16%	16.2%

Figure 4.10: C-NAP1 depleted clones show no defect in cell cycling. A. Wild-type RPE1 cells and C-NAP1 depleted cells from Clones 1, 2 and 3 were stained with 20μg/ml PI and sorted by FACS. 10,000 cells were analysed for each cell line. **B.** Based on the cell cycle profiles in A., the percentage of cells in each stage of the cell cycle was measured using Accuri C6 Sampler software.

We next investigated the impact of permanent C-NAP1 loss on centrosome cohesion. Figure 4.7B demonstrates the marked increase in split centrioles in C-NAP1 deficient cells when compared to wild-type hTERT-RPE1 cells. In all three clones we can see that C-NAP1 deficiency causes a significant increase in the number of centrosomes where the centrioles are greater than 2 μm apart (Fig. 4.11). The percentage of split centrosomes in wild-type cells is 6%, which increases to 42% for Clone 1, 38% for Clone 2 and 36% for Clone 3. This confirms previous observations of centrosome splitting seen after siRNA knockdown of C-NAP1 (Fry *et al.* 1998, Conroy *et al.* 2012).

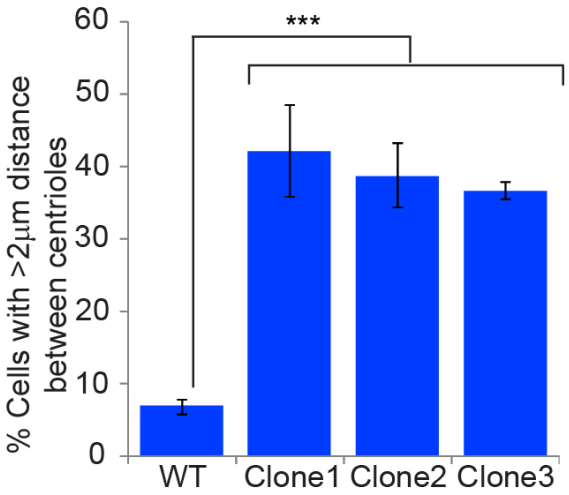

Figure 4.11: CRISPR/Cas9 mediated C-NAP1 depleted clones show an increase in the number of split centrosomes compared to wild-type cells. Cells were stained with anti-Cep135 and anti-γ-tubulin antibodies and cells with an inter-centriolar distance greater than 2 μm were counted. N=3, 200 cells were analysed for each cell line, error bars indicate s.d. ***p<0.001.

In order to confirm this splitting phenotype, we made a rescue cell line using the pcDNA3.1-C-NAP1-BsrLoxP construct generated in Section 4.2. After screening for C-NAP1 expression, rescue clone 1 (R1) was the best candidate for analysis based on its adequate expression and correct localisation (Fig. 4.12).

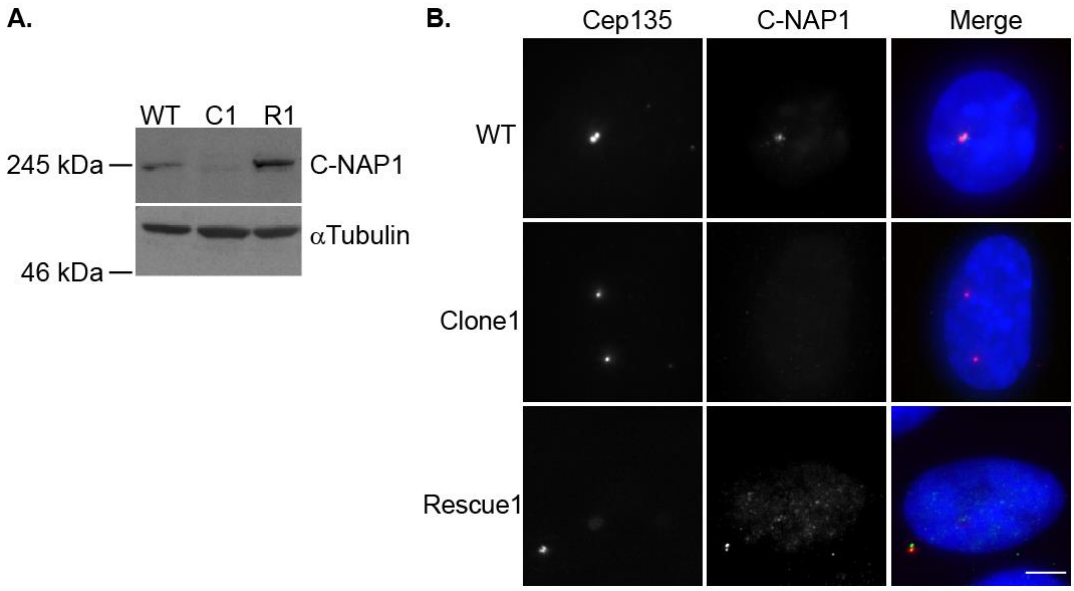

Figure 4.12: C-NAP1 reintroduction can be visualised at the correct size and position by Western blot and IF. A. Western blot for C-NAP1 in wild-type hTERT-RPE1 cells, Clone 1 (C1) and C-NAP1 Rescue cells (R1). α-Tubulin is a loading control. **B.** IF staining of WT, C1 and R1 cells with antibodies to C-NAP1 and Cep135. Scale bar: 5 μm, inset scale bar: 0.5 μm.

After confirming C-NAP1 can be re-expressed at its correct molecular weight and regains its centrosomal localisation, we tested whether the slight overexpression of the protein had an effect on proliferation of the rescue cell line. As displayed in Figure 4.13, R1 cells have an unrestricted proliferation curve similar to wild-type and Clone 1 curves. This assures us that R1 cells have no proliferative defect when expressing C-NAP1 from a locus other than the endogenous one.

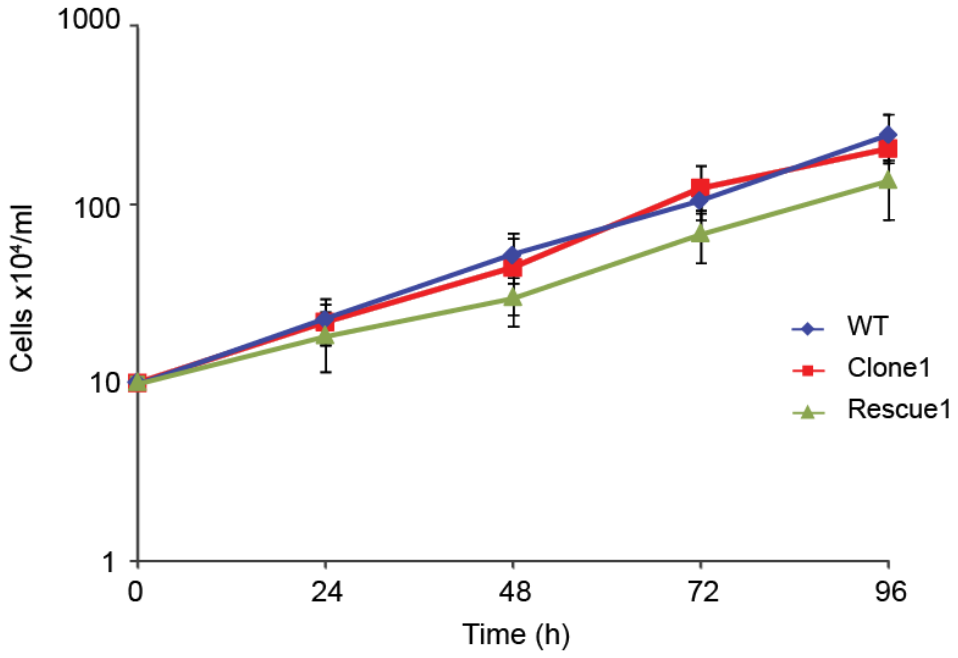

Figure 4.13: C-NAP1 rescue cells show no proliferation defect. Cells were plated at 10 x10^4/ml and counted every 24 hours for 96 hours. N=3, error bars indicate s.d..

Intact centrosome structure was the next critical aspect to check for both the C-NAP1 deficient Clone1 cells and the R1 rescue cell line. In Figure 4.14, we can see that C-NAP1 antibodies do not stain the centrioles in Clone1 cells, whereas there is C-NAP1 present at both of the centrioles in the case of the WT and R1 cells. Cep135 staining for the proximal ends of the microtubule barrels show the centrioles have maintained their structure at the ends normally tethered by C-NAP1 (K. Kim *et al.* 2008). Centrin 3 staining of the lumen of the centrioles in both cases shows the distal centriole structure is intact (Paoletti *et al.* 1996). γ-Tubulin constitutes part of the pericentriolar material (PCM) and is located around the proximal regions of both centrioles, and maintains this pericentriolar localisation in the *C-NAP1* disrupted clone. The mother centriole is identified using antibodies to the appendage protein

ninein and can be clearly identified in all three cell lines. Upon staining with antibodies to PCM1, we can see a disparity in the distribution of the centriolar satellites (Balczon *et al.* 1994). This observation is further characterised in Section 4.9.

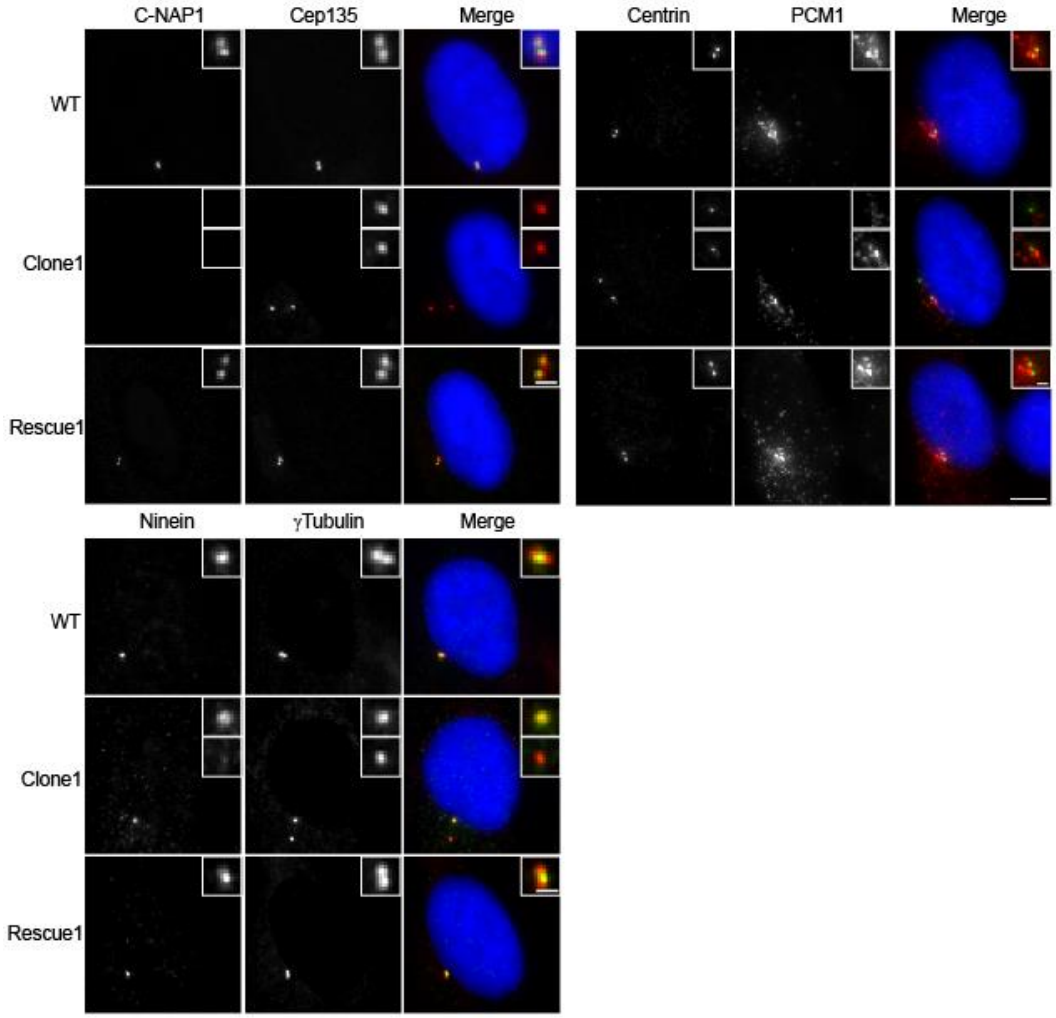

Figure 4.14: Immunofluorescence micrographs show normal localisation of core centrosome proteins in the absence of C-NAP1. WT RPE1 cells, C-NAP1 depleted and C-NAP1 rescue clones stained with centrosome linker marker using 6F2 C8 monoclonal C-NAP1 antibody, centriolar markers Cep135 and centrin3, appendage marker ninein, centrosomal marker γ-tubulin and centriolar satellite marker PCM1. Scale bar: 5 μm, inset scale bar: 1 μm.

4.6 Centrosomal cohesion and linker protein composition of C-NAP1 deficient cells

For all the images in Figure 4.14, in the case of the wild-type and rescue cells we can see the centrioles are in close proximity to each other. As for the C1 cells, there were many more split centrosomes in the population (as has been previously measured in Figure 4.11). R1 cells were stained with antibodies to Cep135 and the number of

centrioles separated by a distance of greater than 2 μm was counted to quantify the percentage of split centrosomes in the rescue cell line. The frequency of intercentriolar distance was rescued from the 30% splitting in cells lacking C-NAP1 to 8% in R1 cells (Fig 4.15).

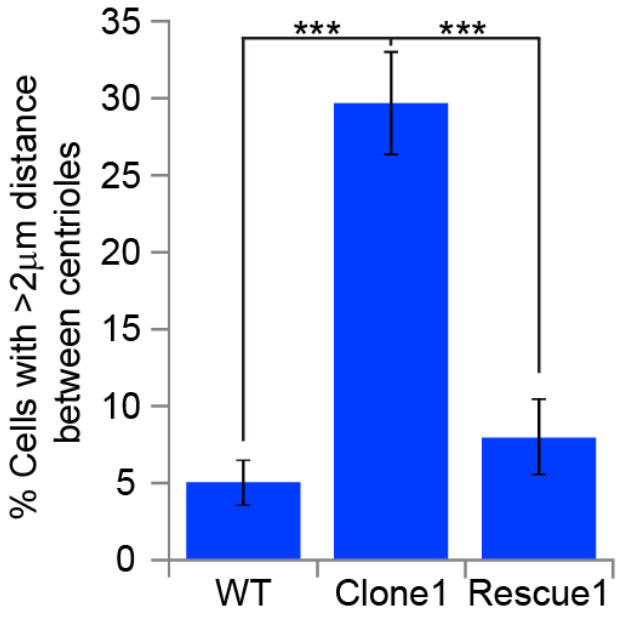

Figure 4.15: Centrosome cohesion can be restored to wild-type levels in C-NAP1 rescue clone R1. Percentages are based on Cep135 staining, 200 cells counted, n=3, error bars indicate s.d.,***p<0.001.

We then investigated the localisation of some of the previously identified interactors of C-NAP1 at the proximal end for the centrioles, Nek2 and rootletin. Staining C-NAP1-deficient and rescue cells with antibodies to these proteins we observed that in C-NAP1-deficient cells there was neither Nek2 nor rootletin at centrosomes, regardless of whether they were separated or in close proximity (Fig. 4.16). There is a recovery of Nek2 and rootletin localisation after reintroduction of the *C-NAP1* cDNA into the *C-NAP1* null background in R1 cells.

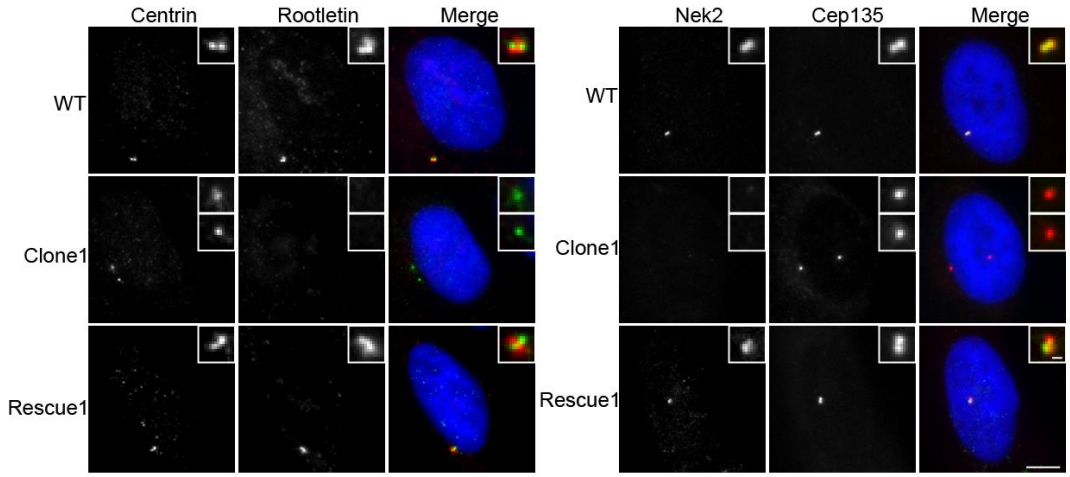

Figure 4.16: Levels of rootletin and Nek2 are significantly decreased at centrosomes where C-NAP1 has been disrupted. IF micrographs of WT cells, C-NAP1 depleted and C-NAP1 rescue cells stained with antibodies to rootletin and Nek2 in combination with centriolar markers centrin and Cep135 respectively. Scale bar: 5 μm, inset scale bar: 0.5 μm.

Nek2 and rootletin are C-NAP1 interacting partners and are found at the proximal ends of the centrioles where they have functions in centrosome cohesion. No detectable Nek2 or rootletin was observed by IF at the centrosome in Clone1 cells, but both Nek2 and rootletin localisation were rescued with C-NAP1 re-introduction. We then verified that these proteins were still being expressed by Western blot analysis. Figure 4.17 confirms that both proteins are still being expressed to wild-type levels in the absence of C-NAP1.

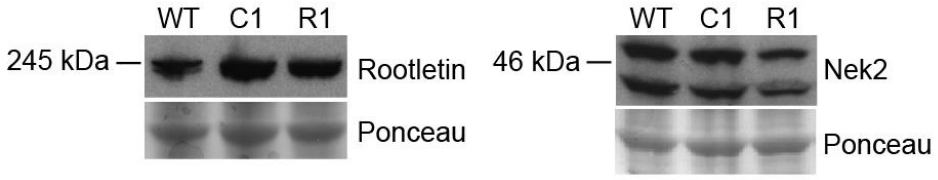

Figure 4.17: Rootletin levels are marginally elevated in C-NAP1 deficient cells whereas Nek2 levels are decreased slightly. WT, C1 and R1 cells immunoblotted for rootletin (left) and Nek2 (right) with Ponceau staining used as a loading control for both.

From the IF and Western blot analysis we can conclude that although rootletin and Nek2 are being expressed in the absence of C-NAP1, they fail to localise to the centrosome. This is an observation that has been previously reported for C-NAP1 and rootletin (Bahe *et al.* 2005, Yang *et al.* 2006).

4.7 C-NAP1 and ciliation

Cilia are produced following the docking of the mother centriole to the plasma membrane and extension of the doublet microtubules to form the axoneme. The primary cilium functions as a sensory organelle and are present on most epithelial cells (Oh and Katsanis 2012). The ability to form cilia was not affected by the loss of C-NAP1 in Clone 1 cells after serum starvation. Cilia were 8-25 μm in length, with an average length of 17 μm in both wildtype and *C-NAP1* disrupted cells (Fig. 4.18). Both experiments are a single repeat however the results show no major discrepancies from the wild-type samples.

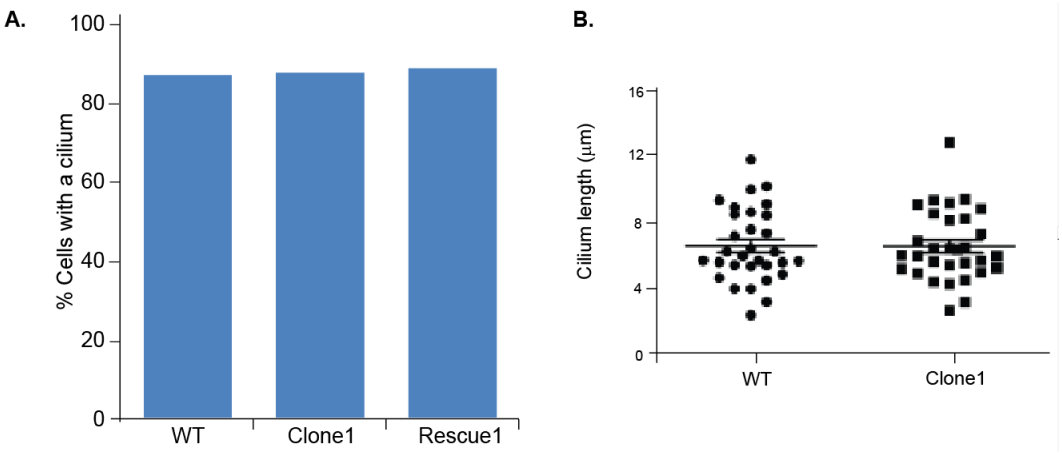

Figure 4.18: C-NAP1 deficiency does not affect ciliation or cilium length. A. Ciliation counts for both wildtype RPE1 cells and *C-NAP1* disrupted Clone1 cells under asynchronous (AS) and serum starved (SS) conditions, n=1. **B.** Cilia length was measured for 30 cells in each case. Error bars indicate s.d.

We have found that the cilia generated in cells lacking C-NAP1 displayed abnormalities in the localisation of rootletin. Rootletin filaments at the proximal end of the mother centriole extend into the cytoplasm anchoring the cilium in the cell. Upon C-NAP1 depletion, rootletin lost this centriolar localisation but long rootletin filaments were found in the cytoplasm in close proximity to the cilium (Fig. 4.19). Whether the loss of the basal body rootlet impacts on cilium function requires further investigation.

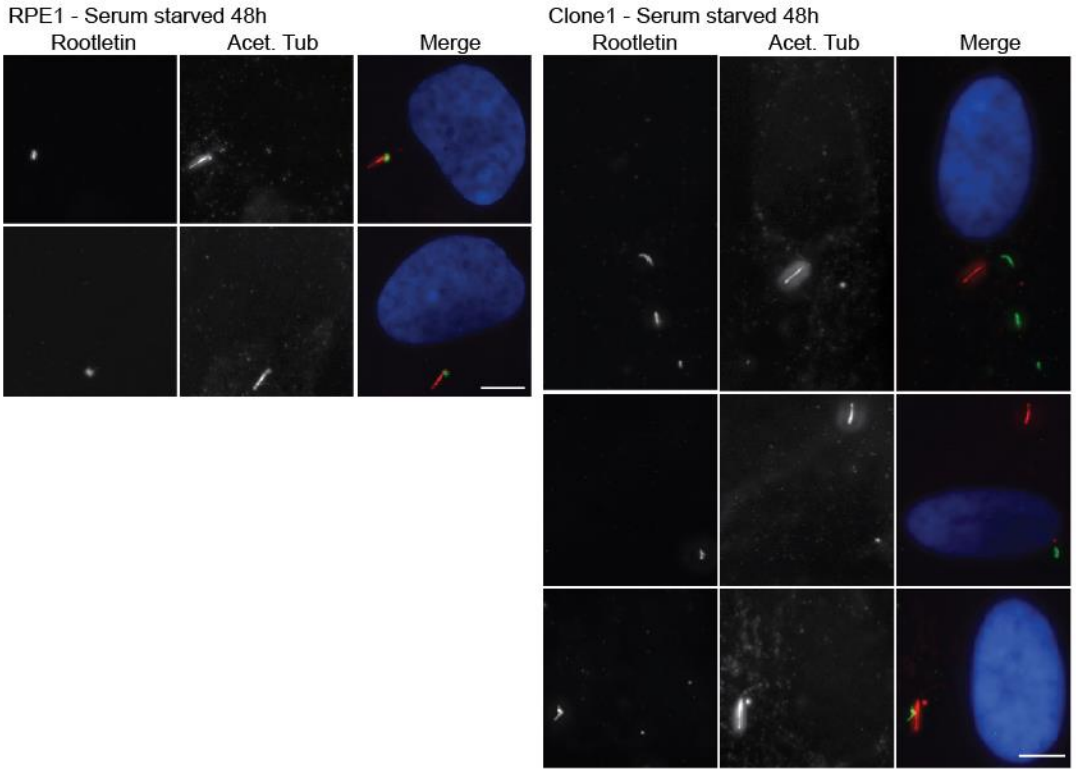

Figure 4.19: Rootletin is displaced from the basal body of cilia in *C-NAP1* disrupted cells. Cilia are stained with acetylated tubulin and rootletin 48 hours after serum starvation. Scale bar: 5μm.

4.8 Microtubule nucleation was not disrupted by the loss of C-NAP1

The ability of centrosomes to nucleate cellular microtubules is one of the key functions of the organelle in both interphase and mitosis. After depolymerisation of microtubules using nocodazole, cells were placed back in warm media without the drug and then fixed at the timepoints indicated in Figure 4.20. There was no difference in the ability of untreated cells to organise microtubules and, following depolymerisation and recovery, based on this single experiment C-NAP1 deficient cells formed microtubule asters of a similar size and in the same time frame as their wild-type counterparts. These preliminary observations lead us to conclude that the premature separation of centrioles does not have an impact on their capacity to nucleate microtubules after depolymerisation.

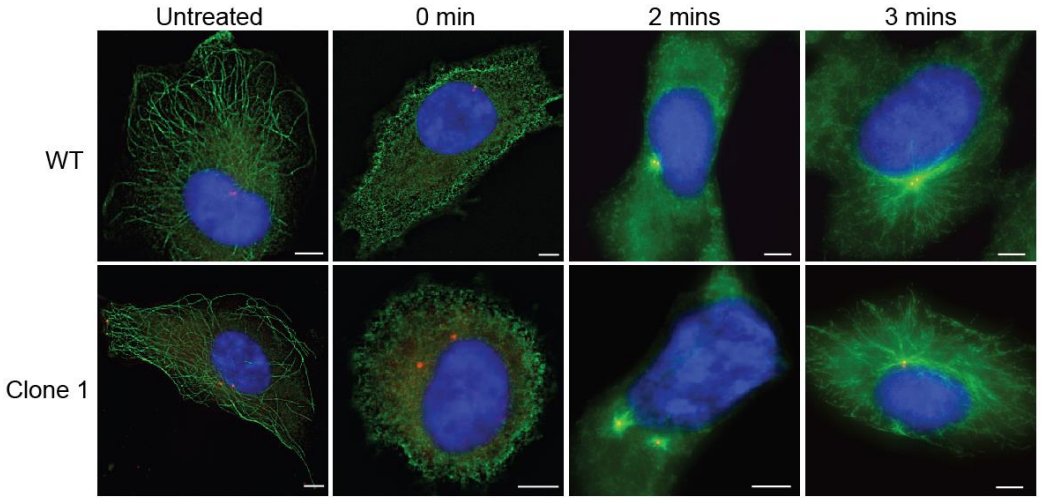

Figure 4.20: *C-NAP1* disrupted cells display no defect in microtubule nucleation after nocodazole treatment. Cells were treated with 2μM of nocodazole for 1 hour then placed on ice for 30 minutes. Untreated cells were fixed and stained with antibodies to αtubulin (green) and Cep135 (red). After the addition of fresh warm media, treated cells were fixed at 0, 2 and 3 minutes and stained as untreated. Scale bar: 5μm.

4.9 C-NAP1 loss results in dispersion of centriolar satellites

Centriolar satellites are centrosome associated protein complexes which have roles in ciliation and transport of proteins to and from the centrosome (Tollenaere *et al.* 2015). Localisation of centriolar satellites was disrupted in cells lacking C-NAP1 as observed by PCM1 staining in Figure 4.14. Satellites are clustered at the centrosome but are also dispersed in the cytosol surrounding the centrosome. Analysis of the distribution of centriolar satellite components PCM1 and OFD1 revealed a decrease in the clustering of satellites at separate centrioles of C-NAP1 null cell as measured by fluorescence intensity in a fixed volume around each centriole (Fig. 4.21). This dispersion was rescued to wild-type intensities upon C-NAP1 re-introduction in both cases.

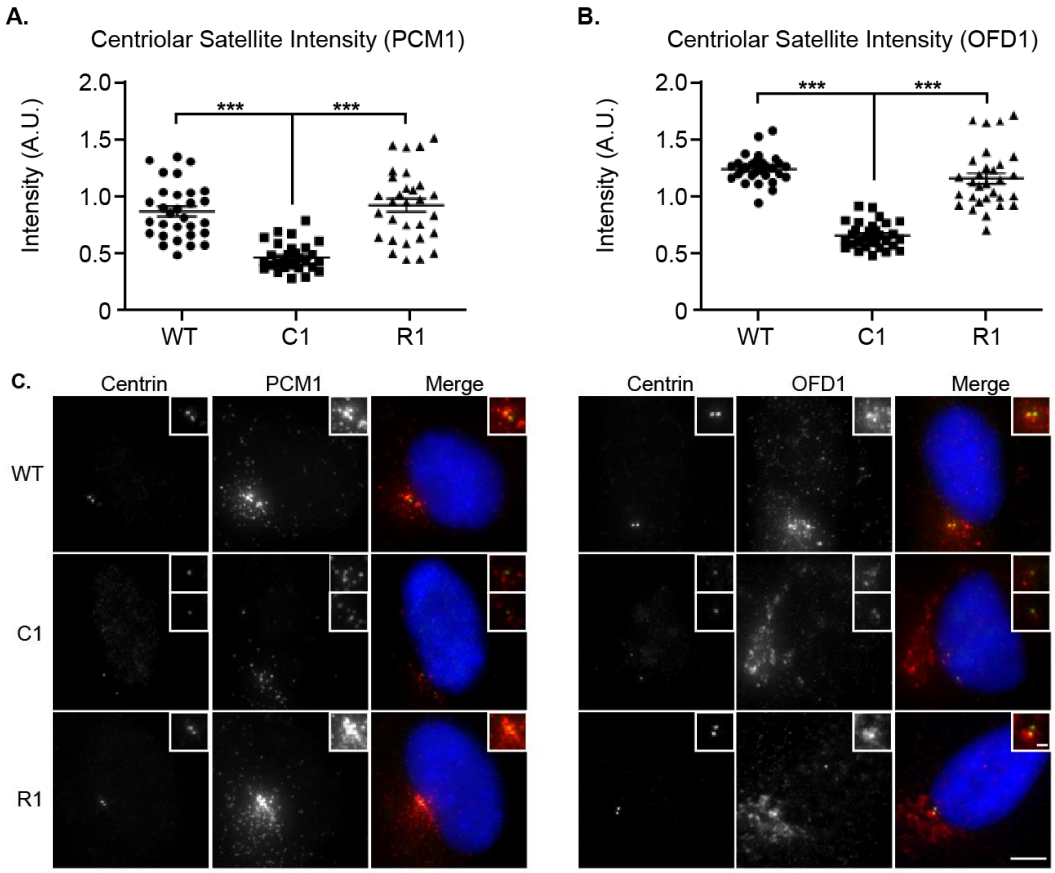

Figure 4.21: C-NAP1 deficient cells have significantly decreased satellite intensity at split centrioles. Average **A.** PCM1 and **B.** OFD1 intensity measurements of 2 pericentriolar volumes (25 μm^2) per cell for 30 individual cells in WT RPE1, C-NAP1 disrupted C1 cells and R1 C-NAP1 rescue cells. N=3, ***p<0.001. **C.** Satellite staining used for intensity measurements, centrin indicates the location of centrioles in each case. Scale bar: 5 μm, inset scale bar: 1 μm.

The increased scattering of PCM1 and OFD1 signal in C-NAP1 depleted cells prompted investigation of the level of protein expression in Clone1 and rescue cells in comparison to wild-type cells. PCM1 and OFD1 levels were not significantly depleted in Clone 1 cells when compared to wild-type or *C-NAP1* rescue cells (Fig. 4.22A, B). There does appear to be an extra band migrating slower than the main OFD1 band in both Clone1 and Rescue1, cells although it has not been verified if this band is related to the OFD1 protein. The levels of other centriolar satellite components, Cep290 and Cep72, was not affected by C-NAP1 depletion (Fig. 4.22B, C).

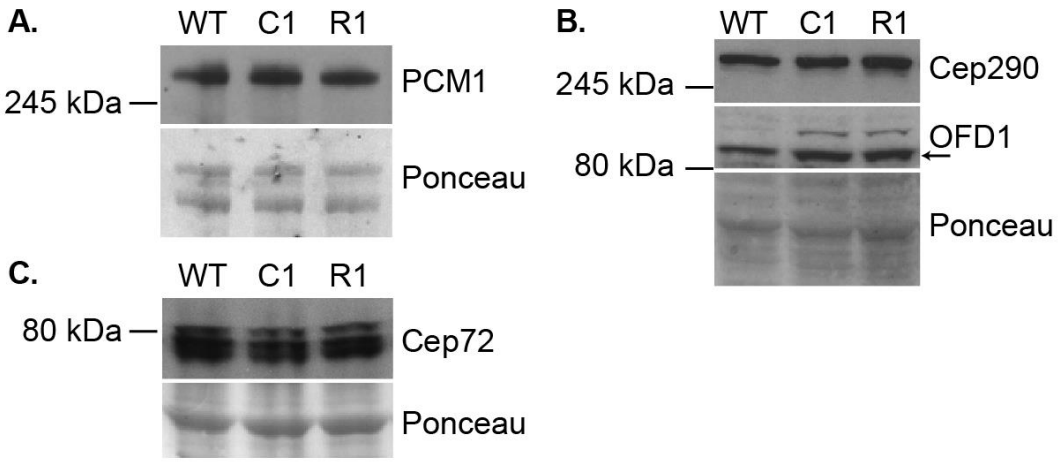

Figure 4.22: Disruption and rescue of C-NAP1 expression has no effect on levels of satellite protein expression in hTERT-RPE1 cells. Wild-type (WT), C-NAP1 disrupted (C1) and rescue (R1) clones immunoblotted for **A.** PCM1, **B.** Cep290 and OFD1 and **C.** Cep72, with Ponceau staining used as a loading control for each.

4.10 DNA damage-induced centrosome amplification in *C-NAP1* disrupted cells

DNA damage is a cause of centrosome amplification in mammalian cells, where cell cycle arrest as part of the DDR can dissociate the DNA replication cycle form the centrosome cycle (Balczon *et al.* 1995). The reduplication of centrosomes can occur during this extended pause in the cell cycle leading to supernumerary centrosomes. We tested if C-NAP1 deficient cells had an abnormal response to γ-irradiation and found that calls lacking C-NAP1 exhibited significantly lower levels of reduplicated centrioles after exposure to ionising radiation (IR) in comparison to their wild-type controls. 48 hours after treatment with 5 Gy of γ-irradiation, C-NAP1 depleted cells exhibited a marked decrease in the number of cells with greater than 2 centrioles when compared to wildtype cells (Fig. 4.23).

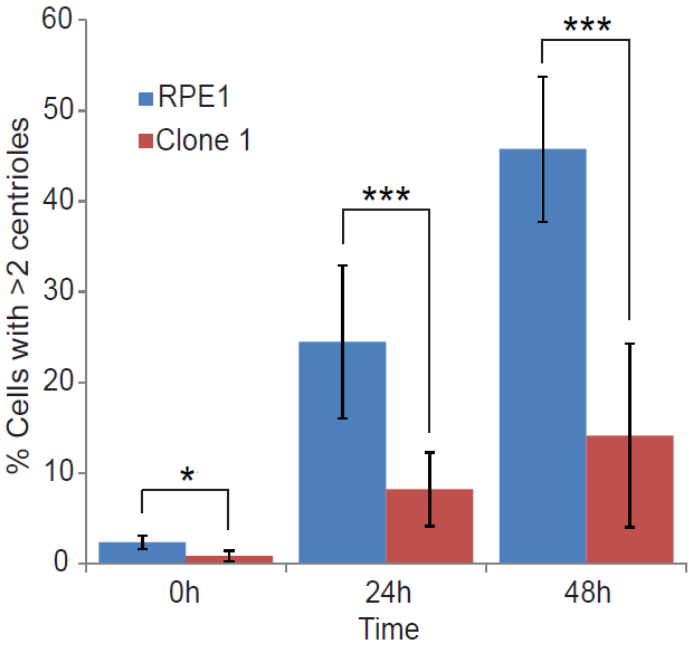

Figure 4.23: Centriole reduplication is suppressed in *C-NAP1* deficient cells. WT RPE1 and Clone 1 cells were treated with 5 Gy IR, then fixed for immunofluorescence at 0 h, 24 h and 48 h. Cells with greater than 2 centrioles were counted based on Cep135 staining. 200 cells were counted for each, N=3, ***p<0.05.

To examine the stage of the cell cycle that both the wildtype and the C-NAP1 deficient cells were in during analysis of centriole reduplication, we performed 1 dimensional (1D) FACS (Fig. 4.24). We can see a significant increase in the percentage of cells in G2/M phase compared to non-irradiated cells for all 4 cell lines (Fig. 4.10). There is also a slight decrease in the number of cells in G1 in all cases and the S phase fraction is almost completely abolished in this single experiment.

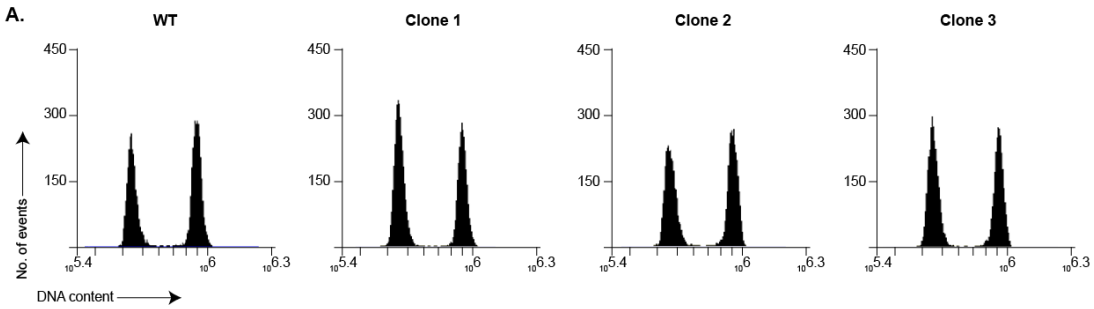

B.

Cell line	Cell cycle stage		
	G1	S	G2/M
WT	42.1%	4.1%	52.3%
Clone 1	51.5%	3.8%	41.4%
Clone 2	46.4%	4.5%	49.1%
Clone 3	51.4%	3.9%	45.1%

Figure 4.24: Wildtype and *C-NAP1* disrupted clones arrest in G2/M after IR. A. FACS profiles of wildtype and Clones 1, 2 and 3 48 h after 5 Gy IR were stained with 20 μg/ml PI and analysed by

FACS. 10,000 cells were analysed for each cell line. **B.** Based on the cell cycle profiles in A., the percentage of cells in each stage of the cell cycle was measured using Accuri C6 Sampler software.

In comparison to wildtype cells, C-NAP1 disrupted cells also displayed a lower number of overduplicated centrioles following exposure to hydroxyurea (Fig. 4.24).

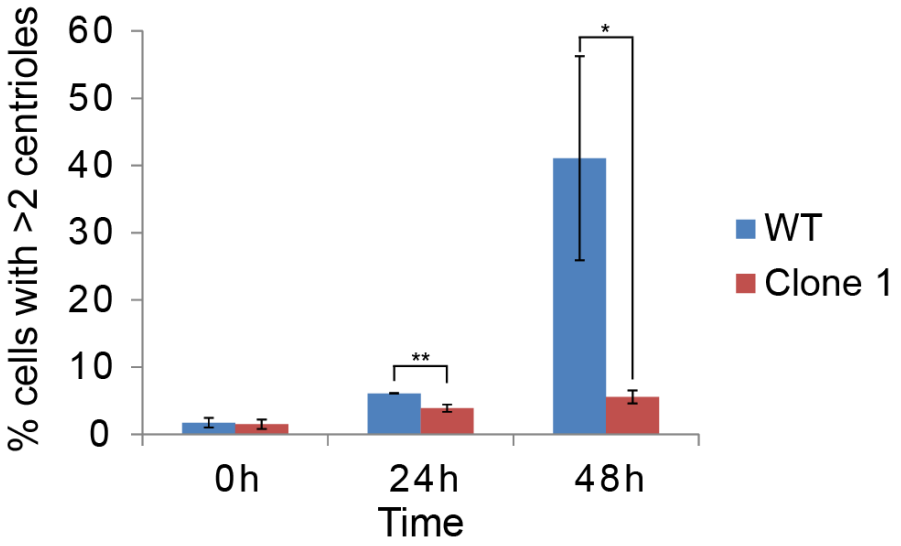

Figure 4.25: Centriole overduplication induced by hydroxyurea is suppressed in the absence of C-NAP1. WT and Clone 1 cells were fixed and stained with Cep135 and γtubulin after incubation with 4 mM HU for 24 and 48 hours. 200 cells were counted for each, N=3, *P<0.03, **P<0.05.

Based on the significant difference between wildtype and C-NAP1 depleted cells, it is possible to speculate that C-NAP1 plays a role in the amplification or reduplication of centrioles during cell cycle arrest after exposure to ionising radiation and replication inhibition. Dysfunction of many DNA damage response proteins and the desynchronization of the centrosome cycle during prolonged checkpoint activation can result in centrosome amplification (Dodson *et al.* 2004, Steere *et al.* 2011). Although centrosome splitting has been reported to contribute to centrosome amplification and reduplication, in the absence of centrosome cohesion protein C-NAP1, cells appear to suppress the assembly of extra centrioles after DNA damage (Ehrhardt and Sluder 2005, Date *et al.* 2006, Saladino *et al.* 2009).

5. Discussion

5.1 Targeting C-NAP1 in DT40 cells

We identified and targeted the insertion of an AIDGFP sequence in the *C-NAP1* locus in the chicken genome. Comparison of the genes flanking the locus and analysis of the chicken EST database confirmed the locus further (Fig. 5.1). During the targeting steps, it became apparent that the C-NAP1 locus was on a trisomic chromosome. Other than trisomy of chromosome 2 and an unidentified minichromosome, the DT40 chromosomes are disomic (Sonoda *et al.* 1998). It is possible that the trisomic chromosome contains the *C-NAP1* locus.

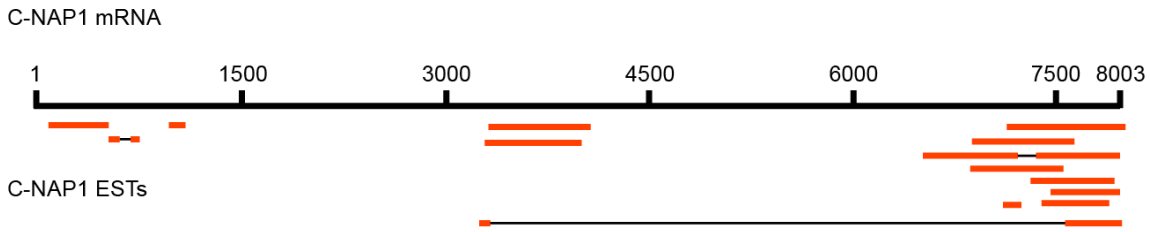

Figure 5.1: Alignment of chicken *C-NAP1* mRNA to EST sequences in the NCBI database. The blck line corresponds to C-NAP1 mRNA with the red lines representing individual EST sequences from th NCBI database.

We confirmed C-NAP1 localisation at the centrosome, although depletion of C-NAP1-AIDGFP had no impact on centrosome cohesion. Centrosome cohesion has been shown to be the key function of C-NAP1 in human cells, which brought the role of the protein in chicken cells into question after we observed no loss of centrosome structure or integrity in DT40 C-NAP1^{off} cells (Mayor *et al.* 2000).

5.2 C-NAP1 and centrosome cohesion

The evolution of CRISPR/Cas9 technology facilitated the expansion of studies on *C-NAP1* in human cells. Generation and phenotypic analysis of stable clones lacking C-NAP1 using a novel monoclonal antibody revealed there was a highly significant increase in intercentriolar distance in these cells. This finding was consistent with previously published data where knockdown of C-NAP1 using autoimmune antibodies or siRNA caused a marked increase in intercentriolar distance (Mayor *et al.* 2000, Bahe *et al.* 2005). The loss of centrosome cohesion was an important observation in human cells that expressed a truncated C-NAP1 protein, due to the fact that there was no increase observed in DT40 cells after C-NAP1 depletion,

which led to confusion over the role of the protein. The depletion of the AIDGFP tagged C-NAP1 protein was confirmed by western blot and immunofluorescence microscopy using the tag itself.

Speculation as to the possible reasons why we did not observe centrosome splitting could hinge on the AIDGFP tag. Other groups have used the AID degron system for the effective and sustained depletion of centrosome proteins in both yeast and human RPE1 cells (Lin *et al.* 2011, Lambrus *et al.* 2015). Depletion of the target proteins in each case (Tub4 and Plk4) was confirmed by immunoblot in both cases, with complete removal of either protein complete within 30 minutes, detected using antibodies to the endogenous protein. In the absence of an antibody to the endogenous chicken C-NAP1 protein, depletion was verified using the GFP tag. Evidence for the unlikely event of the AIDGFP tag being removed from the centrosome without removing the C-NAP1 protein comes from the AID-tagged Plk4 experiments mentioned above. Even if the C-NAP1 protein was embedded and fixed at the proximal ends of the centrioles, auxin-mediated depletion should at least prevent the accumulation of the protein in G1 stage of the next cell cycle, when the linker is re-assembled, thus showing a minimal increase in centrosome splitting.

In addition to the possibility of cleavage of the AIDGFP tag from C-NAP1 upon auxin addition, there is also the possibility that there exist other loci that express C-NAP1. The unexpected observation that the chromosome harbouring *C-NAP1* was trisomic raises the idea of there being other loci in the genome from which *C-NAP1* is transcribed. The 5’ probe used to analyse the *C-NAP1* locus contained exon 29 of the C-NAP1 protein, which would argue against there being alternative loci for the *C-NAP1* gene. As we were unable to resolve the reason(s) behind the lack of impact of C-NAP1 depletion on centrosome cohesion in the chicken system, we therefore chose to analyse *C-NAP1* in human cells in more detail.

5.3 C-NAP1 binding partners and function in ciliation and microtubule regrowth

Re-introduction of C-NAP1 re-established the localisation of rootletin and Nek2 without inducing any overexpression of either protein, as determined by western blot. Since C-NAP1 is considered to be a scaffold protein to which fibrous linker proteins attach, the absence of rootletin from the intercentriolar space is a logical

outcome from the loss of C-NAP1 at proximal centrioles (Bahe *et al.* 2005, Graser *et al.* 2007b). Nek2 localises at the centrosome in a transient manner phosphorylates C-NAP1 and rootletin at the onset of mitosis (Fry *et al.* 1998, Bahe *et al.* 2005, Hames *et al.* 2005). Nek2-mediated phosphorylation occurs at the centrosome meaning the kinase must be trafficked to and from the centrosome, a function mediated by the centriolar satellite complex protein, PCM1 (Hames *et al.* 2005). Activation of Nek2 is dependent on Mst and hSav members of the Hippo signalling pathway and is critical for the localisation of Nek2 at centrosomes (Mardin *et al.* 2010). However, since Nek2 relies on C-NAP1 and rootletin for centrosomal localisation, disruption and loss of C-NAP1, and consequently rootletin, results in the depletion of Nek2 at the centrosome (Bahe *et al.* 2005, Yang *et al.* 2006).

The ability of *C-NAP1* disrupted cells to form cilia was unaffected by the loss of C-NAP1 however a mislocalisation of rootletin occurred after serum starvation. Rootletin formed filament-like structures in the cytoplasm, which were not attached to the basal body. The depolymerisation of intercellular tubulin structures using nocodazole showed *C-NAP1* disruption did not affect the ability of the individual centrioles to form microtubule asters. Split centrosomes displayed the ability to nucleate microtubules as efficiently and within the same time frame as their non-split counterparts.

Rootletin fibres form the striated basal rootlet in ciliated cells which project from the mother centriole into the cytoplasm (Yang *et al.* 2006). Ciliary rootlets are particularly well developed in photoreceptor cells, with individual rootletin monomers associating to form long filament-like structures which are postulated to play roles in intracellular protein transport (Fariss *et al.* 1997, J. Yang *et al.* 2002). As we have observed, the absence of the rootletin docking site on the mother centriole through loss of C-NAP1 not only prevents rootletin localisation in asynchronous cells, but also hinders the recruitment of rootletin to the basal body during ciliogenesis. The large filaments assembled in the cytoplasm of C-NAP1 deficient cells are reminiscent of the long extended fibres seen in photoreceptor cells (J. Yang *et al.* 2002). This mislocalisation does not affect the ciliation capacity of the cell, but whether the functionality of cilia is altered in C-NAP1 deficient cells has not been addressed here.

5.4 Centriolar satellite structure in C-NAP1 disrupted cells

One of the most striking phenotypes observed in cells lacking C-NAP1 was the redistribution of centriolar satellites. In wild-type cells, satellite proteins PCM1 and OFD1 displayed a classical satellite distribution; clustering at the centrosome while maintaining a scattered distribution in the cytoplasm surrounding the centrosome (Balczon *et al.* 1994, Kubo and Tsukita 2003, Tang *et al.* 2013). In cells lacking C-NAP1, split centrosomes rearranged the distribution of their satellites, decreasing the intensity of the complexes in the region of the centrosome and dispersing the signal throughout the cell. The change in PCM1 and OFD1 concentration at the centrosome was rescued upon *C-NAP1* reintroduction and was not due to a change in the expression of either protein as detected by western blot. Satellite proteins Cep72 and Cep290 also maintained their respective expression levels independently of the cells' *C-NAP1* status.

The centriolar satellite complex is a highly dynamic group of proteins, with many more proteins associating with scaffold and motor protein components at different stages of the cell cycle. Other proteins use the satellite network for their delivery to the centrosome or for activation purposes, such as Nek2 and Plk1 (Hames *et al.* 2005, G. Wang *et al.* 2013). As previously discussed, the absence of C-NAP1 does not appear to have an effect on the ability of cells to form a primary cilium; however the question of whether cellular signalling is affected is unknown. OFD1 and PCM1 are both required for the formation of cilia, with depletion of OFD1 preventing the docking of the mother centriole to ciliary vesicles before axoneme elongation (Singla *et al.* 2010). Depletion of PCM1 has been shown to mediate a number of different centrosomal and ciliary defects which are dependent on its role in redistributing proteins between the centrosome and cytoplasmic pools (Kubo *et al.* 1999, Kamiya *et al.* 2008, Stowe *et al.* 2012).

Microtubule nucleation is an activity mediated by the centrosome for which PCM1 is required. PCM1 shuttles ninein and centrin to the centrosome to increase centrosome-mediated radial microtubule organization (Dammermann and Merdes 2002). Compared to wildtype cells, C-NAP1 deficient cells were able to re-establish radial microtubule networks when the cells were subjected to a microtubule regrowth assay using nocodazole. Microtubule nucleation appeared normal in cells lacking C-NAP1, leads us to believe that the centriolar satellite functions in microtubule

nucleation and cilia formation are not affected by the disorganisation of the satellite complexes. The microtubule network in C-NAP1 deficient cell is worthy of further investigation however, due to the integral relationship between the satellites and microtubules for both centrosomal and cellular processes.

5.5 C-NAP1 and the DNA damage response

Finally, the duplication of centrioles after exposure to ionising radiation or hydroxyurea appeared to be suppressed in C-NAP1 depleted cells. Induction of DSBs via exposure to γ–irradiation caused centriole duplication in wildtype cells. Cells lacking C-NAP1 did not produce these extra centrioles after DNA damage. Similarly, in the case of cell cycle arrest in S phase using hydroxyurea, *C-NAP1* disrupted clones did not assemble new centrioles to the same extent as was observed in wildtype cells. Analysis of wildtype and *C-NAP1* disrupted cells by FACS revealed a considerable increase in the percentage of cells in G2/M after exposure to 5 Gy of ionising radiation when compared to untreated cells indicative of cell cycle arrest. p53, which would have been absent in the DT40 model system, is an effector of G2/M cell cycle arrest, influencing transcription and cell cycle progression via the ATM/Chk1 DDR signalling pathway (Fukasawa *et al.* 1996, Taylor and Stark 2001, Dodson *et al.* 2004, Bourke *et al.* 2007). The DDR signalling pathway is functioning to detect DNA damage and induce a checkpoint, however the amplification of centrioles is suppressed. It is possible that cells with split centrioles are incapable of recognising and responding to the DDR signals following irradiation. Analysis of DDR pathway mediator and effector proteins, and centrosomal DDR response proteins, could provide greater insight as to whether the DDR is altered in any way in these cells.

Centriolar satellites are required to transport centrin and γtubulin to the centrosome for the formation of new centrioles (La Terra *et al.* 2005, Prosser *et al.* 2009). It is possible that the depletion of centriolar satellite concentration at the centrosome limits the formation of new centrioles during cell cycle arrest. In order to address this possibility, a combination of satellite protein overexpression and subsequent exposure to IR could be used in an effort to artificially increase the concentration of satellites at the centrosome to an extent in which centrosome amplification would be restored. Experiments to overexpress satellite proteins PCM1 or Cep72 in cells

depleted of C-NAP1 could be performed to rescue the amplification observed in wildtype cells. Analysis of centrosome amplification in *C-NAP1* rescue cells would allow us to understand whether centrosome amplification can occur when centrosome cohesion and centriolar satellite organisation have been re-established.

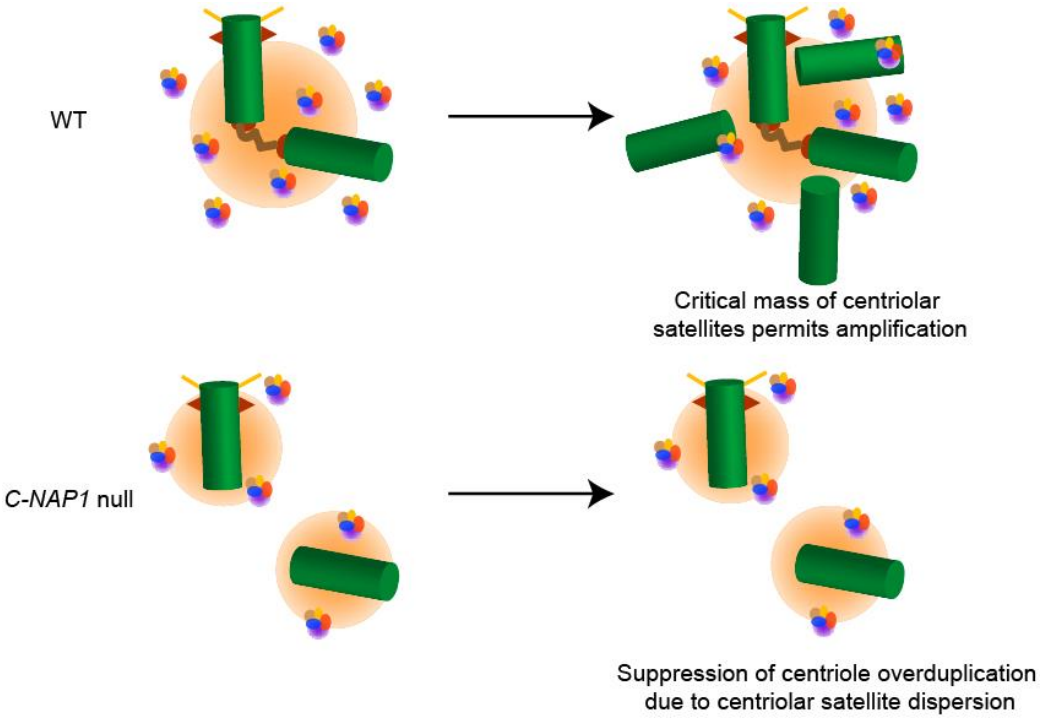

Figure 5.2: Model for suppression of centrosome overduplication in *C-NAP1* deficient cells. In wild-type cells, there is sufficient accumulation of centriolar satellites to facilitate the assembly of new centrioles during IR-induced cell cycle arrest. In the absence of C-NAP1, split centrioles result in a dispersion of the centriolar satellite complexes thus suppressing centriole biogenesis as a critical concentration of centriolar and centrosomal factors cannot be obtained.

We propose a model for the suppression of centrosome overdulpication in the absence of C-NAP1 (Fig. 5.2). Based on our observations, we propose that a critical level of centrosomal satellite accumulation is necessary at the centrosome in order to achieve reduplication of centrioles. In the case of loss of centrosome cohesion, where the centriolar satellite complexes are dispersed, overduplication of the centrioles is not supported due to the inability to accumulate centrin and other centrosome components to amounts sufficient to initiate centriole biogenesis.

6. Conclusions and future perspectives

6. Conclusions and future perspectives

The amplification of centrioles in response to DNA damage is driven by the uncoupling of the centrosome and DNA replication cycles (Balczon *et al.* 1995, Kuriyama *et al.* 2007, Saladino *et al.* 2012). Cell cycle arrest via ATM-Chk1 signalling pathway and blocks the DNA replication cycle but the centrosome duplication cycle can continue (Dodson *et al.* 2004, Bourke *et al.* 2007). The extra centrioles are formed by the accumulation and aggregation of centrin, followed by the assembly of maturation markers such as γtubulin (Kuriyama *et al.* 2007, Prosser *et al.* 2009). Centrosome amplification can also occur by excess accumulation of centriolar satellites following DNA damage (Loffler *et al.* 2013). We found that loss of centrosomal cohesion resulted in a depletion of centriolar satellites at the centrosome. Exposure to ionising radiation suppressed DNA damage-induced centrosome amplification in cells with split centrosomes. We propose a model for centrosome amplification which is dependent on the maintenance of centrosome cohesion to generate a specific local concentration of centriolar satellites in order to facilitate the assembly of supernumerary centrioles during G2 cell cycle arrest.

Further analysis of the links between the DNA damage response and centriolar satellites is required in both wild-type cells and in cells which have lost cohesion. The microtubule network in the cell plays a major role in the cellular trafficking and cytosolic organisation. Split centrosomes could very well cause a change in the way this network assembles and/or its functioning. It would be interesting to see if disruption of the microtubules in combination with DNA damage would allow the formation of new centrioles.

We performed preliminary experiments with the Eg5 inhibitor monastrol in the hope that dynein forces would direct cellular cargo to the centrosome with the underlying idea of trying to bring the centrioles in close proximity to allow the assembly of new centrioles by creating a focus for the microtubule network of the cell. This proved more complicated than initially thought, due to the mitotic block induced by the consequent monopolar spindles from the monastrol. It is likely that the same problems would be encountered should we attempt to address the role of microtubules in the reduplication process using microtubule-targeting drugs.

In relation to the structure of the centrioles in C-NAP1-deficient cells, accurate quantification of the amount of various centriolar and pericentriolar proteins would

provide useful data about the composition of the centrioles. In particular, investigation by microscopy of the compositional changes of PCM proteins which modify their structure during disengagement could reveal some interesting properties of split centrosomes. Analysis of microtubule-anchoring proteins at the centrioles might provide a link between the centrioles and the microtubule network in C-NAP1 null cells.

One option to investigate the role of PCM1 (or other satellite proteins) in the duplication of centrioles after DNA damage would be to deplete PCM1 in wild-type cells. This would address the requirement for satellite function in the IR-induced amplification of centrioles. Similarly, depletion of another centriolar linker protein such as rootletin or even Cep215 could create cells with split centrosomes. We could then isolate a role for the linker or specific linker proteins in centriole duplication by subjecting these cells to DNA damage. Examination of the role of the centriolar linker and the satellites in the DDR could also be performed in other cell lines to confirm observations reported in this work.

The disrupted ciliary rootlet seen in cells lacking C-NAP1 is an interesting phenotype that could be investigated further. An experiment to test the functionality of ciliary signalling pathways in *C-NAP1-/-* cells would be most valuable as it could shed some light on how important the link between the daughter cells and the rootlet structure are for cilia function.

References

Abraham, R. T. (2001) 'Cell cycle checkpoint signaling through the ATM and ATR kinases', *Genes Dev*, 15(17), 2177-96.

Agircan, F. G. and Schiebel, E. (2014) 'Sensors at Centrosomes Reveal Determinants of Local Separase Activity', *PLoS Genetics*, 10(10), e1004672.

Agircan, F. G., Schiebel, E. and Mardin, B. R. (2014) 'Separate to operate: control of centrosome positioning and separation', *Philos Trans R Soc Lond B Biol Sci*, 369(1650).

Ahnesorg, P., Smith, P. and Jackson, S. P. (2006) 'XLF interacts with the XRCC4-DNA ligase IV complex to promote DNA nonhomologous end-joining', *Cell*, 124(2), 301-13.

Akhmanova, A., Hoogenraad, C. C., Drabek, K., Stepanova, T., Dortland, B., Verkerk, T., Vermeulen, W., Burgering, B. M., De Zeeuw, C. I., Grosveld, F. and Galjart, N. (2001) 'Clasps are CLIP-115 and -170 associating proteins involved in the regional regulation of microtubule dynamics in motile fibroblasts', *Cell*, 104(6), 923-35.

Andrews, P. D. (2005) 'Aurora kinases: shining lights on the therapeutic horizon?', *Oncogene*, 24(32), 5005-15.

Antonczak, A. K., Mullee, L. I., Wang, Y., Comartin, D., Inoue, T., Pelletier, L. and Morrison, C. G. (2015) 'Opposing effects of pericentrin and microcephalin on the pericentriolar material regulate CHK1 activation in the DNA damage response', *Oncogene*.

Araki, M., Masutani, C., Takemura, M., Uchida, A., Sugasawa, K., Kondoh, J., Ohkuma, Y. and Hanaoka, F. (2001) 'Centrosome protein centrin 2/caltractin 1 is part of the xeroderma pigmentosum group C complex that initiates global genome nucleotide excision repair', *J Biol Chem*, 276(22), 18665-72.

Archambault, V. and Glover, D. M. (2009) 'Polo-like kinases: conservation and divergence in their functions and regulation', *Nat Rev Mol Cell Biol*, 10(4), 265-275.

Arquint, C., Gabryjonczyk, A. M. and Nigg, E. A. (2014) 'Centrosomes as signalling centres', *Philos Trans R Soc Lond B Biol Sci*, 369(1650).

Ayeni, J. O. and Campbell, S. D. (2014) '"Ready, set, go": checkpoint regulation by Cdk1 inhibitory phosphorylation', *Fly (Austin)*, 8(3), 140-7.

Azimzadeh, J., Hergert, P., Delouvee, A., Euteneuer, U., Formstecher, E., Khodjakov, A. and Bornens, M. (2009) 'hPOC5 is a centrin-binding protein required for assembly of full-length centrioles', *J Cell Biol*, 185(1), 101-14.

Azimzadeh, J. and Marshall, W. F. (2010) 'Building the centriole', *Curr Biol*, 20(18), R816-25.

Baba, T. W., Giroir, B. P. and Humphries, E. H. (1985) 'Cell lines derived from avian lymphomas exhibit two distinct phenotypes', *Virology*, 144(1), 139-51.

Bahe, S., Stierhof, Y. D., Wilkinson, C. J., Leiss, F. and Nigg, E. A. (2005) 'Rootletin forms centriole-associated filaments and functions in centrosome cohesion', *J Cell Biol*, 171(1), 27-33.

Bahmanyar, S., Kaplan, D. D., Deluca, J. G., Giddings, T. H., Jr., O'Toole, E. T., Winey, M., Salmon, E. D., Casey, P. J., Nelson, W. J. and Barth, A. I. (2008) 'beta-Catenin is a Nek2 substrate involved in centrosome separation', *Genes Dev*, 22(1), 91-105.

Bakkenist, C. J. and Kastan, M. B. (2003) 'DNA damage activates ATM through intermolecular autophosphorylation and dimer dissociation', *Nature*, 421(6922), 499-506.

Balczon, R., Bao, L. and Zimmer, W. E. (1994) 'PCM-1, A 228-kD centrosome autoantigen with a distinct cell cycle distribution', *J Cell Biol*, 124(5), 783-93.

Balczon, R., Bao, L., Zimmer, W. E., Brown, K., Zinkowski, R. P. and Brinkley, B. R. (1995) 'Dissociation of centrosome replication events from cycles of DNA synthesis and mitotic division in hydroxyurea-arrested Chinese hamster ovary cells', *The Journal of Cell Biology*, 130(1), 105-115.

Balczon, R., Varden, C. E. and Schroer, T. A. (1999) 'Role for microtubules in centrosome doubling in Chinese hamster ovary cells', *Cell Motil Cytoskeleton*, 42(1), 60-72.

Barenz, F., Mayilo, D. and Gruss, O. J. (2011) 'Centriolar satellites: busy orbits around the centrosome', *Eur J Cell Biol*, 90(12), 983-9.

Barr, A. R. and Gergely, F. (2007) 'Aurora-A: the maker and breaker of spindle poles', *J Cell Sci*, 120(Pt 17), 2987-96.

Bartek, J. and Lukas, J. (2003) 'Chk1 and Chk2 kinases in checkpoint control and cancer', *Cancer Cell*, 3(5), 421-9.

Basto, R., Brunk, K., Vinadogrova, T., Peel, N., Franz, A., Khodjakov, A. and Raff, J. W. (2008) 'Centrosome amplification can initiate tumorigenesis in flies', *Cell*, 133(6), 1032-42.

Basto, R., Lau, J., Vinogradova, T., Gardiol, A., Woods, C. G., Khodjakov, A. and Raff, J. W. (2006) 'Flies without Centrioles', *Cell*, 125(7), 1375-1386.

Baumann, P., Benson, F. E. and West, S. C. (1996) 'Human Rad51 protein promotes ATP-dependent homologous pairing and strand transfer reactions in vitro', *Cell*, 87(4), 757-66.

Baye, L. M., Patrinostro, X., Swaminathan, S., Beck, J. S., Zhang, Y., Stone, E. M., Sheffield, V. C. and Slusarski, D. C. (2011) 'The N-terminal region of centrosomal protein 290 (CEP290) restores vision in a zebrafish model of human blindness', *Hum Mol Genet*, 20(8), 1467-77.

Bazzi, H. and Anderson, K. V. (2014) 'Acentriolar mitosis activates a p53-dependent apoptosis pathway in the mouse embryo', *Proc Natl Acad Sci U S A*, 111(15), E1491-500.

Bermudez, V. P., Lindsey-Boltz, L. A., Cesare, A. J., Maniwa, Y., Griffith, J. D., Hurwitz, J. and Sancar, A. (2003) 'Loading of the human 9-1-1 checkpoint complex onto DNA by the checkpoint clamp loader hRad17-replication factor C complex in vitro', *Proc Natl Acad Sci U S A*, 100(4), 1633-8.

Bernstein, K. A. and Rothstein, R. (2009) 'At loose ends: resecting a double-strand break', *Cell*, 137(5), 807-10.

Bettencourt-Dias, M. and Glover, D. M. (2007) 'Centrosome biogenesis and function: centrosomics brings new understanding', *Nat Rev Mol Cell Biol*, 8(6), 451-63.

Bischoff, F. R. and Ponstingl, H. (1991) 'Catalysis of guanine nucleotide exchange on Ran by the mitotic regulator RCC1', *Nature*, 354(6348), 80-2.

Blagden, S. P. and Glover, D. M. (2003) 'Polar expeditions--provisioning the centrosome for mitosis', *Nat Cell Biol*, 5(6), 505-11.

Bobinnec, Y., Khodjakov, A., Mir, L. M., Rieder, C. L., Edde, B. and Bornens, M. (1998) 'Centriole disassembly in vivo and its effect on centrosome structure and function in vertebrate cells', *J Cell Biol*, 143(6), 1575-89.

Bodnar, A. G., Ouellette, M., Frolkis, M., Holt, S. E., Chiu, C. P., Morin, G. B., Harley, C. B., Shay, J. W., Lichtsteiner, S. and Wright, W. E. (1998) 'Extension of life-span by introduction of

telomerase into normal human cells', *Science*, 279(5349), 349-52.

Bourke, E., Dodson, H., Merdes, A., Cuffe, L., Zachos, G., Walker, M., Gillespie, D. and Morrison, C. G. (2007) 'DNA damage induces Chk1-dependent centrosome amplification', *EMBO Rep*, 8(6), 603-9.

Boveri, T. (1887) 'Ueber den Antheil des Spermatozoon an der Teilung des Eies', *Sitzungsber. Ges. Morph. Physiol. Mu¨nchen*, (3), 151-164.

Bowers, B. and Korn, E. D. (1968) 'The fine structure of Acanthamoeba castellanii. I. The trophozoite', *J Cell Biol*, 39(1), 95-111.

Brito, D. A. and Rieder, C. L. (2006) 'Mitotic checkpoint slippage in humans occurs via cyclin B destruction in the presence of an active checkpoint', *Curr Biol*, 16(12), 1194-200.

Broekhuis, J. R., Verhey, K. J. and Jansen, G. (2014) 'Regulation of Cilium Length and Intraflagellar Transport by the RCK-Kinases ICK and MOK in Renal Epithelial Cells', *PLoS ONE*, 9(9), e108470.

Brown, E. J. and Baltimore, D. (2000) 'ATR disruption leads to chromosomal fragmentation and early embryonic lethality', *Genes Dev*, 14(4), 397-402.

Buerstedde, J. M. and Takeda, S. (1991) 'Increased ratio of targeted to random integration after transfection of chicken B cell lines', *Cell*, 67(1), 179-88.

Bunting, S. F., Callen, E., Wong, N., Chen, H. T., Polato, F., Gunn, A., Bothmer, A., Feldhahn, N., Fernandez-Capetillo, O., Cao, L., Xu, X., Deng, C. X., Finkel, T., Nussenzweig, M., Stark, J. M. and Nussenzweig, A. (2010) '53BP1 inhibits homologous recombination in Brca1-deficient cells by blocking resection of DNA breaks', *Cell*, 141(2), 243-54.

Burma, S., Chen, B. P., Murphy, M., Kurimasa, A. and Chen, D. J. (2001) 'ATM phosphorylates histone H2AX in response to DNA double-strand breaks', *J Biol Chem*, 276(45), 42462-7.

Cann, K. L. and Hicks, G. G. (2007) 'Regulation of the cellular DNA double-strand break response', *Biochem Cell Biol*, 85(6), 663-74.

Carreira, A., Hilario, J., Amitani, I., Baskin, R. J., Shivji, M. K., Venkitaraman, A. R. and Kowalczykowski, S. C. (2009) 'The BRC repeats of BRCA2 modulate the DNA-binding selectivity of RAD51', *Cell*, 136(6), 1032-43.

Casenghi, M., Meraldi, P., Weinhart, U., Duncan, P. I., Körner, R. and Nigg, E. A. (2003) 'Polo-like Kinase 1 Regulates Nlp, a Centrosome Protein Involved in Microtubule Nucleation', *Developmental Cell*, 5(1), 113-125.

Chaki, M., Airik, R., Ghosh, Amiya K., Giles, Rachel H., Chen, R., Slaats, Gisela G., Wang, H., Hurd, Toby W., Zhou, W., Cluckey, A., Gee, H. Y., Ramaswami, G., Hong, C.-J., Hamilton, Bruce A., Červenka, I., Ganji, Ranjani S., Bryja, V., Arts, Heleen H., van Reeuwijk, J., Oud, Machteld M., Letteboer, Stef J. F., Roepman, R., Husson, H., Ibraghimov-Beskrovnaya, O., Yasunaga, T., Walz, G., Eley, L., Sayer, John A., Schermer, B., Liebau, Max C., Benzing, T., Le Corre, S., Drummond, I., Janssen, S., Allen, Susan J., Natarajan, S., O'Toole, John F., Attanasio, M., Saunier, S., Antignac, C., Koenekoop, Robert K., Ren, H., Lopez, I., Nayir, A., Stoetzel, C., Dollfus, H., Massoudi, R., Gleeson, Joseph G., Andreoli, Sharon P., Doherty, Dan G., Lindstrad, A., Golzio, C., Katsanis, N., Pape, L., Abboud, Emad B., Al-Rajhi, Ali A., Lewis, Richard A., Omran, H., Lee, E. Y. H. P., Wang, S., Sekiguchi, JoAnn M., Saunders, R., Johnson, Colin A., Garner, E., Vanselow, K., Andersen, Jens S., Shlomai, J., Nurnberg, G., Nurnberg, P., Levy, S., Smogorzewska, A., Otto, Edgar A. and Hildebrandt, F. (2012) 'Exome Capture Reveals ZNF423 and CEP164 Mutations, Linking Renal Ciliopathies to DNA Damage Response Signaling', *Cell*, 150(3), 533-548.

Chamling, X., Seo, S., Searby, C. C., Kim, G., Slusarski, D. C. and Sheffield, V. C. (2014) 'The

centriolar satellite protein AZI1 interacts with BBS4 and regulates ciliary trafficking of the BBSome', *PLoS Genet*, 10(2), e1004083.

Chao, W. C., Kulkarni, K., Zhang, Z., Kong, E. H. and Barford, D. (2012) 'Structure of the mitotic checkpoint complex', *Nature*, 484(7393), 208-13.

Chavali, P. L., Putz, M. and Gergely, F. (2014) 'Small organelle, big responsibility: the role of centrosomes in development and disease', *Philos Trans R Soc Lond B Biol Sci*, 369(1650).

Cheeseman, I. M. and Desai, A. (2008) 'Molecular architecture of the kinetochore-microtubule interface', *Nat Rev Mol Cell Biol*, 9(1), 33-46.

Chehab, N. H., Malikzay, A., Stavridi, E. S. and Halazonetis, T. D. (1999) 'Phosphorylation of Ser-20 mediates stabilization of human p53 in response to DNA damage', *Proc Natl Acad Sci U S A*, 96(24), 13777-82.

Chen, C., Tian, F., Lu, L., Wang, Y., Xiao, Z., Yu, C. and Yu, X. (2015) 'Characterization of Cep85: A novel antagonist of Nek2A that is involved in the regulation of centrosome disjunction', *Journal of Cell Science*.

Chen, M. S., Ryan, C. E. and Piwnica-Worms, H. (2003) 'Chk1 kinase negatively regulates mitotic function of Cdc25A phosphatase through 14-3-3 binding', *Mol Cell Biol*, 23(21), 7488-97.

Chen, Z., Yang, H. and Pavletich, N. P. (2008) 'Mechanism of homologous recombination from the RecA-ssDNA/dsDNA structures', *Nature*, 453(7194), 489-4.

Chini, C. C. and Chen, J. (2003) 'Human claspin is required for replication checkpoint control', *J Biol Chem*, 278(32), 30057-62.

Cho, S. W., Kim, S., Kim, J. M. and Kim, J. S. (2013) 'Targeted genome engineering in human cells with the Cas9 RNA-guided endonuclease', *Nat Biotechnol*, 31(3), 230-2.

Ciosk, R., Zachariae, W., Michaelis, C., Shevchenko, A., Mann, M. and Nasmyth, K. (1998) 'An ESP1/PDS1 complex regulates loss of sister chromatid cohesion at the metaphase to anaphase transition in yeast', *Cell*, 93(6), 1067-76.

Cizmecioglu, O., Arnold, M., Bahtz, R., Settele, F., Ehret, L., Haselmann-Weiss, U., Antony, C. and Hoffmann, I. (2010) 'Cep152 acts as a scaffold for recruitment of Plk4 and CPAP to the centrosome', *J Cell Biol*, 191(4), 731-9.

Cong, L., Ran, F. A., Cox, D., Lin, S., Barretto, R., Habib, N., Hsu, P. D., Wu, X., Jiang, W., Marraffini, L. A. and Zhang, F. (2013) 'Multiplex genome engineering using CRISPR/Cas systems', *Science*, 339(6121), 819-23.

Conroy, P. C., Saladino, C., Dantas, T. J., Lalor, P., Dockery, P. and Morrison, C. G. (2012) 'C-NAP1 and rootletin restrain DNA damage-induced centriole splitting and facilitate ciliogenesis', *Cell Cycle*, 11(20), 3769-78.

Cunha-Ferreira, I., Rodrigues-Martins, A., Bento, I., Riparbelli, M., Zhang, W., Laue, E., Callaini, G., Glover, D. M. and Bettencourt-Dias, M. (2009) 'The SCF/Slimb ubiquitin ligase limits centrosome amplification through degradation of SAK/PLK4', *Curr Biol*, 19(1), 43-9.

D'Assoro, A. B., Barrett, S. L., Folk, C., Negron, V. C., Boeneman, K., Busby, R., Whitehead, C., Stivala, F., Lingle, W. L. and Salisbury, J. L. (2002a) 'Amplified centrosomes in breast cancer: a potential indicator of tumor aggressiveness', *Breast Cancer Res Treat*, 75(1), 25-34.

D'Assoro, A. B., Lingle, W. L. and Salisbury, J. L. (2002b) 'Centrosome amplification and the development of cancer', *Oncogene*, 21(40), 6146-53.

Dammermann, A., Maddox, P. S., Desai, A. and Oegema, K. (2008) 'SAS-4 is recruited to a dynamic structure in newly forming centrioles that is stabilized by the gamma-tubulin-mediated addition of centriolar microtubules', *J Cell Biol*, 180(4), 771-85.

Dammermann, A. and Merdes, A. (2002) 'Assembly of centrosomal proteins and microtubule organization depends on PCM-1', *J Cell Biol*, 159(2), 255-66.

Date, O., Katsura, M., Ishida, M., Yoshihara, T., Kinomura, A., Sueda, T. and Miyagawa, K. (2006) 'Haploinsufficiency of RAD51B causes centrosome fragmentation and aneuploidy in human cells', *Cancer Res*, 66(12), 6018-24.

David, A., Liu, F., Tibelius, A., Vulprecht, J., Wald, D., Rothermel, U., Ohana, R., Seitel, A., Metzger, J., Ashery-Padan, R., Meinzer, H. P., Grone, H. J., Izraeli, S. and Kramer, A. (2014) 'Lack of centrioles and primary cilia in STIL(-/-) mouse embryos', *Cell Cycle*, 13(18), 2859-68.

De Luca, M., Lavia, P. and Guarguaglini, G. (2006) 'A functional interplay between Aurora-A, Plk1 and TPX2 at spindle poles: Plk1 controls centrosomal localization of Aurora-A and TPX2 spindle association', *Cell Cycle*, 5(3), 296-303.

Delgehyr, N., Sillibourne, J. and Bornens, M. (2005) 'Microtubule nucleation and anchoring at the centrosome are independent processes linked by ninein function', *J Cell Sci*, 118(Pt 8), 1565-75.

Dictenberg, J. B., Zimmerman, W., Sparks, C. A., Young, A., Vidair, C., Zheng, Y., Carrington, W., Fay, F. S. and Doxsey, S. J. (1998) 'Pericentrin and gamma-tubulin form a protein complex and are organized into a novel lattice at the centrosome', *J Cell Biol*, 141(1), 163-74.

Dierick, H. and Bejsovec, A. (1999) 'Cellular mechanisms of wingless/Wnt signal transduction', *Curr Top Dev Biol*, 43, 153-90.

Dodson, H., Bourke, E., Jeffers, L. J., Vagnarelli, P., Sonoda, E., Takeda, S., Earnshaw, W. C., Merdes, A. and Morrison, C. (2004) 'Centrosome amplification induced by DNA damage occurs during a prolonged G2 phase and involves ATM', *EMBO J*, 23(19), 3864-73.

Duelli, D. M., Hearn, S., Myers, M. P. and Lazebnik, Y. (2005) 'A primate virus generates transformed human cells by fusion', *J Cell Biol*, 171(3), 493-503.

Duensing, A., Liu, Y., Perdreau, S. A., Kleylein-Sohn, J., Nigg, E. A. and Duensing, S. (2007) 'Centriole overduplication through the concurrent formation of multiple daughter centrioles at single maternal templates', *Oncogene*, 26(43), 6280-8.

Duensing, A., Liu, Y., Tseng, M., Malumbres, M., Barbacid, M. and Duensing, S. (2006) 'Cyclin-dependent kinase 2 is dispensable for normal centrosome duplication but required for oncogene-induced centrosome overduplication', *Oncogene*, 25(20), 2943-9.

Dzhindzhev, N. S., Tzolovsky, G., Lipinszki, Z., Schneider, S., Lattao, R., Fu, J., Debski, J., Dadlez, M. and Glover, D. M. (2014) 'Plk4 phosphorylates Ana2 to trigger Sas6 recruitment and procentriole formation', *Curr Biol*, 24(21), 2526-32.

Eggert, U. S., Mitchison, T. J. and Field, C. M. (2006) 'Animal cytokinesis: from parts list to mechanisms', *Annu Rev Biochem*, 75, 543-66.

Ehrhardt, A. G. and Sluder, G. (2005) 'Spindle pole fragmentation due to proteasome inhibition', *J Cell Physiol*, 204(3), 808-18.

Elowe, S., Hümmer, S., Uldschmid, A., Li, X. and Nigg, E. A. (2007) 'Tension-sensitive Plk1 phosphorylation on BubR1 regulates the stability of kinetochore–microtubule interactions', *Genes & Development*, 21(17), 2205-2219.

Fabbro, M., Savage, K., Hobson, K., Deans, A. J., Powell, S. N., McArthur, G. A. and Khanna, K. K. (2004) 'BRCA1-BARD1 complexes are required for p53Ser-15 phosphorylation and a G1/S arrest following ionizing radiation-induced DNA damage', *J Biol Chem*, 279(30), 31251-8.

Fais, D. A., Nadezhdina, E. S. and Chentsov, Y. S. (1986) 'The centriolar rim. The structure that maintains the configuration of centrioles and basal bodies in the absence of their microtubules', *Exp Cell Res*, 164(1), 27-34.

Falck, J., Mailand, N., Syljuasen, R. G., Bartek, J. and Lukas, J. (2001) 'The ATM-Chk2-Cdc25A checkpoint pathway guards against radioresistant DNA synthesis', *Nature*, 410(6830), 842-7.

Fang, G., Yu, H. and Kirschner, M. W. (1998) 'Direct binding of CDC20 protein family members activates the anaphase-promoting complex in mitosis and G1', *Mol Cell*, 2(2), 163-71.

Fang, G., Zhang, D., Yin, H., Zheng, L., Bi, X. and Yuan, L. (2014) 'Centlein mediates an interaction between C-Nap1 and Cep68 to maintain centrosome cohesion', *Journal of Cell Science*, 127(8), 1631-1639.

Faragher, A. J. and Fry, A. M. (2003) 'Nek2A kinase stimulates centrosome disjunction and is required for formation of bipolar mitotic spindles', *Mol Biol Cell*, 14(7), 2876-89.

Fariss, R. N., Molday, R. S., Fisher, S. K. and Matsumoto, B. (1997) 'Evidence from normal and degenerating photoreceptors that two outer segment integral membrane proteins have separate transport pathways', *J Comp Neurol*, 387(1), 148-56.

Ferrante, M. I., Romio, L., Castro, S., Collins, J. E., Goulding, D. A., Stemple, D. L., Woolf, A. S. and Wilson, S. W. (2009) 'Convergent extension movements and ciliary function are mediated by ofd1, a zebrafish orthologue of the human oral-facial-digital type 1 syndrome gene', *Hum Mol Genet*, 18(2), 289-303.

Fletcher, L., Cerniglia, G. J., Nigg, E. A., Yend, T. J. and Muschel, R. J. (2004) 'Inhibition of centrosome separation after DNA damage: a role for Nek2', *Radiat Res*, 162(2), 128-35.

Fletcher, L. and Muschel, R. J. (2006) 'The centrosome and the DNA damage induced checkpoint', *Cancer Lett*, 243(1), 1-8.

Florian, S. and Mayer, T. U. (2012) 'The functional antagonism between Eg5 and dynein in spindle bipolarization is not compatible with a simple push-pull model', *Cell Rep*, 1(5), 408-16.

Fong, C. S., Kim, M., Yang, T. T., Liao, J. C. and Tsou, M. F. (2014) 'SAS-6 assembly templated by the lumen of cartwheel-less centrioles precedes centriole duplication', *Dev Cell*, 30(2), 238-45.

Fry, A. M. (2002) 'The Nek2 protein kinase: a novel regulator of centrosome structure', *Oncogene*, 6184-6194.

Fry, A. M., Mayor, T., Meraldi, P., Stierhof, Y. D., Tanaka, K. and Nigg, E. A. (1998) 'C-Nap1, a novel centrosomal coiled-coil protein and candidate substrate of the cell cycle-regulated protein kinase Nek2', *J Cell Biol*, 141(7), 1563-74.

Fu, J. and Glover, D. M. (2012) 'Structured illumination of the interface between centriole and peri-centriolar material', *Open Biol*, 2(8), 120104.

Fukasawa, K. (2008) 'P53, cyclin-dependent kinase and abnormal amplification of centrosomes', *Biochim Biophys Acta*, 1786(1), 15-23.

Fukasawa, K., Choi, T., Kuriyama, R., Rulong, S. and Vande Woude, G. F. (1996) 'Abnormal centrosome amplification in the absence of p53', *Science*, 271(5256), 1744-1747.

Ganem, N. J., Godinho, S. A. and Pellman, D. (2009) 'A mechanism linking extra centrosomes to

chromosomal instability', *Nature*, 460(7252), 278-82.

Ganem, N. J., Storchova, Z. and Pellman, D. (2007) 'Tetraploidy, aneuploidy and cancer', *Curr Opin Genet Dev*, 17(2), 157-62.

Gellert, M. (2002) 'V(D)J recombination: RAG proteins, repair factors, and regulation', *Annu Rev Biochem*, 71, 101-32.

Gilmore, E. C. and Walsh, C. A. (2013) 'Genetic causes of microcephaly and lessons for neuronal development', *Wiley Interdiscip Rev Dev Biol*, 2(4), 461-78.

Godinho, S. A. and Pellman, D. (2014) 'Causes and consequences of centrosome abnormalities in cancer', *Philos Trans R Soc Lond B Biol Sci*, 369(1650).

Godinho, S. A., Picone, R., Burute, M., Dagher, R., Su, Y., Leung, C. T., Polyak, K., Brugge, J. S., Thery, M. and Pellman, D. (2014) 'Oncogene-like induction of cellular invasion from centrosome amplification', *Nature*, 510(7503), 167-71.

Goodarzi, A. A., Yu, Y., Riballo, E., Douglas, P., Walker, S. A., Ye, R., Harer, C., Marchetti, C., Morrice, N., Jeggo, P. A. and Lees-Miller, S. P. (2006) 'DNA-PK autophosphorylation facilitates Artemis endonuclease activity', *Embo j*, 25(16), 3880-9.

Gorbsky, G. J. and Borisy, G. G. (1989) 'Microtubules of the kinetochore fiber turn over in metaphase but not in anaphase', *J Cell Biol*, 109(2), 653-62.

Gorr, I. H., Boos, D. and Stemmann, O. (2005) 'Mutual Inhibition of Separase and Cdk1 by Two-Step Complex Formation', *Molecular Cell*, 19(1), 135-141.

Gottlieb, T. M. and Jackson, S. P. (1993) 'The DNA-dependent protein kinase: Requirement for DNA ends and association with Ku antigen', *Cell*, 72(1), 131-142.

Graser, S., Stierhof, Y. D., Lavoie, S. B., Gassner, O. S., Lamla, S., Le Clech, M. and Nigg, E. A. (2007a) 'Cep164, a novel centriole appendage protein required for primary cilium formation', *J Cell Biol*, 179(2), 321-30.

Graser, S., Stierhof, Y. D. and Nigg, E. A. (2007b) 'Cep68 and Cep215 (Cdk5rap2) are required for centrosome cohesion', *J Cell Sci*, 120(Pt 24), 4321-31.

Gruss, O. J., Carazo-Salas, R. E., Schatz, C. A., Guarguaglini, G., Kast, J., Wilm, M., Le Bot, N., Vernos, I., Karsenti, E. and Mattaj, I. W. (2001) 'Ran Induces Spindle Assembly by Reversing the Inhibitory Effect of Importin α on TPX2 Activity', *Cell*, 104(1), 83-93.

Gu, J., Lu, H., Tsai, A. G., Schwarz, K. and Lieber, M. R. (2007) 'Single-stranded DNA ligation and XLF-stimulated incompatible DNA end ligation by the XRCC4-DNA ligase IV complex: influence of terminal DNA sequence', *Nucleic Acids Res*, 35(17), 5755-62.

Gudi, R., Haycraft, C. J., Bell, P. D., Li, Z. and Vasu, C. (2015) 'Centrobin-mediated regulation of the centrosomal protein 4.1-associated protein (CPAP) level limits centriole length during elongation stage', *J Biol Chem*, 290(11), 6890-902.

Gudi, R., Zou, C., Dhar, J., Gao, Q. and Vasu, C. (2014) 'Centrobin-centrosomal protein 4.1-associated protein (CPAP) interaction promotes CPAP localization to the centrioles during centriole duplication', *J Biol Chem*, 289(22), 15166-78.

Guichard, P., Chretien, D., Marco, S. and Tassin, A. M. (2010) 'Procentriole assembly revealed by cryo-electron tomography', *EMBO J*, 29(9), 1565-72.

Guo, H. Q., Gao, M., Ma, J., Xiao, T., Zhao, L. L., Gao, Y. and Pan, Q. J. (2007) 'Analysis of the cellular centrosome in fine-needle aspirations of the breast', *Breast Cancer Res*, 9(4), R48.

Hames, R. S., Crookes, R. E., Straatman, K. R., Merdes, A., Hayes, M. J., Faragher, A. J. and Fry, A. M. (2005) 'Dynamic recruitment of Nek2 kinase to the centrosome involves microtubules, PCM-1, and localized proteasomal degradation', *Mol Biol Cell*, 16(4), 1711-24.

Hansen, D. V., Loktev, A. V., Ban, K. H. and Jackson, P. K. (2004) 'Plk1 Regulates Activation of the Anaphase Promoting Complex by Phosphorylating and Triggering SCFβTrCP-dependent Destruction of the APC Inhibitor Emi1', *Molecular Biology of the Cell*, 15(12), 5623-5634.

Hardy, T., Lee, M., Hames, R. S., Prosser, S. L., Cheary, D. M., Samant, M. D., Schultz, F., Baxter, J. E., Rhee, K. and Fry, A. M. (2014) 'Multisite phosphorylation of C-Nap1 releases it from Cep135 to trigger centrosome disjunction', *J Cell Sci*, 127(Pt 11), 2493-506.

Harel, A., Chan, R. C., Lachish-Zalait, A., Zimmerman, E., Elbaum, M. and Forbes, D. J. (2003) 'Importin beta negatively regulates nuclear membrane fusion and nuclear pore complex assembly', *Mol Biol Cell*, 14(11), 4387-96.

Harper, J. W., Adami, G. R., Wei, N., Keyomarsi, K. and Elledge, S. J. (1993) 'The p21 Cdk-interacting protein Cip1 is a potent inhibitor of G1 cyclin-dependent kinases', *Cell*, 75(4), 805-16.

Harper, J. W., Elledge, S. J., Keyomarsi, K., Dynlacht, B., Tsai, L. H., Zhang, P., Dobrowolski, S., Bai, C., Connell-Crowley, L., Swindell, E. and et al. (1995) 'Inhibition of cyclin-dependent kinases by p21', *Mol Biol Cell*, 6(4), 387-400.

Hauf, S., Roitinger, E., Koch, B., Dittrich, C. M., Mechtler, K. and Peters, J. M. (2005) 'Dissociation of cohesin from chromosome arms and loss of arm cohesion during early mitosis depends on phosphorylation of SA2', *PLoS Biol*, 3(3), e69.

He, R., Huang, N., Bao, Y., Zhou, H., Teng, J. and Chen, J. (2013) 'LRRC45 is a centrosome linker component required for centrosome cohesion', *Cell Rep*, 4(6), 1100-7.

Helps, N. R., Luo, X., Barker, H. M. and Cohen, P. T. (2000) 'NIMA-related kinase 2 (Nek2), a cell-cycle-regulated protein kinase localized to centrosomes, is complexed to protein phosphatase 1', *Biochem J*, 349(Pt 2), 509-18.

Herzog, F., Primorac, I., Dube, P., Lenart, P., Sander, B., Mechtler, K., Stark, H. and Peters, J. M. (2009) 'Structure of the anaphase-promoting complex/cyclosome interacting with a mitotic checkpoint complex', *Science*, 323(5920), 1477-81.

Hinchcliffe, E. H., Li, C., Thompson, E. A., Maller, J. L. and Sluder, G. (1999) 'Requirement of Cdk2-cyclin E activity for repeated centrosome reproduction in Xenopus egg extracts', *Science*, 283(5403), 851-4.

Hochegger, H., Takeda, S. and Hunt, T. (2008) 'Cyclin-dependent kinases and cell-cycle transitions: does one fit all?', *Nat Rev Mol Cell Biol*, 9(11), 910-6.

Holland, A. J., Lan, W., Niessen, S., Hoover, H. and Cleveland, D. W. (2010) 'Polo-like kinase 4 kinase activity limits centrosome overduplication by autoregulating its own stability', *J Cell Biol*, 188(2), 191-8.

Huertas, P. and Jackson, S. P. (2009) 'Human CtIP mediates cell cycle control of DNA end resection and double strand break repair', *J Biol Chem*, 284(14), 9558-65.

Hunt, T. and Kirschner, M. (1993) 'Cell multiplication', *Curr Opin Cell Biol*, 5(2), 163-5.

Hurtado, L., Caballero, C., Gavilan, M. P., Cardenas, J., Bornens, M. and Rios, R. M. (2011) 'Disconnecting the Golgi ribbon from the centrosome prevents directional cell migration and ciliogenesis', *J Cell Biol*, 193(5), 917-33.

Hutchins, J. R. A., Moore, W. J., Hood, F. E., Wilson, J. S. J., Andrews, P. D., Swedlow, J. R. and

Clarke, P. R. (2004) 'Phosphorylation Regulates the Dynamic Interaction of RCC1 with Chromosomes during Mitosis', *Current Biology*, 14(12), 1099-1104.

Inanc, B., Dodson, H. and Morrison, C. G. (2010) 'A centrosome-autonomous signal that involves centriole disengagement permits centrosome duplication in G2 phase after DNA damage', *Mol Biol Cell*, 21(22), 3866-77.

Inoue, D. and Sagata, N. (2005) 'The Polo-like kinase Plx1 interacts with and inhibits Myt1 after fertilization of Xenopus eggs', *Embo j*, 24(5), 1057-67.

Ishikawa, H., Kubo, A. and Tsukita, S. (2005) 'Odf2-deficient mother centrioles lack distal/subdistal appendages and the ability to generate primary cilia', *Nat Cell Biol*, 7(5), 517-24.

Ishikawa, K., Ishii, H. and Saito, T. (2006) 'DNA damage-dependent cell cycle checkpoints and genomic stability', *DNA Cell Biol*, 25(7), 406-11.

Jackman, M., Lindon, C., Nigg, E. A. and Pines, J. (2003) 'Active cyclin B1-Cdk1 first appears on centrosomes in prophase', *Nat Cell Biol*, 5(2), 143-8.

Jana, S. C., Marteil, G. and Bettencourt-Dias, M. (2014) 'Mapping molecules to structure: unveiling secrets of centriole and cilia assembly with near-atomic resolution', *Curr Opin Cell Biol*, 26, 96-106.

Jiang, X. R., Jimenez, G., Chang, E., Frolkis, M., Kusler, B., Sage, M., Beeche, M., Bodnar, A. G., Wahl, G. M., Tlsty, T. D. and Chiu, C. P. (1999) 'Telomerase expression in human somatic cells does not induce changes associated with a transformed phenotype', *Nat Genet*, 21(1), 111-4.

Jin, H., White, S. R., Shida, T., Schulz, S., Aguiar, M., Gygi, S. P., Bazan, J. F. and Nachury, M. V. (2010) 'The conserved Bardet-Biedl syndrome proteins assemble a coat that traffics membrane proteins to cilia', *Cell*, 141(7), 1208-19.

Joglekar, A. P., Bloom, K. S. and Salmon, E. D. (2010) 'Mechanisms of force generation by end-on kinetochore-microtubule attachments', *Curr Opin Cell Biol*, 22(1), 57-67.

Johnson, V. L., Scott, M. I., Holt, S. V., Hussein, D. and Taylor, S. S. (2004) 'Bub1 is required for kinetochore localization of BubR1, Cenp-E, Cenp-F and Mad2, and chromosome congression', *J Cell Sci*, 117(Pt 8), 1577-89.

Kalab, P., Pu, R. T. and Dasso, M. (1999) 'The ran GTPase regulates mitotic spindle assembly', *Curr Biol*, 9(9), 481-4.

Kallenbach, R. J. and Mazia, D. (1982) 'Origin and maturation of centrioles in association with the nuclear envelope in hypertonic-stressed sea urchin eggs', *Eur J Cell Biol*, 28(1), 68-76.

Kamileri, I., Karakasilioti, I., Sideri, A., Kosteas, T., Tatarakis, A., Talianidis, I. and Garinis, G. A. (2012) 'Defective transcription initiation causes postnatal growth failure in a mouse model of nucleotide excision repair (NER) progeria', *Proc Natl Acad Sci U S A*, 109(8), 2995-3000.

Kamiya, A., Tan, P. L., Kubo, K., Engelhard, C., Ishizuka, K., Kubo, A., Tsukita, S., Pulver, A. E., Nakajima, K., Cascella, N. G., Katsanis, N. and Sawa, A. (2008) 'Recruitment of PCM1 to the centrosome by the cooperative action of DISC1 and BBS4: a candidate for psychiatric illnesses', *Arch Gen Psychiatry*, 65(9), 996-1006.

Karsenti, E. and Vernos, I. (2001) 'The mitotic spindle: a self-made machine', *Science*, 294(5542), 543-7.

Khateb, S., Zelinger, L., Mizrahi-Meissonnier, L., Ayuso, C., Koenekoop, R. K., Laxer, U., Gross, M., Banin, E. and Sharon, D. (2014) 'A homozygous nonsense CEP250 mutation combined with a heterozygous nonsense C2orf71 mutation is associated with atypical Usher syndrome',

J Med Genet, 51(7), 460-9.

Khodjakov, A., Cole, R. W., Oakley, B. R. and Rieder, C. L. (2000) 'Centrosome-independent mitotic spindle formation in vertebrates', *Curr Biol*, 10(2), 59-67.

Khodjakov, A. and Rieder, C. L. (2001) 'Centrosomes enhance the fidelity of cytokinesis in vertebrates and are required for cell cycle progression', *J Cell Biol*, 153(1), 237-42.

Khodjakov, A., Rieder, C. L., Sluder, G., Cassels, G., Sibon, O. and Wang, C. L. (2002) 'De novo formation of centrosomes in vertebrate cells arrested during S phase', *The Journal of Cell Biology*, 158(7), 1171-1181.

Kim, Lee, S., Chang, J. and Rhee, K. (2008) 'A novel function of CEP135 as a platform protein of C-NAP1 for its centriolar localization', *Exp Cell Res*, 314(20), 3692-700.

Kim, J., Krishnaswami, S. R. and Gleeson, J. G. (2008) 'CEP290 interacts with the centriolar satellite component PCM-1 and is required for Rab8 localization to the primary cilium', *Hum Mol Genet*, 17(23), 3796-805.

Kim, J. C., Badano, J. L., Sibold, S., Esmail, M. A., Hill, J., Hoskins, B. E., Leitch, C. C., Venner, K., Ansley, S. J., Ross, A. J., Leroux, M. R., Katsanis, N. and Beales, P. L. (2004) 'The Bardet-Biedl protein BBS4 targets cargo to the pericentriolar region and is required for microtubule anchoring and cell cycle progression', *Nat Genet*, 36(5), 462-70.

Kim, K., Lee, S., Chang, J. and Rhee, K. (2008) 'A novel function of CEP135 as a platform protein of C-NAP1 for its centriolar localization', *Exp Cell Res*, 314(20), 3692-700.

Kim, S. and Dynlacht, B. D. (2013) 'Assembling a primary cilium', *Current Opinion in Cell Biology*, 25(4), 506-511.

Kim, T. S., Park, J. E., Shukla, A., Choi, S., Murugan, R. N., Lee, J. H., Ahn, M., Rhee, K., Bang, J. K., Kim, B. Y., Loncarek, J., Erikson, R. L. and Lee, K. S. (2013) 'Hierarchical recruitment of Plk4 and regulation of centriole biogenesis by two centrosomal scaffolds, Cep192 and Cep152', *Proc Natl Acad Sci U S A*, 110(50), E4849-57.

King, R. W., Peters, J. M., Tugendreich, S., Rolfe, M., Hieter, P. and Kirschner, M. W. (1995) 'A 20S complex containing CDC27 and CDC16 catalyzes the mitosis-specific conjugation of ubiquitin to cyclin B', *Cell*, 81(2), 279-88.

Kirschner, M. and Mitchison, T. (1986) 'Beyond self-assembly: from microtubules to morphogenesis', *Cell*, 45(3), 329-42.

Kitagawa, D., Vakonakis, I., Olieric, N., Hilbert, M., Keller, D., Olieric, V., Bortfeld, M., Erat, M. C., Fluckiger, I., Gonczy, P. and Steinmetz, M. O. (2011) 'Structural basis of the 9-fold symmetry of centrioles', *Cell*, 144(3), 364-75.

Kiyomitsu, T. and Cheeseman, I. M. (2012) 'Chromosome- and spindle-pole-derived signals generate an intrinsic code for spindle position and orientation', *Nat Cell Biol*, 14(3), 311-7.

Kleylein-Sohn, J., Westendorf, J., Le Clech, M., Habedanck, R., Stierhof, Y. D. and Nigg, E. A. (2007) 'Plk4-induced centriole biogenesis in human cells', *Dev Cell*, 13(2), 190-202.

Kline-Smith, S. L. and Walczak, C. E. (2004) 'Mitotic spindle assembly and chromosome segregation: refocusing on microtubule dynamics', *Mol Cell*, 15(3), 317-27.

Klos Dehring, D. A., Vladar, E. K., Werner, M. E., Mitchell, J. W., Hwang, P. and Mitchell, B. J. (2013) 'Deuterosome-mediated centriole biogenesis', *Dev Cell*, 27(1), 103-12.

Kodani, A., Tonthat, V., Wu, B. and Sutterlin, C. (2010) 'Par6 alpha interacts with the dynactin subunit p150 Glued and is a critical regulator of centrosomal protein recruitment', *Mol Biol*

Cell, 21(19), 3376-85.

Kohlmaier, G., Loncarek, J., Meng, X., McEwen, B. F., Mogensen, M. M., Spektor, A., Dynlacht, B. D., Khodjakov, A. and Gonczy, P. (2009) 'Overly long centrioles and defective cell division upon excess of the SAS-4-related protein CPAP', *Curr Biol*, 19(12), 1012-8.

Komarova, Y. A., Akhmanova, A. S., Kojima, S., Galjart, N. and Borisy, G. G. (2002) 'Cytoplasmic linker proteins promote microtubule rescue in vivo', *J Cell Biol*, 159(4), 589-99.

Kops, G. J., Saurin, A. T. and Meraldi, P. (2010) 'Finding the middle ground: how kinetochores power chromosome congression', *Cell Mol Life Sci*, 67(13), 2145-61.

Kops, G. J., Weaver, B. A. and Cleveland, D. W. (2005) 'On the road to cancer: aneuploidy and the mitotic checkpoint', *Nat Rev Cancer*, 5(10), 773-85.

Kratz, A. S., Barenz, F., Richter, K. T. and Hoffmann, I. (2015) 'Plk4-dependent phosphorylation of STIL is required for centriole duplication', *Biol Open*, 4(3), 370-7.

Kubo, A., Sasaki, H., Yuba-Kubo, A., Tsukita, S. and Shiina, N. (1999) 'Centriolar satellites: molecular characterization, ATP-dependent movement toward centrioles and possible involvement in ciliogenesis', *J Cell Biol*, 147(5), 969-80.

Kubo, A. and Tsukita, S. (2003) 'Non-membranous granular organelle consisting of PCM-1: subcellular distribution and cell-cycle-dependent assembly/disassembly', *J Cell Sci*, 116(Pt 5), 919-28.

Kuerbitz, S. J., Plunkett, B. S., Walsh, W. V. and Kastan, M. B. (1992) 'Wild-type p53 is a cell cycle checkpoint determinant following irradiation', *Proc Natl Acad Sci U S A*, 89(16), 7491-5.

Kuriyama, R., Terada, Y., Lee, K. S. and Wang, C. L. (2007) 'Centrosome replication in hydroxyurea-arrested CHO cells expressing GFP-tagged centrin2', *J Cell Sci*, 120(Pt 14), 2444-53.

Kushner, E. J., Ferro, L. S., Liu, J. Y., Durrant, J. R., Rogers, S. L., Dudley, A. C. and Bautch, V. L. (2014) 'Excess centrosomes disrupt endothelial cell migration via centrosome scattering', *J Cell Biol*, 206(2), 257-72.

Kwon, M., Godinho, S. A., Chandhok, N. S., Ganem, N. J., Azioune, A., Thery, M. and Pellman, D. (2008) 'Mechanisms to suppress multipolar divisions in cancer cells with extra centrosomes', *Genes Dev*, 22(16), 2189-203.

La Terra, S., English, C. N., Hergert, P., McEwen, B. F., Sluder, G. and Khodjakov, A. (2005) 'The de novo centriole assembly pathway in HeLa cells: cell cycle progression and centriole assembly/maturation', *J Cell Biol*, 168(5), 713-22.

Lambrus, B. G., Uetake, Y., Clutario, K. M., Daggubati, V., Snyder, M., Sluder, G. and Holland, A. J. (2015) 'p53 protects against genome instability following centriole duplication failure', *J Cell Biol*, 210(1), 63-77.

Lane, H. A. and Nigg, E. A. (1996) 'Antibody microinjection reveals an essential role for human polo-like kinase 1 (Plk1) in the functional maturation of mitotic centrosomes', *J Cell Biol*, 135(6 Pt 2), 1701-13.

Lawo, S., Hasegan, M., Gupta, G. D. and Pelletier, L. (2012) 'Subdiffraction imaging of centrosomes reveals higher-order organizational features of pericentriolar material', *Nat Cell Biol*, 14(11), 1148-58.

Leber, B., Maier, B., Fuchs, F., Chi, J., Riffel, P., Anderhub, S., Wagner, L., Ho, A. D., Salisbury, J. L., Boutros, M. and Kramer, A. (2010) 'Proteins required for centrosome clustering in cancer cells', *Sci Transl Med*, 2(33), 33ra38.

Lee, J. H. and Paull, T. T. (2005) 'ATM activation by DNA double-strand breaks through the Mre11-Rad50-Nbs1 complex', *Science*, 308(5721), 551-4.

Lee, K. and Rhee, K. (2012) 'Separase-dependent cleavage of pericentrin B is necessary and sufficient for centriole disengagement during mitosis', *Cell Cycle*, 11(13), 2476-85.

Li, J., D'Angiolella, V., Seeley, E. S., Kim, S., Kobayashi, T., Fu, W., Campos, E. I., Pagano, M. and Dynlacht, B. D. (2013) 'USP33 regulates centrosome biogenesis via deubiquitination of the centriolar protein CP110', *Nature*, 495(7440), 255-9.

Lieber, M. R. (2010) 'The mechanism of double-strand DNA break repair by the nonhomologous DNA end-joining pathway', *Annu Rev Biochem*, 79, 181-211.

Lieber, M. R. and Karanjawala, Z. E. (2004) 'Ageing, repetitive genomes and DNA damage', *Nat Rev Mol Cell Biol*, 5(1), 69-75.

Lim, H. H., Zhang, T. and Surana, U. (2009) 'Regulation of centrosome separation in yeast and vertebrates: common threads', *Trends Cell Biol*, 19(7), 325-33.

Lin, S. Y., Rai, R., Li, K., Xu, Z. X. and Elledge, S. J. (2005) 'BRIT1/MCPH1 is a DNA damage responsive protein that regulates the Brca1-Chk1 pathway, implicating checkpoint dysfunction in microcephaly', *Proc Natl Acad Sci U S A*, 102(42), 15105-9.

Lin, T.-c., Neuner, A. and Schiebel, E. (2015) 'Targeting of γ-tubulin complexes to microtubule organizing centers: conservation and divergence', *Trends in Cell Biology*, 25(5), 296-307.

Lin, T. C., Gombos, L., Neuner, A., Sebastian, D., Olsen, J. V., Hrle, A., Benda, C. and Schiebel, E. (2011) 'Phosphorylation of the yeast gamma-tubulin Tub4 regulates microtubule function', *PLoS One*, 6(5), e19700.

Lin, Y. C., Chang, C. W., Hsu, W. B., Tang, C. J., Lin, Y. N., Chou, E. J., Wu, C. T. and Tang, T. K. (2013) 'Human microcephaly protein CEP135 binds to hSAS-6 and CPAP, and is required for centriole assembly', *EMBO J*, 32(8), 1141-54.

Lingle, W. L., Barrett, S. L., Negron, V. C., D'Assoro, A. B., Boeneman, K., Liu, W., Whitehead, C. M., Reynolds, C. and Salisbury, J. L. (2002) 'Centrosome amplification drives chromosomal instability in breast tumor development', *Proc Natl Acad Sci U S A*, 99(4), 1978-83.

Liu, W.-F., Yu, S.-S., Chen, G.-J. and Li, Y.-Z. (2006) 'DNA Damage Checkpoint, Damage Repair, and Genome Stability', *Acta Genetica Sinica*, 33(5), 381-390.

Loffler, H., Fechter, A., Liu, F. Y., Poppelreuther, S. and Kramer, A. (2013) 'DNA damage-induced centrosome amplification occurs via excessive formation of centriolar satellites', *Oncogene*, 32(24), 2963-72.

Loffler, H., Lukas, J., Bartek, J. and Kramer, A. (2006) 'Structure meets function--centrosomes, genome maintenance and the DNA damage response', *Exp Cell Res*, 312(14), 2633-40.

Loncarek, J., Hergert, P., Magidson, V. and Khodjakov, A. (2008) 'Control of daughter centriole formation by the pericentriolar material', *Nat Cell Biol*, 10(3), 322-8.

Lopes, C. A., Prosser, S. L., Romio, L., Hirst, R. A., O'Callaghan, C., Woolf, A. S. and Fry, A. M. (2011) 'Centriolar satellites are assembly points for proteins implicated in human ciliopathies, including oral-facial-digital syndrome 1', *J Cell Sci*, 124(Pt 4), 600-12.

Lossaint, G., Larroque, M., Ribeyre, C., Bec, N., Larroque, C., Decaillet, C., Gari, K. and Constantinou, A. (2013) 'FANCD2 binds MCM proteins and controls replisome function upon activation of s phase checkpoint signaling', *Mol Cell*, 51(5), 678-90.

Lou, Z., Chini, C. C., Minter-Dykhouse, K. and Chen, J. (2003) 'Mediator of DNA damage

checkpoint protein 1 regulates BRCA1 localization and phosphorylation in DNA damage checkpoint control', *J Biol Chem*, 278(16), 13599-602.

Luders, J. and Stearns, T. (2007) 'Microtubule-organizing centres: a re-evaluation', *Nat Rev Mol Cell Biol*, 8(2), 161-7.

Luo, X., Tang, Z., Rizo, J. and Yu, H. (2002) 'The Mad2 spindle checkpoint protein undergoes similar major conformational changes upon binding to either Mad1 or Cdc20', *Mol Cell*, 9(1), 59-71.

Ma, Y., Pannicke, U., Schwarz, K. and Lieber, M. R. (2002) 'Hairpin opening and overhang processing by an Artemis/DNA-dependent protein kinase complex in nonhomologous end joining and V(D)J recombination', *Cell*, 108(6), 781-94.

Macurek, L., Lindqvist, A., Lim, D., Lampson, M. A., Klompmaker, R., Freire, R., Clouin, C., Taylor, S. S., Yaffe, M. B. and Medema, R. H. (2008) 'Polo-like kinase-1 is activated by aurora A to promote checkpoint recovery', *Nature*, 455(7209), 119-123.

Madlener, S., Rosner, M., Krieger, S., Giessrigl, B., Gridling, M., Vo, T. P. N., Leisser, C., Lackner, A., Raab, I., Grusch, M., Hengstschläger, M., Dolznig, H. and Krupitza, G. (2009) 'Short 42°C heat shock induces phosphorylation and degradation of Cdc25A which depends on p38MAPK, Chk2 and 14.3.3', *Human Molecular Genetics*, 18(11), 1990-2000.

Magidson, V., O'Connell, C. B., Loncarek, J., Paul, R., Mogilner, A. and Khodjakov, A. (2011) 'The spatial arrangement of chromosomes during prometaphase facilitates spindle assembly', *Cell*, 146(4), 555-67.

Mali, P., Yang, L., Esvelt, K. M., Aach, J., Guell, M., DiCarlo, J. E., Norville, J. E. and Church, G. M. (2013) 'RNA-guided human genome engineering via Cas9', *Science*, 339(6121), 823-6.

Malumbres, M. and Barbacid, M. (2005) 'Mammalian cyclin-dependent kinases', *Trends in Biochemical Sciences*, 30(11), 630-641.

Man, X., Megraw, T. L. and Lim, Y. P. (2015) 'Cep68 can be regulated by Nek2 and SCF complex', *Eur J Cell Biol*, 94(3-4), 162-72.

Manning, J. A., Shalini, S., Risk, J. M., Day, C. L. and Kumar, S. (2010) 'A direct interaction with NEDD1 regulates gamma-tubulin recruitment to the centrosome', *PLoS One*, 5(3), e9618.

Mardin, B. R., Isokane, M., Cosenza, M. R., Kramer, A., Ellenberg, J., Fry, A. M. and Schiebel, E. (2013) 'EGF-induced centrosome separation promotes mitotic progression and cell survival', *Dev Cell*, 25(3), 229-40.

Mardin, B. R., Lange, C., Baxter, J. E., Hardy, T., Scholz, S. R., Fry, A. M. and Schiebel, E. (2010) 'Components of the Hippo pathway cooperate with Nek2 kinase to regulate centrosome disjunction', *Nat Cell Biol*, 12(12), 1166-76.

Mardin, B. R. and Schiebel, E. (2012) 'Breaking the ties that bind: new advances in centrosome biology', *J Cell Biol*, 197(1), 11-8.

Martin, G. M., Smith, A. C., Ketterer, D. J., Ogburn, C. E. and Disteche, C. M. (1985) 'Increased chromosomal aberrations in first metaphases of cells isolated from the kidneys of aged mice', *Isr J Med Sci*, 21(3), 296-301.

Martin, S. A., Lord, C. J. and Ashworth, A. (2010) 'Therapeutic targeting of the DNA mismatch repair pathway', *Clin Cancer Res*, 16(21), 5107-13.

Marumoto, T., Zhang, D. and Saya, H. (2005) 'Aurora-A - a guardian of poles', *Nat Rev Cancer*, 5(1), 42-50.

Matsuo, K., Ohsumi, K., Iwabuchi, M., Kawamata, T., Ono, Y. and Takahashi, M. (2012) 'Kendrin is

a novel substrate for separase involved in the licensing of centriole duplication', *Curr Biol*, 22(10), 915-21.

Mayor, T., Hacker, U., Stierhof, Y. D. and Nigg, E. A. (2002) 'The mechanism regulating the dissociation of the centrosomal protein C-Nap1 from mitotic spindle poles', *J Cell Sci*, 115(Pt 16), 3275-84.

Mayor, T., Stierhof, Y. D., Tanaka, K., Fry, A. M. and Nigg, E. A. (2000) 'The centrosomal protein C-Nap1 is required for cell cycle-regulated centrosome cohesion', *J Cell Biol*, 151(4), 837-46.

Meek, K., Gupta, S., Ramsden, D. A. and Lees-Miller, S. P. (2004) 'The DNA-dependent protein kinase: the director at the end', *Immunol Rev*, 200, 132-41.

Mennella, V., Keszthelyi, B., McDonald, K. L., Chhun, B., Kan, F., Rogers, G. C., Huang, B. and Agard, D. A. (2012) 'Subdiffraction-resolution fluorescence microscopy reveals a domain of the centrosome critical for pericentriolar material organization', *Nat Cell Biol*, 14(11), 1159-68.

Meraldi, P., Honda, R. and Nigg, E. A. (2002) 'Aurora-A overexpression reveals tetraploidization as a major route to centrosome amplification in p53-/- cells', *EMBO J*, 21(4), 483-92.

Meraldi, P., Lukas, J., Fry, A. M., Bartek, J. and Nigg, E. A. (1999) 'Centrosome duplication in mammalian somatic cells requires E2F and Cdk2-cyclin A', *Nat Cell Biol*, 1(2), 88-93.

Mi, J., Guo, C., Brautigan, D. L. and Larner, J. M. (2007) 'Protein phosphatase-1alpha regulates centrosome splitting through Nek2', *Cancer Res*, 67(3), 1082-9.

Mimori-Kiyosue, Y. and Tsukita, S. (2003) '"Search-and-Capture" of Microtubules through Plus-End-Binding Proteins (+TIPs)', *Journal of Biochemistry*, 134(3), 321-326.

Mitchison, T. and Kirschner, M. (1984) 'Dynamic instability of microtubule growth', *Nature*, 312(5991), 237-42.

Molinari, M. (2000) 'Cell cycle checkpoints and their inactivation in human cancer', *Cell Prolif*, 33(5), 261-74.

Morrison, C., Sonoda, E., Takao, N., Shinohara, A., Yamamoto, K. and Takeda, S. (2000) 'The controlling role of ATM in homologous recombinational repair of DNA damage', *Embo j*, 19(3), 463-71.

Moynahan, M. E. and Jasin, M. (2010) 'Mitotic homologous recombination maintains genomic stability and suppresses tumorigenesis', *Nat Rev Mol Cell Biol*, 11(3), 196-207.

Mullins, J. M. and Biesele, J. J. (1973) 'Cytokinetic activities in a human cell line: the midbody and intercellular bridge', *Tissue Cell*, 5(1), 47-61.

Musacchio, A. and Salmon, E. D. (2007) 'The spindle-assembly checkpoint in space and time', *Nat Rev Mol Cell Biol*, 8(5), 379-93.

Nachury, M. V. (2014) 'How do cilia organize signalling cascades?', *Philos Trans R Soc Lond B Biol Sci*, 369(1650).

Nachury, M. V., Loktev, A. V., Zhang, Q., Westlake, C. J., Peranen, J., Merdes, A., Slusarski, D. C., Scheller, R. H., Bazan, J. F., Sheffield, V. C. and Jackson, P. K. (2007) 'A core complex of BBS proteins cooperates with the GTPase Rab8 to promote ciliary membrane biogenesis', *Cell*, 129(6), 1201-13.

Nakajima, N. I., Hagiwara, Y., Oike, T., Okayasu, R., Murakami, T., Nakano, T. and Shibata, A. (2015) 'Pre-exposure to ionizing radiation stimulates DNA double strand break end

resection, promoting the use of homologous recombination repair', *PLoS One*, 10(3), e0122582.

Nakamura, A., Arai, H. and Fujita, N. (2009) 'Centrosomal Aki1 and cohesin function in separase-regulated centriole disengagement', *J Cell Biol*, 187(5), 607-14.

Nasmyth, K. (2001) 'Disseminating the genome: joining, resolving, and separating sister chromatids during mitosis and meiosis', *Annu Rev Genet*, 35, 673-745.

Nigg, E. A. (2002) 'Centrosome aberrations: cause or consequence of cancer progression?', *Nat Rev Cancer*, 2(11), 815-25.

Nigg, E. A. (2006) 'Origins and consequences of centrosome aberrations in human cancers', *Int J Cancer*, 119(12), 2717-23.

Nigg, E. A. (2007) 'Centrosome duplication: of rules and licenses', *Trends Cell Biol*, 17(5), 215-21.

Nigg, E. A. and Raff, J. W. (2009) 'Centrioles, centrosomes, and cilia in health and disease', *Cell*, 139(4), 663-78.

Niida, H. and Nakanishi, M. (2006) 'DNA damage checkpoints in mammals', *Mutagenesis*, 21(1), 3-9.

Nishimura, K., Fukagawa, T., Takisawa, H., Kakimoto, T. and Kanemaki, M. (2009) 'An auxin-based degron system for the rapid depletion of proteins in nonplant cells', *Nat Methods*, 6(12), 917-22.

Oh, E. C. and Katsanis, N. (2012) 'Cilia in vertebrate development and disease', *Development*, 139(3), 443-8.

Oikawa, T., Okuda, M., Ma, Z., Goorha, R., Tsujimoto, H., Inokuma, H. and Fukasawa, K. (2005) 'Transcriptional control of BubR1 by p53 and suppression of centrosome amplification by BubR1', *Mol Cell Biol*, 25(10), 4046-61.

Oshimori, N., Li, X., Ohsugi, M. and Yamamoto, T. (2009) 'Cep72 regulates the localization of key centrosomal proteins and proper bipolar spindle formation', *EMBO J*, 28(14), 2066-76.

Oshimori, N., Ohsugi, M. and Yamamoto, T. (2006) 'The Plk1 target Kizuna stabilizes mitotic centrosomes to ensure spindle bipolarity', *Nat Cell Biol*, 8(10), 1095-101.

Ou, Y. Y., Mack, G. J., Zhang, M. and Rattner, J. B. (2002) 'CEP110 and ninein are located in a specific domain of the centrosome associated with centrosome maturation', *J Cell Sci*, 115(Pt 9), 1825-35.

Pagan, J. K., Marzio, A., Jones, M. J., Saraf, A., Jallepalli, P. V., Florens, L., Washburn, M. P. and Pagano, M. (2015) 'Degradation of Cep68 and PCNT cleavage mediate Cep215 removal from the PCM to allow centriole separation, disengagement and licensing', *Nat Cell Biol*, 17(1), 31-43.

Palazzo, R. E., Vaisberg, E., Cole, R. W. and Rieder, C. L. (1992) 'Centriole duplication in lysates of Spisula solidissima oocytes', *Science*, 256(5054), 219-21.

Panic, M., Hata, S., Neuner, A. and Schiebel, E. (2015) 'The centrosomal linker and microtubules provide dual levels of spatial coordination of centrosomes', *PLoS Genet*, 11(5), e1005243.

Paoletti, A., Moudjou, M., Paintrand, M., Salisbury, J. L. and Bornens, M. (1996) 'Most of centrin in animal cells is not centrosome-associated and centrosomal centrin is confined to the distal lumen of centrioles', *J Cell Sci*, 109 (Pt 13), 3089-102.

Paridaen, J. T., Wilsch-Brauninger, M. and Huttner, W. B. (2013) 'Asymmetric inheritance of centrosome-associated primary cilium membrane directs ciliogenesis after cell division',

Cell, 155(2), 333-44.

Pearson, C. G., Osborn, D. P., Giddings, T. H., Jr., Beales, P. L. and Winey, M. (2009) 'Basal body stability and ciliogenesis requires the conserved component Poc1', *J Cell Biol*, 187(6), 905-20.

Peters, J.-M. (2006) 'The anaphase promoting complex/cyclosome: a machine designed to destroy', *Nat Rev Mol Cell Biol*, 7(9), 644-656.

Petrie, R. J., Doyle, A. D. and Yamada, K. M. (2009) 'Random versus directionally persistent cell migration', *Nat Rev Mol Cell Biol*, 10(8), 538-49.

Piel, M., Meyer, P., Khodjakov, A., Rieder, C. L. and Bornens, M. (2000) 'The respective contributions of the mother and daughter centrioles to centrosome activity and behavior in vertebrate cells', *J Cell Biol*, 149(2), 317-30.

Piel, M., Nordberg, J., Euteneuer, U. and Bornens, M. (2001) 'Centrosome-dependent exit of cytokinesis in animal cells', *Science*, 291(5508), 1550-3.

Prosser, S. L., Straatman, K. R. and Fry, A. M. (2009) 'Molecular dissection of the centrosome overduplication pathway in S-phase-arrested cells', *Mol Cell Biol*, 29(7), 1760-73.

Quintyne, N. J. and Schroer, T. A. (2002) 'Distinct cell cycle–dependent roles for dynactin and dynein at centrosomes', *The Journal of Cell Biology*, 159(2), 245-254.

Rass, U., Compton, S. A., Matos, J., Singleton, M. R., Ip, S. C., Blanco, M. G., Griffith, J. D. and West, S. C. (2010) 'Mechanism of Holliday junction resolution by the human GEN1 protein', *Genes Dev*, 24(14), 1559-69.

Rieder, C. L. (1981) 'The structure of the cold-stable kinetochore fiber in metaphase PtK1 cells', *Chromosoma*, 84(1), 145-58.

Rieder, C. L., Davison, E. A., Jensen, L. C., Cassimeris, L. and Salmon, E. D. (1986) 'Oscillatory movements of monooriented chromosomes and their position relative to the spindle pole result from the ejection properties of the aster and half-spindle', *J Cell Biol*, 103(2), 581-91.

Rieder, C. L. and Salmon, E. D. (1998) 'The vertebrate cell kinetochore and its roles during mitosis', *Trends Cell Biol*, 8(8), 310-8.

Saito, Y., Fujimoto, H. and Kobayashi, J. (2013) 'Role of NBS1 in DNA damage response and its relationship with cancer development', *Translational Cancer Research*, 2(3), 178-189.

Saladino, C., Bourke, E., Conroy, P. C. and Morrison, C. G. (2009) 'Centriole separation in DNA damage-induced centrosome amplification', *Environ Mol Mutagen*, 50(8), 725-32.

Saladino, C., Bourke, E. and Morrison, C. G. (2012) 'The Centrosome: Cell and Molecular Mechanisms of Functions and Dysfunctions in Disease', *ed H. Schatten (New York, NY: Humana Press)*, 223-241.

Sancar, A., Lindsey-Boltz, L. A., Unsal-Kacmaz, K. and Linn, S. (2004) 'Molecular mechanisms of mammalian DNA repair and the DNA damage checkpoints', *Annu Rev Biochem*, 73, 39-85.

Sankaran, S., Crone, D. E., Palazzo, R. E. and Parvin, J. D. (2007) 'BRCA1 regulates gamma-tubulin binding to centrosomes', *Cancer Biol Ther*, 6(12), 1853-7.

Satir, P., Pedersen, L. B. and Christensen, S. T. (2010) 'The primary cilium at a glance', *J Cell Sci*, 123(Pt 4), 499-503.

Satyanarayana, A. and Kaldis, P. (2009) 'Mammalian cell-cycle regulation: several Cdks, numerous cyclins and diverse compensatory mechanisms', *Oncogene*, 28(33), 2925-39.

Sawin, K. E. and Mitchison, T. J. (1995) 'Mutations in the kinesin-like protein Eg5 disrupting localization to the mitotic spindle', *Proc Natl Acad Sci U S A*, 92(10), 4289-93.

Schneider, L., Clement, C. A., Teilmann, S. C., Pazour, G. J., Hoffmann, E. K., Satir, P. and Christensen, S. T. (2005) 'PDGFRalphaalpha signaling is regulated through the primary cilium in fibroblasts', *Curr Biol*, 15(20), 1861-6.

Schnerch, D. and Nigg, E. A. (2015) 'Structural centrosome aberrations favor proliferation by abrogating microtubule-dependent tissue integrity of breast epithelial mammospheres', *Oncogene*.

Schockel, L., Mockel, M., Mayer, B., Boos, D. and Stemmann, O. (2011) 'Cleavage of cohesin rings coordinates the separation of centrioles and chromatids', *Nat Cell Biol*, 13(8), 966-72.

Schon, O., Friedler, A., Bycroft, M., Freund, S. M. and Fersht, A. R. (2002) 'Molecular mechanism of the interaction between MDM2 and p53', *J Mol Biol*, 323(3), 491-501.

Shaltiel, I. A., Krenning, L., Bruinsma, W. and Medema, R. H. (2015) 'The same, only different - DNA damage checkpoints and their reversal throughout the cell cycle', *J Cell Sci*, 128(4), 607-20.

Shao, S., Liu, R., Wang, Y., Song, Y., Zuo, L., Xue, L., Lu, N., Hou, N., Wang, M., Yang, X. and Zhan, Q. (2010) 'Centrosomal Nlp is an oncogenic protein that is gene-amplified in human tumors and causes spontaneous tumorigenesis in transgenic mice', *J Clin Invest*, 120(2), 498-507.

Shekhar, M. P., Lyakhovich, A., Visscher, D. W., Heng, H. and Kondrat, N. (2002) 'Rad6 overexpression induces multinucleation, centrosome amplification, abnormal mitosis, aneuploidy, and transformation', *Cancer Res*, 62(7), 2115-24.

Shieh, S. Y., Ahn, J., Tamai, K., Taya, Y. and Prives, C. (2000) 'The human homologs of checkpoint kinases Chk1 and Cds1 (Chk2) phosphorylate p53 at multiple DNA damage-inducible sites', *Genes Dev*, 14(3), 289-300.

Shiloh, Y. (2003) 'ATM and related protein kinases: safeguarding genome integrity', *Nat Rev Cancer*, 3(3), 155-68.

Singla, V., Romaguera-Ros, M., Garcia-Verdugo, J. M. and Reiter, J. F. (2010) 'Ofd1, a human disease gene, regulates the length and distal structure of centrioles', *Dev Cell*, 18(3), 410-24.

Sir, J. H., Putz, M., Daly, O., Morrison, C. G., Dunning, M., Kilmartin, J. V. and Gergely, F. (2013) 'Loss of centrioles causes chromosomal instability in vertebrate somatic cells', *J Cell Biol*, 203(5), 747-56.

Sironi, L., Melixetian, M., Faretta, M., Prosperini, E., Helin, K. and Musacchio, A. (2001) 'Mad2 binding to Mad1 and Cdc20, rather than oligomerization, is required for the spindle checkpoint', *Embo j*, 20(22), 6371-82.

Skoufias, D. A., Andreassen, P. R., Lacroix, F. B., Wilson, L. and Margolis, R. L. (2001) 'Mammalian mad2 and bub1/bubR1 recognize distinct spindle-attachment and kinetochore-tension checkpoints', *Proc Natl Acad Sci U S A*, 98(8), 4492-7.

Somyajit, K., Basavaraju, S., Scully, R. and Nagaraju, G. (2013) 'ATM- and ATR-mediated phosphorylation of XRCC3 regulates DNA double-strand break-induced checkpoint activation and repair', *Mol Cell Biol*, 33(9), 1830-44.

Sonnen, K. F., Gabryjonczyk, A. M., Anselm, E., Stierhof, Y. D. and Nigg, E. A. (2013) 'Human Cep192 and Cep152 cooperate in Plk4 recruitment and centriole duplication', *J Cell Sci*, 126(Pt 14), 3223-33.

Sonnen, K. F., Schermelleh, L., Leonhardt, H. and Nigg, E. A. (2012) '3D-structured illumination microscopy provides novel insight into architecture of human centrosomes', *Biol Open*, 1(10), 965-76.

Sonoda, E., Sasaki, M. S., Buerstedde, J. M., Bezzubova, O., Shinohara, A., Ogawa, H., Takata, M., Yamaguchi-Iwai, Y. and Takeda, S. (1998) 'Rad51-deficient vertebrate cells accumulate chromosomal breaks prior to cell death', *EMBO J*, 17(2), 598-608.

Sonoda, E., Takata, M., Yamashita, Y. M., Morrison, C. and Takeda, S. (2001) 'Homologous DNA recombination in vertebrate cells', *Proc Natl Acad Sci U S A*, 98(15), 8388-94.

Sorensen, C. S., Syljuasen, R. G., Falck, J., Schroeder, T., Ronnstrand, L., Khanna, K. K., Zhou, B. B., Bartek, J. and Lukas, J. (2003) 'Chk1 regulates the S phase checkpoint by coupling the physiological turnover and ionizing radiation-induced accelerated proteolysis of Cdc25A', *Cancer Cell*, 3(3), 247-58.

Sorokin, S. P. (1968a) 'Centriole formation and ciliogenesis', *Aspen Emphysema Conf*, 11, 213-6.

Sorokin, S. P. (1968b) 'Reconstructions of centriole formation and ciliogenesis in mammalian lungs', *J Cell Sci*, 3(2), 207-30.

Spalluto, C., Wilson, D. I. and Hearn, T. (2012) 'Nek2 localises to the distal portion of the mother centriole/basal body and is required for timely cilium disassembly at the G2/M transition', *Eur J Cell Biol*, 91(9), 675-86.

Spektor, A., Tsang, W. Y., Khoo, D. and Dynlacht, B. D. (2007) 'Cep97 and CP110 suppress a cilia assembly program', *Cell*, 130(4), 678-90.

Staples, C. J., Myers, K. N., Beveridge, R. D., Patil, A. A., Lee, A. J., Swanton, C., Howell, M., Boulton, S. J. and Collis, S. J. (2012) 'The centriolar satellite protein Cep131 is important for genome stability', *J Cell Sci*, 125(Pt 20), 4770-9.

Steere, N., Wagner, M., Beishir, S., Smith, E., Breslin, L., Morrison, C. G., Hochegger, H. and Kuriyama, R. (2011) 'Centrosome amplification in CHO and DT40 cells by inactivation of cyclin-dependent kinases', *Cytoskeleton (Hoboken)*, 68(8), 446-58.

Stinchcombe, J. C., Bossi, G., Booth, S. and Griffiths, G. M. (2001) 'The immunological synapse of CTL contains a secretory domain and membrane bridges', *Immunity*, 15(5), 751-61.

Stinchcombe, J. C. and Griffiths, G. M. (2014) 'Communication, the centrosome and the immunological synapse', *Philos Trans R Soc Lond B Biol Sci*, 369(1650).

Stinchcombe, J. C., Salio, M., Cerundolo, V., Pende, D., Arico, M. and Griffiths, G. M. (2011) 'Centriole polarisation to the immunological synapse directs secretion from cytolytic cells of both the innate and adaptive immune systems', *BMC Biol*, 9, 45.

Stowe, T. R., Wilkinson, C. J., Iqbal, A. and Stearns, T. (2012) 'The centriolar satellite proteins Cep72 and Cep290 interact and are required for recruitment of BBS proteins to the cilium', *Mol Biol Cell*, 23(17), 3322-35.

Strnad, P., Leidel, S., Vinogradova, T., Euteneuer, U., Khodjakov, A. and Gonczy, P. (2007) 'Regulated HsSAS-6 levels ensure formation of a single procentriole per centriole during the centrosome duplication cycle', *Dev Cell*, 13(2), 203-13.

Sudakin, V., Chan, G. K. and Yen, T. J. (2001) 'Checkpoint inhibition of the APC/C in HeLa cells is mediated by a complex of BUBR1, BUB3, CDC20, and MAD2', *J Cell Biol*, 154(5), 925-36.

Sumara, I., Vorlaufer, E., Stukenberg, P. T., Kelm, O., Redemann, N., Nigg, E. A. and Peters, J. M. (2002) 'The dissociation of cohesin from chromosomes in prophase is regulated by Polo-like

kinase', *Mol Cell*, 9(3), 515-25.

Sung, P. and Robberson, D. L. (1995) 'DNA strand exchange mediated by a RAD51-ssDNA nucleoprotein filament with polarity opposite to that of RecA', *Cell*, 82(3), 453-61.

Szollosi, D. and Ozil, J. P. (1991) 'De novo formation of centrioles in parthenogenetically activated, diploidized rabbit embryos', *Biol Cell*, 72(1-2), 61-6.

Takahashi, M., Shibata, H., Shimakawa, M., Miyamoto, M., Mukai, H. and Ono, Y. (1999) 'Characterization of a novel giant scaffolding protein, CG-NAP, that anchors multiple signaling enzymes to centrosome and the golgi apparatus', *J Biol Chem*, 274(24), 17267-74.

Takai, H., Naka, K., Okada, Y., Watanabe, M., Harada, N., Saito, S., Anderson, C. W., Appella, E., Nakanishi, M., Suzuki, H., Nagashima, K., Sawa, H., Ikeda, K. and Motoyama, N. (2002) 'Chk2-deficient mice exhibit radioresistance and defective p53-mediated transcription', *EMBO J*, 21(19), 5195-205.

Takata, M., Sasaki, M. S., Sonoda, E., Morrison, C., Hashimoto, M., Utsumi, H., Yamaguchi-Iwai, Y., Shinohara, A. and Takeda, S. (1998) 'Homologous recombination and non-homologous end-joining pathways of DNA double-strand break repair have overlapping roles in the maintenance of chromosomal integrity in vertebrate cells', *Embo j*, 17(18), 5497-508.

Takisawa, H., Mimura, S. and Kubota, Y. (2000) 'Eukaryotic DNA replication: from pre-replication complex to initiation complex', *Curr Opin Cell Biol*, 12(6), 690-6.

Tamura, K., Stecher, G., Peterson, D., Filipski, A. and Kumar, S. (2013) 'MEGA6: Molecular Evolutionary Genetics Analysis version 6.0', *Mol Biol Evol*, 30(12), 2725-9.

Tanenbaum, M. E. and Medema, R. H. (2010) 'Mechanisms of centrosome separation and bipolar spindle assembly', *Dev Cell*, 19(6), 797-806.

Tang, C. J., Lin, S. Y., Hsu, W. B., Lin, Y. N., Wu, C. T., Lin, Y. C., Chang, C. W., Wu, K. S. and Tang, T. K. (2011) 'The human microcephaly protein STIL interacts with CPAP and is required for procentriole formation', *EMBO J*, 30(23), 4790-804.

Tang, Z., Lin, M. G., Stowe, T. R., Chen, S., Zhu, M., Stearns, T., Franco, B. and Zhong, Q. (2013) 'Autophagy promotes primary ciliogenesis by removing OFD1 from centriolar satellites', *Nature*, 502(7470), 254-7.

Tasouri, E. and Tucker, K. L. (2011) 'Primary cilia and organogenesis: is Hedgehog the only sculptor?', *Cell Tissue Res*, 345(1), 21-40.

Tayeh, M. K., Yen, H. J., Beck, J. S., Searby, C. C., Westfall, T. A., Griesbach, H., Sheffield, V. C. and Slusarski, D. C. (2008) 'Genetic interaction between Bardet-Biedl syndrome genes and implications for limb patterning', *Hum Mol Genet*, 17(13), 1956-67.

Taylor, W. R. and Stark, G. R. (2001) 'Regulation of the G2/M transition by p53', *Oncogene*, 20(15), 1803-15.

Thein, K. H., Kleylein-Sohn, J., Nigg, E. A. and Gruneberg, U. (2007) 'Astrin is required for the maintenance of sister chromatid cohesion and centrosome integrity', *J Cell Biol*, 178(3), 345-54.

Tollenaere, M. A., Mailand, N. and Bekker-Jensen, S. (2015) 'Centriolar satellites: key mediators of centrosome functions', *Cell Mol Life Sci*, 72(1), 11-23.

Tournebize, R., Andersen, S. S., Verde, F., Doree, M., Karsenti, E. and Hyman, A. A. (1997) 'Distinct roles of PP1 and PP2A-like phosphatases in control of microtubule dynamics during mitosis', *Embo j*, 16(18), 5537-49.

Tsang, W. Y., Bossard, C., Khanna, H., Peranen, J., Swaroop, A., Malhotra, V. and Dynlacht, B. D. (2008) 'CP110 suppresses primary cilia formation through its interaction with CEP290, a protein deficient in human ciliary disease', *Dev Cell*, 15(2), 187-97.

Tsang, W. Y. and Dynlacht, B. D. (2013) 'CP110 and its network of partners coordinately regulate cilia assembly', *Cilia*, 2(1), 9.

Tsou, M. F. and Stearns, T. (2006a) 'Controlling centrosome number: licenses and blocks', *Current Opinion in Cell Biology*, 18(1), 74-78.

Tsou, M. F. and Stearns, T. (2006b) 'Mechanism limiting centrosome duplication to once per cell cycle', *Nature*, 442(7105), 947-51.

Tsou, M. F., Wang, W. J., George, K. A., Uryu, K., Stearns, T. and Jallepalli, P. V. (2009) 'Polo kinase and separase regulate the mitotic licensing of centriole duplication in human cells', *Dev Cell*, 17(3), 344-54.

Tsvetkov, L., Xu, X., Li, J. and Stern, D. F. (2003) 'Polo-like kinase 1 and Chk2 interact and co-localize to centrosomes and the midbody', *J Biol Chem*, 278(10), 8468-75.

Tutt, A., Gabriel, A., Bertwistle, D., Connor, F., Paterson, H., Peacock, J., Ross, G. and Ashworth, A. (1999) 'Absence of Brca2 causes genome instability by chromosome breakage and loss associated with centrosome amplification', *Curr Biol*, 9(19), 1107-10.

Ueda, S., Takeishi, Y., Ohashi, E. and Tsurimoto, T. (2012) 'Two serine phosphorylation sites in the C-terminus of Rad9 are critical for 9-1-1 binding to TopBP1 and activation of the DNA damage checkpoint response in HeLa cells', *Genes Cells*, 17(10), 807-16.

Uetake, Y. and Sluder, G. (2004) 'Cell cycle progression after cleavage failure: mammalian somatic cells do not possess a "tetraploidy checkpoint"', *J Cell Biol*, 165(5), 609-15.

van Breugel, M., Hirono, M., Andreeva, A., Yanagisawa, H. A., Yamaguchi, S., Nakazawa, Y., Morgner, N., Petrovich, M., Ebong, I. O., Robinson, C. V., Johnson, C. M., Veprintsev, D. and Zuber, B. (2011) 'Structures of SAS-6 suggest its organization in centrioles', *Science*, 331(6021), 1196-9.

Vuolo, L., Herrera, A., Torroba, B., Menendez, A. and Pons, S. (2015) 'Ciliary adenylyl cyclases control the Hedgehog pathway', *J Cell Sci*, 128(15), 2928-37.

Wade, R. H. (2007) 'Microtubules: an overview', *Methods Mol Med*, 137, 1-16.

Walker, J. R., Corpina, R. A. and Goldberg, J. (2001) 'Structure of the Ku heterodimer bound to DNA and its implications for double-strand break repair', *Nature*, 412(6847), 607-14.

Wallace, S. S., Murphy, D. L. and Sweasy, J. B. (2012) 'Base excision repair and cancer', *Cancer Lett*, 327(1-2), 73-89.

Wallingford, J. B. and Mitchell, B. (2011) 'Strange as it may seem: the many links between Wnt signaling, planar cell polarity, and cilia', *Genes Dev*, 25(3), 201-13.

Wang, G., Chen, Q., Zhang, X., Zhang, B., Zhuo, X., Liu, J., Jiang, Q. and Zhang, C. (2013) 'PCM1 recruits Plk1 to the pericentriolar matrix to promote primary cilia disassembly before mitotic entry', *J Cell Sci*, 126(Pt 6), 1355-65.

Wang, G., Jiang, Q. and Zhang, C. (2014) 'The role of mitotic kinases in coupling the centrosome cycle with the assembly of the mitotic spindle', *J Cell Sci*, 127(Pt 19), 4111-22.

Wang, H., Powell, S. N., Iliakis, G. and Wang, Y. (2004) 'ATR affecting cell radiosensitivity is dependent on homologous recombination repair but independent of nonhomologous end joining', *Cancer Res*, 64(19), 7139-43.

Wang, H., Yang, H., Shivalila, C. S., Dawlaty, M. M., Cheng, A. W., Zhang, F. and Jaenisch, R. (2013) 'One-step generation of mice carrying mutations in multiple genes by CRISPR/Cas-mediated genome engineering', *Cell*, 153(4), 910-8.

Wang, X., Yang, Y., Duan, Q., Jiang, N., Huang, Y., Darzynkiewicz, Z. and Dai, W. (2008) 'sSgo1, a Major Splice Variant of Sgo1, Functions in Centriole Cohesion Where It Is Regulated by Plk1', *Developmental Cell*, 14(3), 331-341.

Wang, Z., Wu, T., Shi, L., Zhang, L., Zheng, W., Qu, J. Y., Niu, R. and Qi, R. Z. (2010) 'Conserved motif of CDK5RAP2 mediates its localization to centrosomes and the Golgi complex', *J Biol Chem*, 285(29), 22658-65.

Watanabe, N., Arai, H., Nishihara, Y., Taniguchi, M., Hunter, T. and Osada, H. (2004) 'M-phase kinases induce phospho-dependent ubiquitination of somatic Wee1 by SCFbeta-TrCP', *Proc Natl Acad Sci U S A*, 101(13), 4419-24.

West, R. B., Yaneva, M. and Lieber, M. R. (1998) 'Productive and nonproductive complexes of Ku and DNA-dependent protein kinase at DNA termini', *Mol Cell Biol*, 18(10), 5908-20.

White, R. A., Pan, Z. and Salisbury, J. L. (2000) 'GFP-centrin as a marker for centriole dynamics in living cells', *Microsc Res Tech*, 49(5), 451-7.

Wiese, C., Wilde, A., Moore, M. S., Adam, S. A., Merdes, A. and Zheng, Y. (2001) 'Role of importin-beta in coupling Ran to downstream targets in microtubule assembly', *Science*, 291(5504), 653-6.

Wiese, C. and Zheng, Y. (2000) 'A new function for the [ggr] -tubulin ring complex as a microtubule minus-end cap', *Nat Cell Biol*, 2(6), 358-364.

Wollman, R., Civelekoglu-Scholey, G., Scholey, J. M. and Mogilner, A. (2008) 'Reverse engineering of force integration during mitosis in the Drosophila embryo', *Mol Syst Biol*, 4, 195.

Wong, C. and Stearns, T. (2003) 'Centrosome number is controlled by a centrosome-intrinsic block to reduplication', *Nat Cell Biol*, 5(6), 539-44.

Wong, Y. L., Anzola, J. V., Davis, R. L., Yoon, M., Motamedi, A., Kroll, A., Seo, C. P., Hsia, J. E., Kim, S. K., Mitchell, J. W., Mitchell, B. J., Desai, A., Gahman, T. C., Shiau, A. K. and Oegema, K. (2015) 'Cell biology. Reversible centriole depletion with an inhibitor of Polo-like kinase 4', *Science*, 348(6239), 1155-60.

Wu, C. L., Classon, M., Dyson, N. and Harlow, E. (1996) 'Expression of dominant-negative mutant DP-1 blocks cell cycle progression in G1', *Mol Cell Biol*, 16(7), 3698-706.

Wu, L. and Hickson, I. D. (2003) 'The Bloom's syndrome helicase suppresses crossing over during homologous recombination', *Nature*, 426(6968), 870-4.

Xu, X., Weaver, Z., Linke, S. P., Li, C., Gotay, J., Wang, X. W., Harris, C. C., Ried, T. and Deng, C. X. (1999) 'Centrosome amplification and a defective G2-M cell cycle checkpoint induce genetic instability in BRCA1 exon 11 isoform-deficient cells', *Mol Cell*, 3(3), 389-95.

Yang, H., Jeffrey, P. D., Miller, J., Kinnucan, E., Sun, Y., Thoma, N. H., Zheng, N., Chen, P. L., Lee, W. H. and Pavletich, N. P. (2002) 'BRCA2 function in DNA binding and recombination from a BRCA2-DSS1-ssDNA structure', *Science*, 297(5588), 1837-48.

Yang, J., Adamian, M. and Li, T. (2006) 'Rootletin interacts with C-Nap1 and may function as a physical linker between the pair of centrioles/basal bodies in cells', *Mol Biol Cell*, 17(2), 1033-40.

Yang, J., Liu, X., Yue, G., Adamian, M., Bulgakov, O. and Li, T. (2002) 'Rootletin, a novel coiled-

coil protein, is a structural component of the ciliary rootlet', *J Cell Biol*, 159(3), 431-40.

Yazdi, P. T., Wang, Y., Zhao, S., Patel, N., Lee, E. Y. and Qin, J. (2002) 'SMC1 is a downstream effector in the ATM/NBS1 branch of the human S-phase checkpoint', *Genes Dev*, 16(5), 571-82.

Yi, J., Wu, X., Chung, A. H., Chen, J. K., Kapoor, T. M. and Hammer, J. A. (2013) 'Centrosome repositioning in T cells is biphasic and driven by microtubule end-on capture-shrinkage', *J Cell Biol*, 202(5), 779-92.

Zhang, S., Hemmerich, P. and Grosse, F. (2007) 'Centrosomal localization of DNA damage checkpoint proteins', *J Cell Biochem*, 101(2), 451-65.

Zhang, Y., Wang, Y., Wei, Y., Ma, J., Peng, J., Wumaier, R., Shen, S., Zhang, P. and Yu, L. (2015) 'The tumor suppressor proteins ASPP1 and ASPP2 interact with C-Nap1 and regulate centrosome linker reassembly', *Biochem Biophys Res Commun*, 458(3), 494-500.

Zhao, H., Zhu, L., Zhu, Y., Cao, J., Li, S., Huang, Q., Xu, T., Huang, X., Yan, X. and Zhu, X. (2013) 'The Cep63 paralogue Deup1 enables massive de novo centriole biogenesis for vertebrate multiciliogenesis', *Nat Cell Biol*, 15(12), 1434-44.

Zhu, Z., Chung, W. H., Shim, E. Y., Lee, S. E. and Ira, G. (2008) 'Sgs1 helicase and two nucleases Dna2 and Exo1 resect DNA double-strand break ends', *Cell*, 134(6), 981-94.

Zimmerman, W. C., Sillibourne, J., Rosa, J. and Doxsey, S. J. (2004) 'Mitosis-specific anchoring of gamma tubulin complexes by pericentrin controls spindle organization and mitotic entry', *Mol Biol Cell*, 15(8), 3642-57.

Zou, L. and Elledge, S. J. (2003) 'Sensing DNA Damage Through ATRIP Recognition of RPA-ssDNA Complexes', *Science*, 300(5625), 1542-1548.

Appendix: Poster presentations and publications

Poster Presentations

- **EMBO Centrosomes and spindle pole bodies International Conference**
  C-NAP1 in centrosome integrity and DNA damage responses
  Anne-Marie M. Flanagan, David C.A. Gaboriau, Ciaran G. Morrison
  30 September – 3 October 2014, Lisbon, Portugal

- **American Society for Cell Biology, Annual Meeting**
  C-Nap1, Centrosomal Linker Protein?
  Anne-Marie M. Flanagan, Ciaran G. Morrison
  14 - 18 December 2013, New Orleans, USA

- **Microscopy Society of Ireland Annual Meeting – Poster Prize**
  The Role of C-Nap1 in Centrosome Duplication and DNA Damage
  Anne-Marie M. Flanagan, Ciaran G. Morrison
  21 -23 August 2013, Galway, Ireland

- **UL-NUIG Alliance Research Day**
  The Role of C-Nap1 in Centrosome Duplication and DNA Damage
  Anne-Marie M. Flanagan, Ciaran G. Morrison
  11 April 2013, Galway, Ireland

Publications

- **SUMO ligase activity of vertebrate Mms21/Nse2 is required for efficient DNA repair but not for Smc5/6 complex stability**
  Kliszczak, Maciej, Stephan, Anna K., Flanagan, Anne-Marie M., Morrison, Ciaran G.
  DNA Repair, 2012 Oct 1;11(10):799-810.